Machine learning prediction of nanofluid thermal and flow characteristics

Ekene Jude Onyiriuka

Submitted in accordance with the requirements for the degree of Doctor of Philosophy

The University of Leeds

School of Mechanical Engineering

March 2024

Intellectual property and publications

The thesis includes article manuscripts that have been written and peer-reviewed in academic journals, recognised to be relevant to the field of the candidate's research and academically reputable. They have been presented as they appear in the published form and are self-contained. The papers present original work. The manuscripts included in the thesis report are findings based on original, theoretical, empirical work, and modelling that form a part of the research conducted during the candidate's post-graduate research studies. The candidate confirms that the work submitted is his own. The candidates confirm that appropriate credit has been given where references have been made to the work of others.

List of published work presented as thesis chapters

Onyiriuka, Ekene Jude. "Predicting the accuracy of nanofluid heat transfer coefficient's computational fluid dynamics simulations using neural networks." Heat Transfer (2023). https://doi.org/10.1002/htj.22833

Onyiriuka, Ekene J. "Single phase nanofluid thermal conductivity and viscosity prediction using neural networks and its application in a heated pipe of a circular cross-section." Heat Transfer (2023). https://doi.org/10.1002/htj.22838

Onyiriuka, E. Predictive modelling of thermal conductivity in single-material nanofluids: a novel approach. Bull Natl Res Cent 47, 140 (2023). https://doi.org/10.1186/s42269-023-01115-9

List of other published work during the candidate's study in University of Leeds

Onyiriuka, E. Optimising Al2O3–water nanofluid. Bull Natl Res Cent 48, 2 (2024). https://doi.org/10.1186/s42269-023-01162-2

Onyiriuka, E. Modeling nanofluid viscosity: comparing models and optimizing feature selection—a novel approach. Bull Natl Res Cent 47, 139 (2023). https://doi.org/10.1186/s42269-023-01114-w

Onyiriuka, E. Modelling the thermal conductivity of nanofluids using a novel model of models approach. J Therm Anal Calorim (2023). https://doi.org/10.1007/s10973-023-12642-y

Ewim, D.R.E., Adelaja, A.OEwim, D.R.E., Adelaja, A.O., **Onyiriuka, E.J.** Modelling of heat transfer coefficients during condensation inside an enhanced inclined tube. J Therm Anal Calorim 146, 103–115 (2021). https://doi.org/10.1007/s10973-020-09930-2

Ewim, D. R., Shote, A. S., **Onyiriuka, E. J.**, Adio, S. A., & Kaood, A. Thermal performance of nano refrigerants: a short review. J Mech Eng Res Dev, 44, 89-115 (2021).

Ewim, D. R. E., Okwu, M. O., **Onyiriuka, E. J**., Abiodun, A. S., Abolarin, S. M., & Kaood, A. A quick review of the applications of artificial neural networks (ANN) in the modelling of thermal systems (2021).

Conferences

Ekene J Onyiriuka, Daniel R E Ewim, Sogo M Abolarin An optimization technique to identify simulation assumptions for various nanofluids using machine learning. Proceedings of the 17th International Heat Transfer Conference, IHTC-17, 14 – 18 **August 2023**, Cape Town, South Africa

This format has been chosen since the candidate is of a lecturing and research background from the University of Benin. This format will aid his career goals in lecturing and aid him in moving higher in the academic cadre.

The thesis has been constructed into three main sections, namely, the introduction section -Chapter One to Chapter Three, the manuscript section - Chapter Four to Chapter Six and the discussion section - Chapter Seven.

THE AUTHOR

The author was educated at the University of Benin Demonstration Secondary and Primary School, and at the University of Benin, from which he graduated with flying colours in Mechanical Engineering in November 2013. After this, the author was employed as a graduate assistant at the University of Benin before commencing his master's degree in mechanical engineering, thermal power engineering option in November 2017. On completing this the author was promoted to Lecturer status. Thereafter, he proceeded to Doctoral study under the sponsorship of the Tertiary Education Trust Fund (TETFund).

ACKNOWLEDGEMENTS

Firstly, the author wishes to thank Dr Jongrae Kim and Dr Jung-uk Shim for their help and support during the supervision of the work. Funding was provided by Tertiary Education Trust Fund (TETFund), and the author greatly acknowledges and appreciates this. Special thanks to Professor David Barton of the Institute of Design, Robotics & Optimization, who attended the biweekly progress report meetings and offered valuable insights in each meeting.

All members of the Academic and teaching staff, Visiting, Honorary and Emeritus Professors, and support staff of the School of Mechanical Engineering have contributed, in one way or another, to this work; while it is not possible to mention them individually, the Author would like to express his sincere appreciation to all. Special thanks go to Michelle Byrne and Joanne Sah, for their contribution to the success of the program.

The author wishes to appreciate the diverse roles played by the wider university community, including the University of Leeds student union, and the student services.

Abstract

This research presents a study on the prediction of nanofluid thermal and flow characteristics using machine learning. The modelling and simulation of nanofluid is a useful tool in predicting nanofluid thermal and flow characteristics. It aids design of new products and helps researchers fully forecast how the fluid will behave under different conditions and settings.

The present study has been successful in improving the accuracy of nanofluid simulations and the thermal and flow characteristics prediction. Through a series of analyses using machine learning, new nanofluid models have been created, and tested, and new insights have been produced both on the nanofluids aspect and the machine learning aspect.

From the study, it was observed that three (3) modelling assumptions namely dispersion, Buongiorno, and discrete phase model (DPM) showed high accuracy in modelling nanofluids. They all have an accuracy within 5%, with the dispersion model being the best for both constant and temperature-dependent property assumptions. The discrete phase model (DPM) model seems to do better in turbulent flow than in laminar flow, while the Buongiorno models do better under laminar flow conditions. The single phase model and mixture models were observed to be the worst and only recommended where there are no other choices. The accuracy of the single phase model can be considerably improved by the substitution of the thermophysical properties of the nanofluid with an accurate machine learning model. The feature selection method based on the physics of the problem is a highly effective machine learning modelling strategy with the possibility of higher accuracy and generalization. Neural network models are considerably effective in modelling nanofluids' thermophysical properties.

Keywords: Nanofluids, Thermophysical properties, Heat transfer, Machine learning, Simulation

Contents

List of figures

List of tables

List of symbols and abbreviations

AI	Artificial intelligence
ANFIS	Adaptive Neuro Fuzzy Inference System
ANN	Artificial neural network
b	Biases
BF	Base fluid
BFa	Base fluid thermal diffusivity $(m^2/s)\ e+07$
BFbp	Base fluid boiling point (^{o}C)
BFcp	Base fluid specific heat capacity $(J\ /\ (kg.K))$
BFd	Base fluid density (kg/m^3)
BFde	Base fluid dielectric constant $(-)$
BFk	Base fluid thermal conductivity $(W/\ (m.K))$
BFkv	Base fluid kinematic viscosity $(m^2/s)\ e+07$
BFst	Base fluid surface tension (mN/m)
BFv	Base fluid viscosity $(Pa.s)$
BM	Model assumptions
BUO	Buongiorno's Model
CDM	Combined model of discrete phase and mixture phase
CFD	Computational fluid dynamics

CONST	Constant thermophysical properties assumption
Cp	Specific heat capacity (kJ/kgK)
D, d	Diameter (m)
DLS	Dynamics light scattering
DIS	Dispersion Model
DP	Particle size diameter (nm)
DPM	Discrete Phase Model
EG	Ethylene-Glycol
ENT	Percentage enhancement of nanofluid thermal conductivity $(\%)$
EUL	Eulerian-Eulerian Model
GA	Genetic Algorithm
GEO	Flow Geometry
GMDH	Group method of data handling
GPR	Gaussian Process Regressor
$\bar{h}$	Mean value of observed heat transfer coefficient
k	Thermal conductivity (W/mK)
kNN	K nearest neighbor
L	Length of pipe (m)
LSSVM	Least square support vector machine

M	Molar mass
MAE	Mean absolute error
MIX	Mixture Model
ML	Machine learning
MLP	Multi-layered Perceptron
MSE	Mean Square Error
MWCNT	Multi-walled carbon nanotube
N	Avogadro's number
N	Number
n	Output
NFSA	Novel feature selection algorithms
NFS-Different	Novel feature selection with different statistical characteristics
NFS-Similar	Novel feature selection with similar statistical characteristics
NPa	Nanoparticle thermal diffusivity $(m^2/s)\ e+07$
NPcp	Nanoparticle-specific heat capacity $(J\ /\ (kg.K))$
NPd	Nanoparticle density (kg/m^3)
NPde	Nanoparticle dielectric constant $(-)$
NPek	Nanoparticle electrical conductivity (mMS/m)

NPk	Nanoparticle thermal conductivity $(W/(m.K))$
NPmp	Nanoparticle melting point (^{o}C)
NPms	Nanoparticle magnetic susceptibility $(-)$
NPri	Nanoparticle refractive index $(-)$
Nu	Nusselt's number
R^2	R-squared value
RBF	Radial Basis Function
Re	Renold's number
ReLU	Rectified Linear Unit
RMSE	Root mean squared error
PA	Property assumption
PD	Percentage deviation
Pr	Prandtl's number
PS	Particle size
PT	Particle type
PV	Particle volume fraction $(\%)$
PVT	Photovoltaic-thermal systems
SEM	Scanning electron microscope
SPM	Single-Phase Model

SS_{reg}	Explained sum of squares
SS_{tot}	Total sum of squares
SVF	Volume concentration
SVM	Support vector machine
T	Temperature (K)
TC	Nanofluid temperature (^{o}C)
TEM	Transmission electron microscopy
UV	Ultraviolet
$\vec{\boldsymbol{v}}$	Velocity (m/s)
VAR	Variable thermophysical properties assumption
VOF	Volume of fluid
w	Weights
WHC	Wall heat flux
x	Input

Greek

α	Arbitrary scaling factor
β	Volumetric thermal expansion
κ	Boltzmann constant

μ	Viscosity $(\mathrm{Pa.s})$
π	3.14159
ρ	Density (kg/m^3)
ϕ	Volume concentration
ω	Frequency

Subscripts

bf	Basefluid
f	Base fluid
i	Data point
m	Max packing fraction
nf	Nanofluid
p	Particle
$pred$	Prediction

Superscript

$pred$	Prediction

Chapter 1 Introduction

1.1 Research background

Water is an essential element of nature and has been proven to be immensely beneficial to the world. It is used for basic necessities such as drinking, cooking, and powering large machinery [4, 5]. As a conventional fluid, it is also used in heat transfer to cool hotter surfaces or fluids and heat up colder surfaces or fluids [4, 5]. Researchers have worked together to improve the properties of fluids used for heat transfer. Their goal is to make life better for everyone by investing more resources in harnessing the properties of water and other conventional heat transfer fluids, while also reducing the cost of their operation.

In the early 1990s, Choi, working at the Argonne National Laboratory in the United States introduced the concept of nanofluids. His main goal in developing nanofluids was to improve the heat transfer capabilities of conventional heat transfer fluids, [6]. Nanofluids are created by dispersing nanoparticles, typically measuring between 1 and 200 nanometres, into a base fluid, such as water, oil, or synthetics. The nanoparticles used are mostly metallic, oxides, or carbon-based. The objective of introducing nanoparticles into the base fluid, as proposed by Choi, is to improve the efficiency of cooling systems and heat transfer processes.

Nanoparticles possess unique properties at the nanoscale, including a high thermal conductivity and large surface area-to-volume ratio. These properties can enhance fluid heat transfer performance [6-8]. The idea of nanofluids has garnered attention due to their promising potential for various applications, such as cooling systems in automobiles and electronics, solar energy systems, and heat exchangers in industries. The aim of incorporating nanoparticles into the fluid is to enhance heat dissipation by taking advantage of the large surface area-to-volume ratio, reduce energy consumption by lowering the viscosity due to temperature changes, and improve overall thermal performance in these applications [8-11].

Many researchers have attempted to understand and accurately model the phenomenon of enhanced heat transfer, thermal conductivity, and flow of nanofluids. However, the complex relationships between these factors have resulted in varying results, models and conflicting conclusions in research journals and papers authored by different researchers.

Figure 1-1, the record of research works containing the word “nanofluid” as analysed on the Web of Science, shows that up until July of 2024, there have been 24,165 records and further shows the increasing trend of research articles in this nanofluids area over the years from 1997 to 2024.

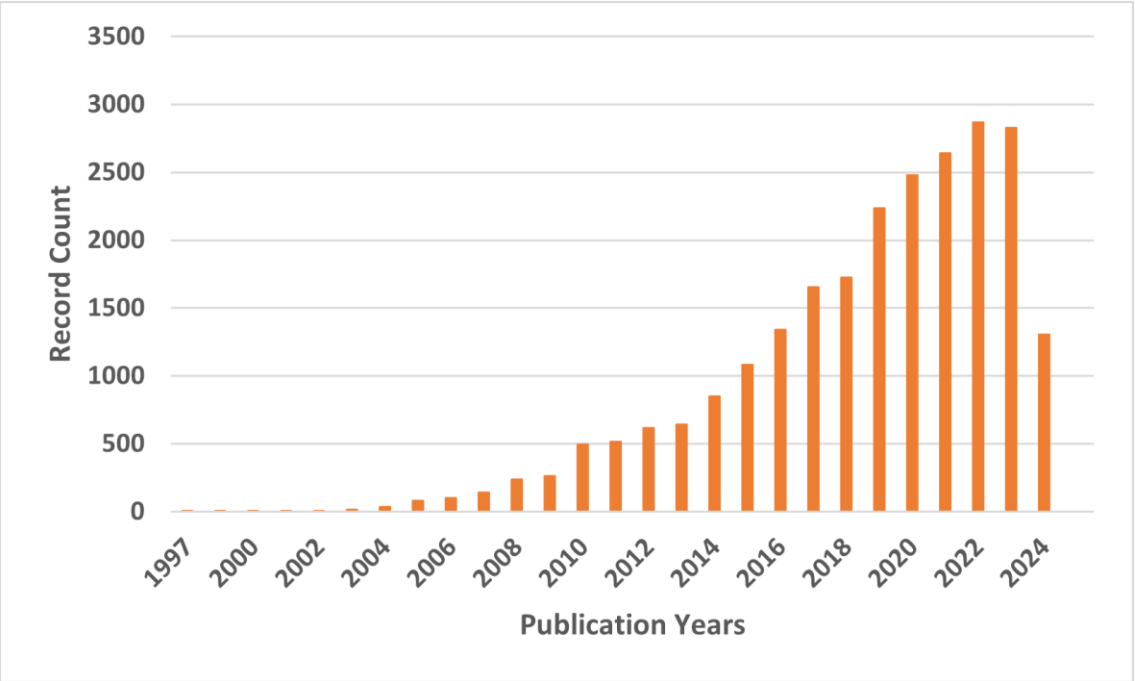

Figure 1-1 Research interest in nanofluids since the year 1990 till date.

Research problem

The focus of this study is to address the research problem of accurately predicting and modelling the properties of nanofluids. Nanofluids are suspensions of nanoparticles in base fluids that exhibit unique thermophysical properties, which can potentially enhance heat transfer efficiency. However, the behaviour of nanofluids is complex and difficult to understand due to the intricate interplay between various nanofluid parameters and the interactions between the nanoparticle and base fluid.

There are three main gaps in the current research on nanofluids.

Gap one pertains to the need for a model to predict the best assumption for simulating a particular nanofluid. Different assumptions provide varying levels of accuracy, depending on the nanofluid configuration and flow conditions.

Gap two is related to the accuracy of the single-phase model for simulating single material nanofluids. A temperature-based neural network model needs to be developed as an additional equation to improve the representation of the thermal conductivity and viscosity of the single-material nanofluid in the single-phase model.

Finally, gap three involves the development of a more generalised approach for predicting the thermophysical properties of single material nanofluids through a novel feature selection approach.

1.2 Aims and Objectives

The study aims to provide a comprehensive understanding of nanofluid behaviour based on its features, develop accurate predictive models, and offer practical guidance for the application of nanofluid models in various single-phase simulations in the industry:

1. Explore the accuracy of nanofluid simulations under different conditions such as modelling treatments, Reynolds numbers, particle sizes, volume fractions, and property assumptions (constant vs. temperature-dependent properties) in both laminar and turbulent flow regimes.
2. Enhance the precision of nanofluid models, specifically the single-phase model, by enhancing their representation of the nanofluid's thermal conductivity and viscosity. This is applied to nanofluid flow in heated pipes with circular cross-sections. Additionally, clear instructions and guidelines are provided on how to incorporate these improved models into computational fluid dynamics (CFD) simulations, using software such as COMSOL.
3. Compare different modelling approaches, such as artificial neural networks (ANNs), robust linear regression, and ensembles approaches, to determine the most effective method for predicting nanofluid properties.
4. Develop accurate predictive models using machine learning algorithms to simulate the behaviour and properties of nanofluids specifically the thermal conductivity of nanofluids.

Overall, the work aims to apply machine learning to improve the modelling and simulation of single material nanofluids which helps to push the boundaries of its application in the real world.

1.3 Outline of the thesis

Chapter 1 presents an introduction into nanofluids, what they are and where they are applied. It gives a brief history of nanofluids along with the current research interests in the field. It states the research problems, and the study’s aims and objectives. The outline of the thesis is presented too.

Chapter 2 presents the literature review on nanofluids: the story of nanofluids, their preparation, stability, applications, their model of thermophysical properties, machine learning methods, and machine learning for predicting their thermophysical properties.

Chapter 3 presents the introduction to the published papers included in the thesis and supporting details of three research papers investigating the prediction of the nanofluids modelling accuracy in different flow regimes, the improvement of the single-phase modelling approach and the prediction of the thermophysical property of nanofluids.

Chapter 4 is a paper titled “Predicting the accuracy of nanofluid heat transfer coefficient’s computational fluid dynamics simulations using neural networks” as published in the Wiley Heat Transfer Journal. It contains the application of neural network algorithms to predict the accuracy of nanofluid simulations [12].

Chapter 5 is a paper titled “Single phase nanofluid thermal conductivity and viscosity prediction using neural networks and its application in a heated pipe of circular cross-section” as published in the Wiley Heat Transfer Journal. It contains the improvement of the single-phase simulation by incorporating the accurate nanofluid’s thermophysical properties models in the single-phase simulation governing equation [13].

Chapter 6 is a paper titled “Predictive modelling of thermal conductivity in single material nanofluids: a novel approach”, as published in the Bulletin of the National Research Centre. It contains a novel method of feature selection for the prediction of the thermal conductivity of single material nanofluids [14].

Chapter 7 presents the analysis of key findings, and limitations of the study in which three research papers are discussed each investigating the prediction of the nanofluids modelling accuracy in different flow regimes. The improvement of the single-phase modelling approach and the prediction of the thermophysical property of nanofluids.

Chapter 8 presents the conclusions and outlook of the study. It states the major contributions of the study and the future directions.

Chapters 4 – 6 are self-contained papers [12-14] which have their own numbering systems of sections, figures, tables and references and they do not follow the numbering system of the whole thesis.

Chapter 2 Literature review

In this chapter, the topics discussed include the story of nanofluids, their preparation, stability, applications, their model of thermophysical properties, machine learning methods, and machine learning for predicting their thermophysical properties.

2.1 Nanofluids: the story

Nanotechnology traces its roots back to 1959 when Nobel Prize winner Richard Feynman presented the concept of miniaturising machines. Since then, miniaturisation has become a popular method in modern science and technology [15]. 40 years later, Nobel Prize winner H. Rohrer wrote a concise report on the opportunities and challenges of the Nano Age [15]. The size of the millimetre scale in the 1950s has decreased to the atomic scale of today [16]. Nanofluids have a strong connection to miniaturisation and nanotechnology [15]. The use of nanofluids is a recent approach to improve the thermal conductivity of liquids. The low thermal conductivity of conventional heat transfer fluids (HTFs) limits their various applications [17].

In the 1990s, Choi provided a definition for nanofluids as a type of heat transfer fluid that utilises nanotechnology. These fluids are created by suspending small particles, fibres, or tubes (typically less than 1% volume) with lengths ranging from 1 to 50 nanometres within traditional heat transfer fluids [6]. This definition has changed over the years. Researchers now consider particles up to 150 nm and include hybrids in fluids [18]. Nanofluids have several advantages over traditional fluids, including enhanced thermal properties, greater stability, customisable features, multifunctionality, and environmental benefits [19].

There are three primary categories of nanofluids: simple nanofluids which consist of non-metals, metals, and oxides such as [water]/Al_2O_3, TiO_2, Cu, ZnO, and CuO; hybrid nanofluids which include [water]/Al_2O_3 + Cu; and ionic nanofluids such as [C4mim][NTf2]/Al_2O_3 [20].

In the future, new methods for controlling the properties of nanofluids at a macroscale level by manipulating their microscale physics will be developed. These efforts will focus on understanding the properties of thermal waves and how they interact with heat diffusion. Another area of focus is constructal nanofluids, which do not require a uniform dispersion of nanoparticles in the base fluid. Instead, they have a tree-like configuration and are widely accepted for use in sustainable energy systems at various scales [21].

The next section discusses its constituents and preparation.

2.2 Nanofluid preparation

Nanofluids are created using nanoparticles, stirrers, ultrasonic vibrations, and base fluids. They can be prepared through single-step, two-step, or novel methods. However, agglomeration remains a major challenge during their creation.

Regarding preparation, the different methods used to produce nanofluids, including two-step and one-step processes. Two-step processes involve synthesising nanoparticles separately and then dispersing them in the base fluid, while one-step processes involve simultaneous nanoparticle synthesis and dispersion in the base fluid [22].

The importance of surface modifications is to enhance nanoparticle dispersion and stability in the fluids. Stability is a crucial factor for the practical application of nanofluids. The review examines various techniques to improve nanofluids' stability, such as surfactants, polymers, and ultrasonic treatment. The challenges are associated with long-term stability and the tendency of nanoparticles to agglomerate over time [22].

The main thermophysical properties of nanofluids include thermal conductivity, viscosity, specific heat capacity, and density. Adding nanoparticles influences these properties and hence the importance of understanding their behaviour to optimise the heat transfer performance [22].

Enhancing thermal conductivity is a significant advantage of nanofluids, enabling better heat transfer than conventional fluids. The heat transfer characteristics of nanofluids are explored, focusing on convective heat transfer in different applications. The following nanofluid features: nanoparticle concentration, size, and shape impacts on heat transfer performance. Different mechanisms are involved, such as Brownian motion, thermophoresis, and agglomeration effects, which affect nanofluids' overall heat transfer behaviour [22].

Lastly, the applications of nanofluids across various industries are stated, including electronics cooling, automotive systems, solar energy, and biomedical applications. Each application's potential benefits and challenges highlight the need for further research to optimise nanofluid formulations and their integration into practical systems. The above provides a comprehensive overview of nanofluids, encompassing their preparation methods, stability issues, and effects of nanofluid features on its thermophysical properties, heat transfer characteristics, and potential applications in different fields [22].

A highlight of the importance of a paradigm shift in research methods that focuses on reproducing previous studies to validate their findings. The study emphasises the significance of nanofluids, due to their enhanced thermal properties [23].

These properties make them promising for various engineering applications, such as heat transfer systems and cooling technologies. The researchers highlight the importance of reproducibility in scientific studies, as it ensures the reliability and validity of research findings. They emphasise the need for rigorous experimental protocols and careful documentation to replicate studies successfully [23].

In addition, the authors discuss experimental techniques used to investigate nanofluid behaviour, such as differential scanning calorimetry, thermogravimetric analysis, and viscosity measurement methods. They emphasise the need for standardised experimental protocols to ensure accurate and comparable results across studies [23].

The article underscores the importance of reproducibility, rigorous experimental protocols, and standardised methods in advancing research on nanofluid synthesis, thermal properties, and experimental techniques in engineering [23].

2.2.1 One step preparation method

By using the one step method, the need for processes such as drying, storage, transportation, and dispersion of nanoparticles is eliminated. Stable nanofluids are prepared through the physical vapor deposition technique, which involves direct evaporation and condensation of nanoparticles, effectively reducing their accumulation. However, this method has two major drawbacks: the presence of residual reactants in the nanofluid and its high cost [24].

2.2.2 Two step preparation method

This is an affordable and effective way to create nanofluids on a larger scale. The process involves obtaining nanoparticles through various methods and dispersing them in a fluid. However, one potential issue is that nanoparticles may clump together, so surfactants are often added to prevent instability. There is a need for a more cost-effective and efficient method of preparing nanofluids to improve their scalability [25].

This section focused on the preparation of nanofluids, including the methods used and their limitations. The following section delves into the challenges of nanofluid stability and nanoparticle sedimentation, as well as techniques for assessing and enhancing stability.

2.3 Nanofluid stability issues

The stability of nanofluids depends on the balance between the repulsive force of the electrical double layer and the attractive force of Van der Waals [22]. For the nanofluid to be stable, the repulsive force between the nanoparticles should be stronger than the attractive force between them [22].

Analysing parameters required to properly define nanofluids for heat transfer applications involves examining various factors influencing their thermal properties and performance [26]. Nanofluids are colloidal suspensions of nanoparticles in a base fluid, typically used to enhance heat transfer in various applications [26].

Here is a summary of the key parameters that need to be considered [26]:

Base Fluid: The choice of base fluid is crucial, as it affects the overall thermal conductivity, viscosity, and stability of the nanofluid. Common base fluids include water, ethylene glycol, and oils, each with different properties and application suitability.

Nanoparticles: The selection of nanoparticles plays a significant role in determining the heat transfer characteristics of the nanofluid. Parameters such as material composition, size, shape, and concentration of nanoparticles should be considered. Common nanoparticles include metal oxides (e.g., alumina, titania), carbon nanotubes, and graphene.

Concentration: The concentration of nanoparticles in the nanofluid is an important parameter. Higher concentrations generally increase thermal conductivity but may result in higher viscosity and reduced stability. Optimal nanoparticle concentration depends on the specific application and desired heat transfer enhancement.

Stability: Nanofluid stability is critical to ensure long-term performance. Factors affecting stability include particle agglomeration, sedimentation, and the presence of surfactants or dispersants. Stability is essential to maintain uniform dispersion and prevent clogging or fouling of heat transfer surfaces.

Thermal Conductivity: The thermal conductivity enhancement provided by nanofluids is a key parameter. It depends on the nanoparticles' choice, concentration, and interactions with the base fluid. Experimental measurements and theoretical models predict and optimise thermal conductivity enhancement.

Viscosity: Nanofluids typically exhibit higher viscosity than the base fluid due to the presence of nanoparticles. The viscosity affects pumping power requirements and pressure drop in heat transfer systems. Balancing heat transfer enhancement with manageable viscosity is crucial for practical applications.

Particle Size Distribution: The size distribution of nanoparticles influences the overall behaviour of nanofluids. Narrow particle size distributions can improve stability and prevent particle settling. Particle size also affects Brownian motion, which contributes to enhanced heat transfer.

Surface Functionalization: Surface modification or functionalisation of nanoparticles can enhance their dispersion and stability within the base fluid. It involves attaching chemical groups or surfactants to the nanoparticle surface to improve compatibility with the base fluid and prevent agglomeration.

2.3.1 Evaluation of nanofluid stability

There exist various techniques to assess the stability of nanofluids. One such method is UV visible spectroscopy.

UV visible spectroscopy: which measures the amount of light absorbed by the nanofluid and provides an estimate of the nanoparticle's concentration [27]. However, this method has limitations, as it cannot be used for highly concentrated or dark-coloured nanofluids and can be time-consuming [27].

Zeta potential: Zeta potential is measured to determine the potential difference between nanoparticles and base fluid [28]. A value between 40 and 60 mV indicates good stability, while a value above 60 mV indicates excellent stability [28]. The limit in this method are the lack of attractive force information and the requirement for a dilute sample with zeta potential [29].

Dynamics light scattering (DLS): The Dynamics Light Scattering (DLS) method is used to measure the particle size and concentration of a sample over time [29]. The nanofluid is exposed to light and the fluctuations in the scattered light are measured at specific intervals [29]. The rate of fluctuation over time indicates the diffusion of molecules, or how stable the nanofluid is. It is important to note that a clear, homogeneous, and diluted sample is necessary for accurate measurements [29-33].

Thermophysical properties: Thermophysical properties are varied over time and correlated with stability [34-36]. The accuracy of measuring equipment and motion of nanoparticles are the limitation of this approach [37].

Centrifugation method: The centrifugation method involves using a spread analyser separator (centrifuge) to visually inspect the sedimentation of nanofluid, making it a quick method [38].

Electron microscopy: Electron microscopy methods are used to measure particle size, but only for low particle concentrations using TEM or SEM [39].

Sedimentation photograph capturing method: A cluster of fixed nanoparticles is placed in a glass vial and photographed at equal intervals to observe sedimentation [40]. This is the most straightforward method to estimate stability [25, 40].

3- ω method: This method involves evaluation of the change in thermal conductivity caused by sedimentation [39, 41, 42].

2.3.2 Methods of enhancing stability

The methods for enhancing stability of nanofluids can be divided into physical and chemical methods [43].

Physical methods involve mechanical action, examples are [43]:

1. Ultrasonication
2. Magnetic stirring
3. High shear stirring

Chemical methods involve the addition of chemicals to create a stable fluid, examples are [43]:

1. Addition of surfactants
2. Surface modification techniques
3. pH variation

The next section presents the applications of nanofluids.

2.4 Applications of nanofluids

The hydrothermal performance of different alumina hybrid nanofluid types in a plate heat exchanger has been investigated for their heat transfer capabilities [1]. Alumina hybrid nanofluids consist of alumina nanoparticles with other oxides dispersed in a base fluid, typically deionised water [1]. These nanofluids exhibit enhanced thermal conductivity and convective heat transfer properties compared to their base fluids, making them attractive for various heat transfer applications as shown in Figure 2-1 [1]. In Figure 2-1, the coolant flow rate ranges from 2 to 4 lpm, denoted by notations 2, 2.5, 3, 3.5, and 4 [1]. Several studies have examined the hydrothermal performance of different alumina hybrid nanofluid types in plate heat exchangers [1].

The performance evaluation is typically based on parameters such as heat transfer coefficient, pressure drop, and overall heat transfer rate [44]. The results of these studies indicate that adding alumina nanoparticles to the base fluid improves the heat transfer performance of the nanofluid in a plate heat exchanger [44]. The enhanced thermal conductivity of the nanofluid leads to increased heat transfer rates between the hot and cold fluid streams in the heat exchanger [1].

However, the specific thermal performance of different alumina hybrid nanofluid types can vary depending on nanoparticle concentration, particle size, base fluid properties, and operating conditions [44]. It is important to note that the optimal performance of alumina hybrid nanofluids in plate heat exchangers may require careful optimisation and consideration of these parameters [1].

Overall, alumina hybrid nanofluids have shown promising thermal performance in plate heat exchangers, offering improved heat transfer rates compared to traditional heat transfer fluids [44]. Further research and experimentation are necessary to explore and optimise the specific characteristics and operating conditions for different alumina hybrid nanofluid types in plate heat exchanger applications [1].

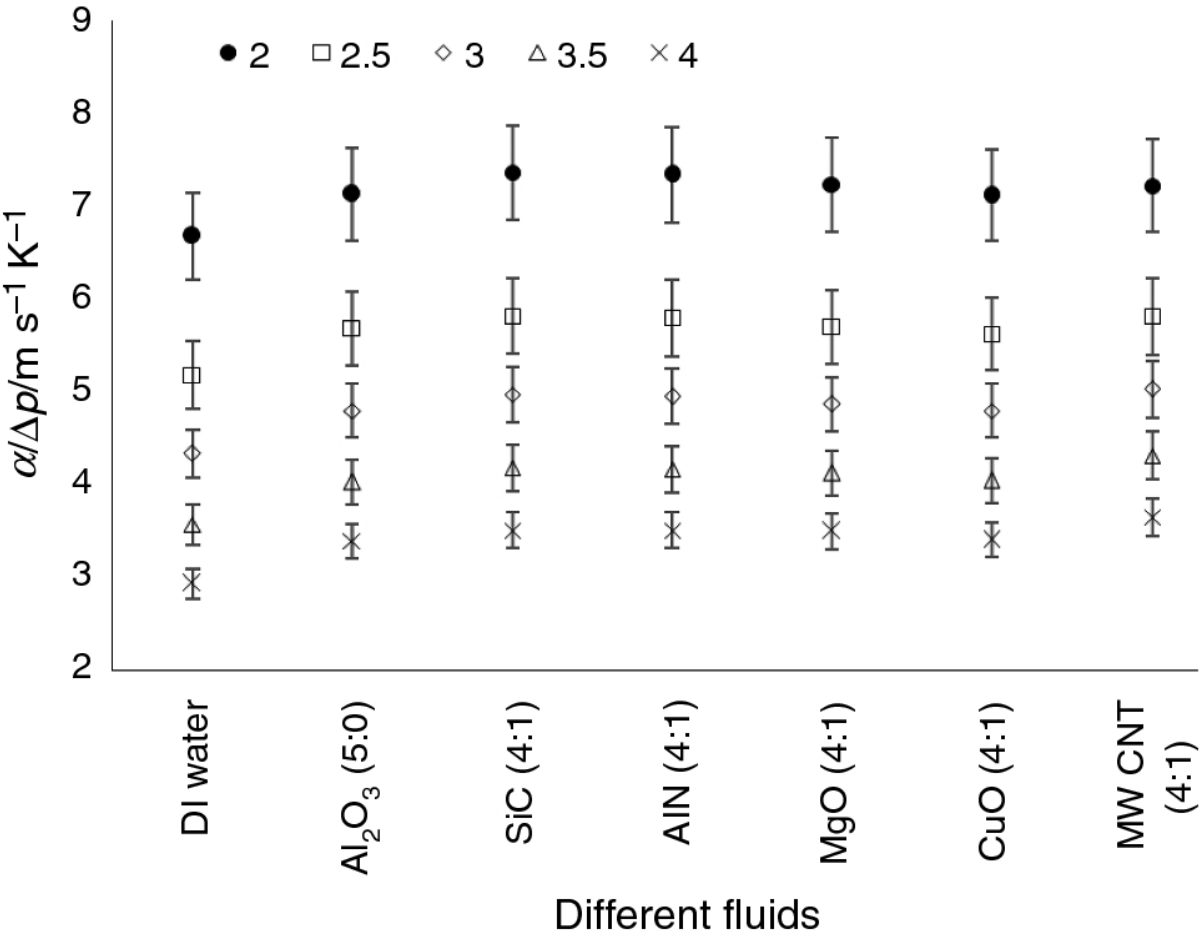

Figure 2-1 Variation of heat transfer coefficient to pressure drop ratio with flow rate where the representation of the hybrid nanofluid as a nanoparticle (x:y), where x is the volume of Al_2O_3 and y is the volume of another nanoparticle [1]. Reprinted with permission.

An investigation of the effect of zirconium oxide nanofluid on the behaviour of a photovoltaic-thermal (PVT) system was carried out [44]. The study aimed to determine the impact of incorporating zirconium oxide nanofluid into the system on its performance [44]. A PVT system combines photovoltaic and thermal technologies to generate both electricity and heat from solar energy [44].

The addition of nanofluids, which are colloidal suspensions of nanoparticles in a base fluid, has been explored to enhance the efficiency of PVT systems [44]. The experimental study involved the preparation of zirconium oxide nanofluid and its integration into a PVT system [44]. The nanofluid was circulated through a heat exchanger, facilitating heat transfer between the photovoltaic module and the fluid [44]. Various parameters were monitored and measured to evaluate the system's performance [44].

The results of the study indicated several significant findings [44]. Firstly, incorporating zirconium oxide nanofluid reduced the temperature of the photovoltaic module, thereby improving its electrical efficiency [44]. The nanofluid enhanced the heat transfer characteristics of the system, resulting in better cooling of the module and reduced temperature-related losses [44].

Secondly, using zirconium oxide nanofluid increased the overall thermal efficiency of the PVT system [44]. The nanofluid facilitated improved heat dissipation and thermal conductivity, leading to enhanced thermal energy extraction from the system [44]. Furthermore, the experimental study revealed that the addition of zirconium oxide nanofluid positively influenced the electrical output of the photovoltaic module [44]. The reduced operating temperature of the module resulted in reduced electrical losses and improved power generation efficiency [44].

Overall, the findings of the experimental study demonstrated that incorporating zirconium oxide nanofluid in a PVT system can significantly enhance its performance [44]. The nanofluid improved the cooling and thermal characteristics of the system, leading to increased electrical and thermal efficiency [44]. These results suggest that zirconium oxide nanofluid holds promise as a potential technology for enhancing the performance of photovoltaic-thermal systems [44].

Investigation of the impact of temperature on the electrical and thermal behaviour of a photovoltaic/thermal (PV/T) system, which is cooled using silicon carbide (SiC) nanofluid [45]. The experimental study compares the performance of the PV/T system under different temperature conditions [45]. Using SiC nanofluid as a coolant in the PV/T system aims to enhance its overall efficiency by improving both the electrical and thermal aspects [45].

The researchers measure various parameters to evaluate the system's performance, including electrical efficiency, thermal efficiency, heat transfer coefficient, and overall system efficiency [45]. The findings reveal that temperature significantly influences the electrical and thermal behaviour of the PV/T system [45].

The system's electrical efficiency decreases as the temperature increases due to increased resistive losses [45]. This decrease in electrical efficiency is attributed to the increase in temperature-dependent resistances within the PV cells [45]. However, the thermal efficiency of the system improves as the temperature rises [45]. The SiC nanofluid coolant effectively enhances the heat transfer coefficient, improving thermal performance [45]. The nanofluid facilitates better heat dissipation, thus reducing the temperature of the PV cells and maintaining their efficiency [45].

Comparing the experimental results under different temperature conditions, it is observed that the overall efficiency of the PV/T system is optimised at a specific temperature range [45]. This indicates an optimal temperature at maximisation of the system's combined electrical and thermal performance [45].

The study demonstrates that temperature plays a crucial role in the electrical and thermal behaviour of a PV/T system cooled using SiC nanofluid [45]. While higher temperatures negatively affect the electrical efficiency, they positively impact the thermal efficiency [45]. Using SiC nanofluid as a coolant helps maintain the PV cells' efficiency by effectively dissipating heat, improving overall system efficiency [45].

Investigations have been conducted to explore the thermal properties of CeO_2/water nanofluids in the context of heat transfer applications [2]. CeO_2, also known as cerium oxide or ceria, is a promising nanomaterial due to its unique properties, including high thermal stability and excellent thermal conductivity [2].

When dispersed in water, CeO_2 nanoparticles form nanofluids, which exhibit enhanced heat transfer characteristics compared to conventional fluids [2]. Several studies have focused on determining the thermal conductivity of CeO_2/water nanofluids [2].

Experimental measurements have shown that the addition of CeO_2 nanoparticles increases the thermal conductivity of water significantly [2]. The enhancement in thermal conductivity is attributed to the interfacial layers [2]. The exact enhancement levels vary with nanoparticle concentration and other features, as Figure 2-2 shows [2]. In Figure 2-2, ϕ represents the volume fraction in percentage of the CeO_2/water nanofluids [2].

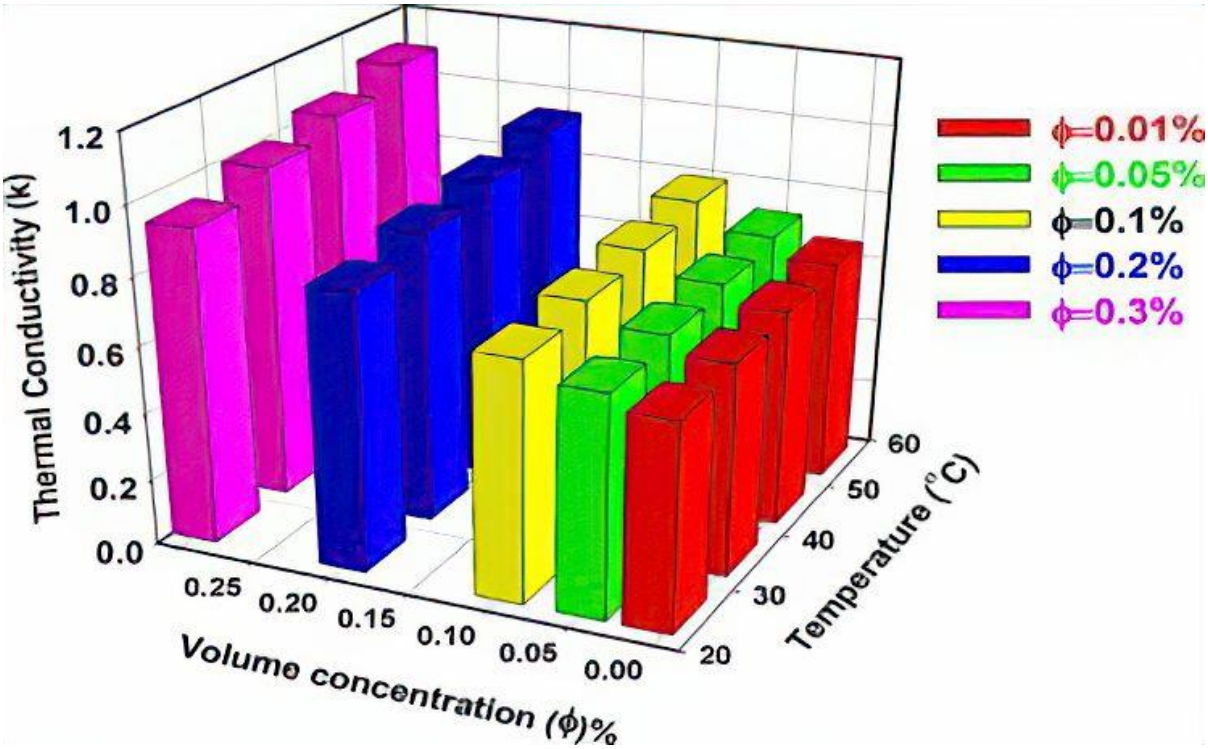

Figure 2-2 Thermal conductivity of nanofluid with temperature rise [2]. Reprinted with permission.

The study "Nanofluid Structural Forces Alter Solid Wetting, Enhancing Oil Recovery" investigates the effects of nanofluid structural forces on solid wetting and their potential to improve oil recovery processes [46]. The research focuses on utilising nanofluids, suspensions of nanoparticles in a base fluid, to modify the wetting behaviour of solid surfaces in oil reservoirs [46]. By introducing nanofluids into the reservoir, the researchers observed that the nanoparticles exerted structural forces on the solid surfaces, altering their wetting characteristics [46].

The nanofluid-induced forces led to enhanced spreading and improved contact between the oil and the reservoir rock, facilitating the displacement and recovery of oil [46]. The study highlights the importance of the interplay between nanofluid properties, such as particle concentration, size, and surface chemistry, and their influence on solid wetting [46]. Understanding these factors is crucial for designing optimised nanofluid formulations that can effectively modify the wetting behaviour and improve oil recovery efficiency [46].

The findings suggest that nanofluids can enhance oil recovery processes by altering the wetting properties of solid surfaces in reservoirs [46]. Further research and development in this field could lead to applying nanofluids as a promising strategy for improving oil extraction and reducing energy costs in the petroleum industry [46].

Recent advances in using nanofluids in renewable energy systems have shown promising potential for enhancing their efficiency and performance [3]. Nanofluids combine nanoparticles dispersed in a base fluid, such as water or oil [3]. Adding nanoparticles to these fluids can significantly alter their thermal, electrical, and optical properties, making them suitable for various renewable energy applications [3].

In solar energy systems, nanofluids have been explored to improve the absorption and conversion of sunlight into electricity or heat [3]. Nanoparticles with high solar absorptivity can be added to solar cells or solar thermal collectors to enhance their efficiency by increasing light absorption [3]. Additionally, nanofluids can be used as heat transfer fluids in concentrated solar power plants, improving heat transfer rates and overall system performance [3].

Similarly, nanofluids have shown potential in wind energy systems [3]. By incorporating nanoparticles into the lubricating oils of wind turbines, their friction and wear characteristics can be improved, leading to reduced maintenance and enhanced energy output [3]. Nanofluids can also be utilised in energy storage systems, such as advanced batteries, to enhance heat dissipation and efficiency [3].

However, the uptake of nanofluids in renewable energy systems also raises environmental implications that need careful consideration [3]. One of the primary concerns is the potential release of nanoparticles into the environment during the manufacturing, usage, or disposal stages [3]. Nanoparticles may adversely affect ecosystems and human health if they accumulate in the environment [3]. Therefore, it is crucial to assess the lifecycle environmental impact of nanofluid technologies and implement appropriate safety measures to prevent nanoparticle release, as shown in Figure 2-3 [3].

Furthermore, the production of nanoparticles and their incorporation into nanofluids require additional energy and resources, which may offset the benefits gained in renewable energy systems [3]. The environmental footprint of nanoparticle synthesis processes and the potential for increased energy consumption during nanofluid production should be evaluated to ensure the overall sustainability of the technology [3]. To mitigate the environmental implications, ongoing research focuses on developing eco-friendly nanoparticles and optimising nanofluid formulations to minimise their potential harm [3].

Additionally, efforts are underway to investigate the fate and transport of nanoparticles in the environment to understand their long-term effects better [3]. In

summary, recent advances in using nanofluids in renewable energy systems have demonstrated their potential for improving efficiency and performance [3]. However, the environmental implications of using nanofluids must be carefully assessed and mitigated through sustainable practices and further research [3].

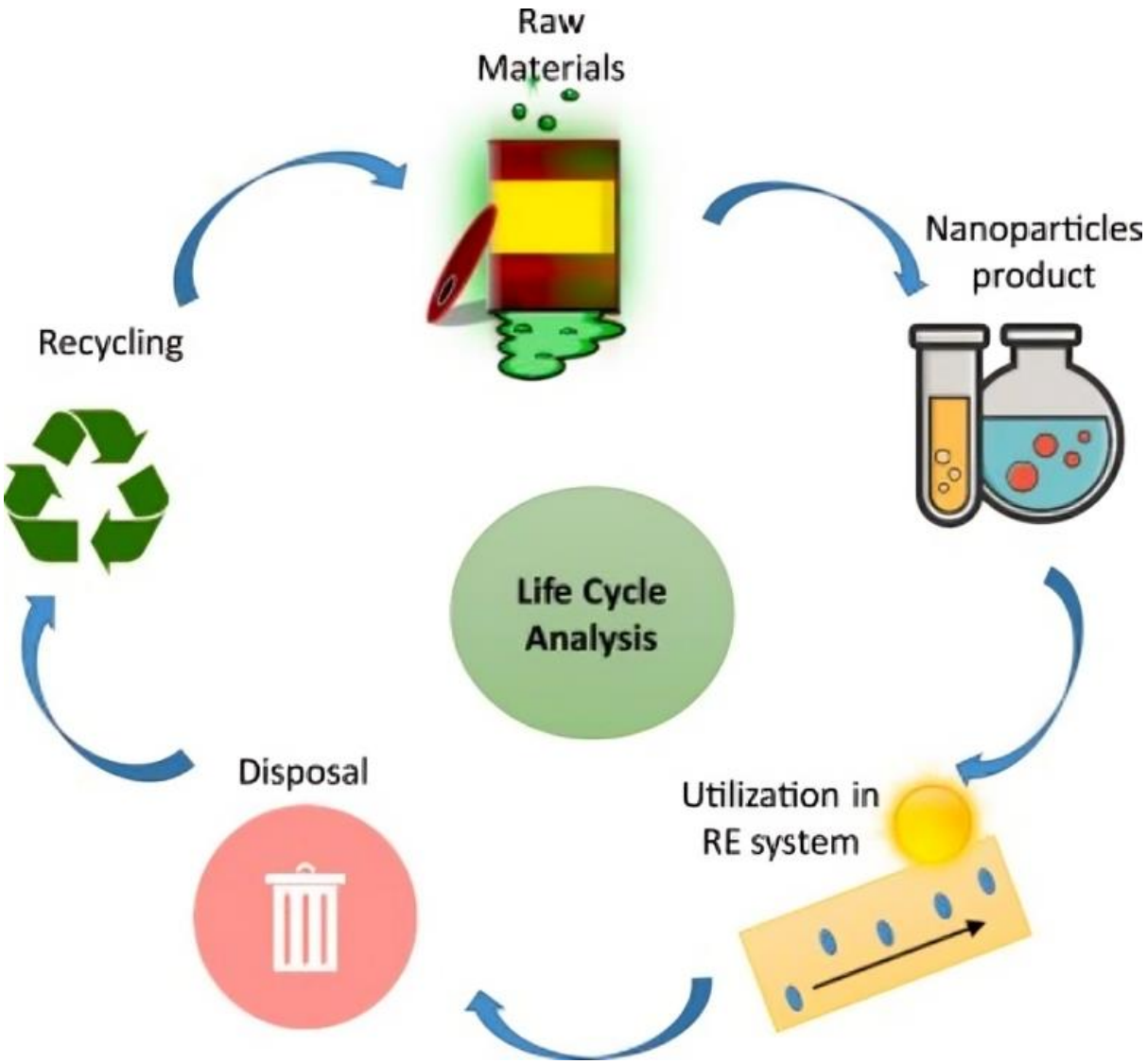

Figure 2-3 Life cycle analysis of nanofluids used in a renewable energy system [3]. Reprinted with permission.

Geometrical effects, when combined with nanofluid, have significantly enhanced heat transfer in heat exchangers. When nanofluids are used in heat exchangers, their unique properties interact with the system's geometry, resulting in improved heat transfer performance [47].

One geometrical effect that enhances heat transfer is using extended surfaces, such as fins or ribs, in the heat exchanger design [47]. These surfaces increase the contact area between the nanofluid and the surrounding fluid, facilitating more efficient heat transfer [47]. The addition of nanofluids further enhances this effect by improving the thermal conductivity of the base fluid, allowing for better heat transfer across the extended surfaces [47].

Additionally, the geometry of the heat exchanger itself can be optimised to promote turbulent flow, which enhances convective heat transfer [47]. Introducing nanofluids into the system can further augment this effect by increasing the fluid viscosity and promoting turbulence, leading to enhanced heat transfer rates [47].

Moreover, nanofluids with specific geometrical configurations, such as microchannels or porous media, can further enhance heat transfer [47]. These structures provide increased surface area and promote better mixing of the nanofluid, resulting in improved heat transfer performance [47].

This section explored the wide-ranging applications of nanofluids, showcasing their potential in different domains. The next section presents models of nanofluid thermophysical properties.

2.5 Models of nanofluid properties

Nanofluids have thermal properties that affect their behavior in various flow scenarios [22]. Finding an accurate model for these properties has been a long-standing challenge, with theoretical, experimental, and empirical models being explored [22, 31, 48]. The thermophysical properties in question are density, viscosity, thermal conductivity, and specific heat capacity.

2.5.1 Thermal conductivity

The property that indicates a material's capacity to transmit heat is known as thermal conductivity [49]. It is measured in Watts per meter per Kelvin. The modification of Maxwell's equation was focused particularly on the form, distribution of particles, particulate shell structure, and volume concentration [50]. Hamilton improved the Maxwell model by considering the volume fraction, conductivity of the base fluid and nanoparticles, and particle shape [51]. The theoretical and experimental models are presented for each thermophysical property. The theoretical models are based on the physics of nanofluids, while the experimental models rely on experimental results.

Theoretically based models

Maxwell [52], Equation 1.

$$k_{nf} = \frac{k_p+2k_f+2\phi(k_p-k_f)}{k_p+2k_f-\phi(k_p-k_f)} k_f \quad (1)$$

This correlation is only useful for small-concentration spherical particles ($\phi \ll 1$)

Ahmed [50], Equation 2.

$$k_{nf} = \frac{k_p+2k_f-2\phi(k_p-k_f)}{k_p+2k_f+\phi(k_p-k_f)} k_f \quad (2)$$

Dogonchi and Ganji [53], Equation 3.

$$k_{nf} = \frac{k_p+2k_f-2\phi(k_p-k_f)}{k_p+2k_f+2\phi(k_p-k_f)} k_f \quad (3)$$

Experimentally based correlations

Relations were established using results from an experiment on the thermal conductivity of Al_2O_3-water and Al_2O_3-EG nanofluids. The correlations were good for a nanoparticle size of 28 nm [54].

Maiga [54], Equations 4 and 5.

Al_2O_3/water:

$$k_{nf} = (4.97\phi^2 + 2.72\phi + 1)k_f \quad (4)$$

Al_2O_3/ethylene glycol:

$$k_{nf} = (28.905\phi^2 + 2.8273\phi + 1)k_f \quad (5)$$

Khanafer, Vafai [55] suggested Equation 6, a method for determining the thermal conductivity of Al_2O_3-water and CuO-water nanofluids, suitable for nanoparticles around 13 nm and 80 nm in size, with volume fractions of about 15%.

$$\frac{k_{nf}}{k_f} = 1 + 1.0112\phi + 2.4375\phi\left(\frac{47}{d_p(nm)}\right) - 0.0248\phi_p\left(\frac{k_p}{0.613}\right) \quad (6)$$

Corcione [56], Model was for nanoparticles with sizes ranging from 10 to 150 nm, and volume concentrations between 0.2% and 9% at temperatures around 294 to 324 K. This correlation takes into account Brownian motion and is represented by the following Equations 7 and 8:

$$\frac{k_{nf}}{k_f} = 1 + 4.4{Re_p}^{0.4}{Pr_f}^{0.66}\left(\frac{T}{T_{freeze}}\right)^{10}\left(\frac{k_p}{k_f}\right)^{0.03}\phi^{0.66} \quad (7)$$

$$Re_p = \frac{2\rho_f\kappa_B T}{\pi\,{\mu_f}^2 d_p} \quad (8)$$

Rudyak and Minakov [57], stated in their paper that theoretical models are unable to predict thermal conductivity. Their equation (Equation 9) had an error of 3% and is given by:

$$k_{nf} = k_f \left[1 + \left[0.0193 + 0.00383 \left(\frac{\rho_p}{\rho_f}\right)\right] \sqrt{\phi \frac{d_p}{d_f}}\right] \quad 9$$

d_f is the carrier fluid molecule's effective size.

2.5.2 Viscosity

Many researchers have investigated the viscosity of nanofluid [58-67]. The viscosity of a nanofluid is the nanofluid's resistance to flow. Viscosity refers to the fluid's resistance to flow. Viscosity is typically measured in Pascal-seconds (Pa*s) or N.s/m^2. Fluids can be broadly classified as Newtonian or non-Newtonian based on whether the shear stress is linearly related to the shear rate.

Theoretically based models

Brinkman introduced a model (Equation 10) for spherical particles, which is valid for particle volume fractions of up to 4% [68].

$$\mu_{nf} = \frac{\mu_f}{(1-\phi)^{2.5}} \quad 10$$

A model (Equation 11) based on the theory of particulate mixture kinetics was introduced by Einstein for volume concentrations less than or equal to 1% [69]:

$$\mu_{nf} = \mu_f(1 + 2.5\phi) \quad 11$$

Krieger and Dougherty [70] suggested a model (Equation 12) for single material nanofluids in which the equation is applicable for a wider range of nanoparticle concentration.

$$\mu_{nf} = \mu_f \left(1 - \frac{\phi}{\phi_m}\right)^{-[\mu]\phi_m} \quad 12$$

Where $[\mu]$ for hard spheres = 2.5 and ϕ_m is the maximum packing fraction of 0.605.

Experimentally based correlations

Singh, Anoop [71] applied experimental data modelling to improve Einstein's model as Equation 13.

$$\mu_{nf} = \mu_f(1 + 10\phi) \quad 13$$

Maiga, Palm [54] also presented models for specific nanofluids: Al_2O_3-water, and Al_2O_3-EG nanofluids, in Equations 14 and 15.

$$\mu_{nf} = (123\phi^2 + 7.3\phi + 1)\mu_f \quad 14$$

$$\mu_{nf} = (306\phi^2 - 0.19\phi + 1)\mu_f \quad 15$$

Corcione [56] suggetsed a model for viscosity which is given thus in Equations 16 and 17:

$$\mu_{nf} = \mu_f \left[\frac{1}{1-34.87\left(\frac{d_p}{d_f}\right)^{-0.3} \phi^{1.03}} \right] \quad 16$$

Where $d_f = \left[\frac{6M}{N\,\pi\,\rho_{f,0}}\right]^{1/3}$ 17

N is Avogadro's number and $\rho_{f,0}$ is the density of the base fluid at 293 K. There is a strong correlation with experimental data for nanoparticle sizes ranging from 25 to 200 nm, concentrations ranging from 0.01% to 7.1%, and temperatures ranging from 293 K to 333 K.

2.5.3 Density

Density is the mass-to-volume ratio of a substance and is expressed in kg/m^3 units [72]. In Equation 18 the effective mixture density is given.

$$\rho_{nf} = (1-\phi)\rho_f + \phi\rho_p \quad 18$$

2.5.4 Specific heat capacity

Specific heat capacity is the amount of heat necessary to raise the temperature of one kilogram (kg) of a nanofluid by 1 Kelvin. It unit is Joules per kilogram per degree Kelvin (J/kgK).

Nanofluids' specific heat capacity is calculated using the formula (Equation 20 or 21) by [73]:

$$\rho_{nf}Cp_{nf} = (1-\phi)(Cp_f\rho_f) + \phi(Cp_p\rho_p) \quad 20$$

The specific heat capacity of any nanofluids can be determined using Equation 21 if the density of the nanoparticles is similar to the base fluid.

$$Cp_{nf} = (1-\phi)Cp_f + \phi Cp_p \quad 21$$

2.5.5 Thermal expansion coefficient

The coefficient of volumetric thermal expansion for nanofluids measures the change in volume per 1 degree Kelvin increase in temperature, and its unit is 1/K. This coefficient is important for both mixed and natural convection problems. It is calculated using Equation 22-23 [73]:

$$\rho_{nf}\beta_{nf} = (1-\phi)(\beta_f\rho_f) + \phi(\beta_p\rho_p) \quad 22$$

Similarly, the thermal expansion coefficient of a nanofluid can be determined using the Equation 23 if the density of the nanoparticles is similar to the base fluid:

$$\beta_{nf} = (1 - \phi)\beta_f + \phi\beta_p \quad (23)$$

This section presented nanofluid thermophysical property models in both theoretically based and experimentally based models. The next section presents machine learning and its models.

2.6 Machine learning methods

Machine learning has been around for a long time and has been widely used in various applications, such as Optical Character Recognition (OCR) and spam filters in the 1990s [74]. Since then, it has been integrated into numerous products and features, providing better recommendations and enabling voice search. Machine learning is the practice of programming computers so that they can learn from data [74]. Arthur Samuel defined it in 1959 as "the field of study that gives computers the ability to learn without being explicitly programmed [75]." The examples used for learning in the system are referred to as the training set, while each example is called the training instance or sample [74]. Machine learning is most suitable for problems that require a lot of tuning or rules, as well as for solving complex problems with no clear solution [74]. It is also well-suited for environments with constantly changing data. Machine learning can be utilized to gain insights into large-scale problems [74].

There are different Machine learning types [74]:

1. Trained with or without human supervision: Supervised, Unsupervised, Semi-supervised, Reinforcement Learning.
2. Learn “on the fly”: Online learning or Batch learning.
3. Learn by comparing new data to known data points or detect patterns in the training data and build a predictive model: instance-based or model-based learning.

2.6.1 Machine learning algorithms

Machine learning methods are those algorithms that are programmed to learn from data in a particular fashion. They range from artificial neural networks (ANN) to linear regressions and decision trees. Below are some examples of these methods.

Artificial neural networks (ANN)

The artificial neural network is designed based on the biological neural network. It consists of an interconnection of nodes (neurons) [76]. There are three critical parts in every neural network: the character of the node, topology of the network, and rules of learning [76]. The character of the nodes controls how the signal is handled at the node, including the number of inputs and outputs, the weight, and the activation function [76]. The topology of the network determines the organization and connection of the nodes. The rules of learning are concerned with weight initialization and adjustment [76].

Decision trees

The decision tree algorithm is a machine learning algorithm that makes predictions based on roots and leaves [77]. It consists of nodes for decision, branches, and leaves. The tree is structured inverted, going from roots to leaves, with the roots at the top and the leaves at the bottom, containing information about the outcome of the category [77]. The roots hold the mixed category or the initial dataset [77]. The tree then grows to the first node where a split is made into categories based on a feature variable [77]. A parent population can be split into many patterns; hence, the one with the most purity is desired [77].

Linear regression

The linear regression is a straightforward machine learning algorithm used to predict the response from a single feature variable [78]. It assumes a linear relationship between the predictor variable and the response/target variable [78].

Support vector machines

The support vector machine (SVM) is a non-probabilistic two-class linear classifier [79]. It separates the dataset using a decision boundary called the hyperplane [79]. This separation is done by solving a constrained quadratic optimization that is based on a structural risk minimization [79].

Random forest

The random forest algorithm is an ensemble method that utilises regression trees [80]. In this algorithm, the regression trees are trained independently using bootstrapped data, and the predictions are generated by averaging the output of the trees [80].

K nearest neighbour

The K Nearest Neighbors (kNN) algorithm is a case-based machine learning method that uses all the training data for classification [81]. To improve its accuracy,

representatives need to be utilized to represent the entire training data for classification [81]. This involves building an inductive learning model from the training dataset and using it (the representatives) for classification [81]. One way to evaluate the algorithm is through its performance. Although K Nearest Neighbors (kNN) is a simple method, it is quite effective in classification, especially in text categorization [81].

In this section machine learning and its models have been presented. The next section presents machine learning prediction of nanofluid thermophysical properties.

2.7 Machine learning for predicting thermophysical properties of nanofluids

Machine learning has been used to predict various thermal and flow characteristics of nanofluids, including thermal conductivity, viscosity, and heat transfer coefficients. A variety of studies have been presented.

2.7.1 Machine learning prediction for the thermal conductivity of nanofluids

In an experiment, nanoparticles were added to mineral oil, and an increase in the thermal conductivity of the resulting nanofluid was observed [82]. In the study, both non-linear regression and an adaptive neuro-fuzzy inference system (ANFIS) were tested [82]. The results indicated that the ANFIS model aligned very well with the experimental data and the non-linear regression model [82]. Specifically, the root mean squared error for the ANFIS model was lower for silver, copper, and titanium oxide compared to the multi-walled carbon nanotube (MWCNT) and diamond–mineral oil nanofluids [82]. The ANFIS model utilized two input variables: concentration and particle type. It was designed to simultaneously determine the viscosity and thermal conductivity of the nanofluid in question [82]. These results suggested the potential for improved thermal characteristics in various nanofluid applications, including the cooling of electronic systems [82].

The thermal conductivity of Al_2O_3 water nanofluids was predicted using machine learning in a study [83]. Three machine learning algorithms, namely Artificial Neural Network (ANN), Self-organizing map, and least square support vector machine (LSSVM) algorithms, were tested [83]. The possible inputs, such as temperature,

particle size, and concentration, were compared to determine their significance [83]. The results showed an increase in the thermal conductivity ratio with higher temperature and concentration [83]. The best results were obtained from the Genetically optimized Least square Support Vector Machine [83]. The other two methods, Self Organizing Maps and Artificial Neural Networks, demonstrated similar correlation coefficients of 0.88125 and 0.87575, respectively [83].

A database for nanofluids' thermophysical properties was introduced in a study [48]. The database was built using MATLAB and was divided into two parts [48]. The first part utilized Gaussian regression, which drew information from experimental data collected from various literature sources [48]. The Gaussian regression model used kernel functions commonly used in the analysis of nanofluid thermophysical properties [48]. The second part of the database employed a neural network, specifically designed for efficiency [48]. This neural network was trained using data from the database, as well as additional data points from the outputs of the Gaussian regression model [48]. It was claimed in the study that this nanofluid database filled a gap in the existing literature and provided thermodynamically consistent results, with minimal discrepancies due to computational precision challenges [48]. The accuracy of the NanoFEx was reported to be over 93% in forecasting important thermophysical properties [48].

The friction factor and heat transfer characteristics of glycerol-based and ethylene glycol silicon dioxide nanofluids flowing through a circular tube with constant heat flux applied to the tube wall was investigated [84]. The goal was to address the challenge of balancing heat transfer and pressure drop [84]. This has applications in the automotive industry, electronics cooling, and renewable energy systems [84]. A range of Reynolds numbers from 1300 to 21,000 was tested, with nanoparticle volume concentrations of up to 1.0% [84]. It was found that the nanofluids exhibited higher heat transfer coefficients and lower friction factors compared to the base fluids [84]. The nanofluid showed the highest enhancement in heat transfer of 8.3% and 5.4% for ethylene glycol-based and glycerol silicon dioxide nanofluid, with relative friction factor penalties of approximately 75% and 30%, respectively [84]. Five machine learning algorithms were employed to model the non-linear data: random forest, decision tree, linear regression, extreme gradient boosting, and adaptive boosting [84]. It was revealed that extreme gradient boosting (mean squared error of 0.045 for the test set) and random forest (mean squared error of 0.069 for the test set) were the most effective algorithms for the problem [84]. The findings suggest that machine learning algorithms can accurately predict the thermal characteristics of nanofluids, making them a reliable method for enhancing the application of nanofluids in various heat and flow systems [84].

The thermal conductivity of the nanofluid was predicted using a combination of molecular modeling and machine learning algorithms to analyze iron oxide CO_2 nanofluids [85]. The predictions of machine learning models were compared against the predicted thermal conductivity [85]. Decision trees, K-nearest neighbors, and linear regression machine learning algorithms were applied, using particle size, volume concentrations, and temperature as inputs [85]. It was found that the decision trees were the most accurate model, achieving a 99% success rate [85].

2.7.2 Machine learning prediction for the viscosity of nanofluids

The dynamic viscosity of nanofluids (Al_2O_3, TiO_2, ZnO water nanofluids) was studied, as this property is important for heat transfer and pressure loss calculations [86]. Nanofluids, which are known to be effective heat transfer fluids, had their dynamic viscosity experimentally measured across various volume concentrations (0.1–1.0%) and temperatures (20–50 ^oC) [86]. A multi-layer perceptron artificial neural network (ANN) was developed to predict the dynamic viscosity of the nanofluids [86]. The genetic algorithm (GA) was used to optimize the dynamic viscosity, and it was found to be more computationally intensive but more accurate [86]. It was concluded that a trade-off between computation resources and accuracy needs to be considered for both models [86]. Ultimately, the results suggested that the dynamic viscosity of nanofluids can be predicted using the artificial neural network (ANN) model, which is more efficient than traditional theoretical and experimental methods [86].

The viscosity of non-Newtonian nanofluids with a water/ethylene-glycol (EG) base was predicted using four different nanofluids: MWCNT-alumina/water-EG, Fe_3O_4-Ag/EG, MWCNT-SiO_2/EG-water, and Fe_3O_4-Ag/water-EG [87]. These nanofluids were employed as input data for an artificial neural network (ANN), which took temperatures, particle concentrations, and shear rates as inputs and predicted viscosity as the output [87]. The performance of the ANN was compared with three correlations using evaluation metrics such as coefficient of determination, average absolute deviation, and sum of squared error [87]. The ANN was found to outperform the correlations, achieving a coefficient of determination of 0.99, while the best correlation achieved 0.98, which was only 0.01 lower than the ANN [87].

The viscosity of nanofluids was predicted by comparing different machine learning algorithms [88]. It was found that the models were generally aimed at analyzing the rheological behavior with respect to various factors, conducting spatial-temporal analysis, correlating flow curves, and applying soft sensors [88]. It was also noted that models designed for one type of fluid can be adapted for use with other fluids, particularly in terms of rheological behavior and flow curve correlations [88]. It was observed that artificial neural networks and support vector machines are typically

suitable for low variability and small datasets [88]. For more complex problems involving a large number of variables and larger datasets, hybrid approaches that combine metaheuristic optimization and machine learning are recommended [88]. A reproducibility checklist was proposed to ensure consistent results for future research. Overall, valuable guidance for using machine learning to predict nanofluid viscosity was provided by the report [88].

The response surface methodology was applied to predict the dynamic viscosity of a hybrid nanofluid [89]. The hybrid nanofluid consisted of CuO nanoparticles in 80% ethylene glycol (EG) and 20% water [89]. A range of temperature values (15 – 50 ^{o}C), volume concentrations of 0.05 – 1%, and shear rates of 26.6 to 933.1 s^{-1} were tested [89]. Models including cubic, quadratic, quartic, and 2FI were studied, and their performance was compared using metrics such as coefficient of determination, correlation deviation, reliability, standard deviation, and P-values [89]. The quartic model was determined to be the best and was used to improve the nanofluid's viscosity [89]. An optimization study was carried out to minimize both the inputs and outputs [89]. The minimum values selected were T = 25.303 ^{o}C, SVF = 0.05%, SR = 26.660 s^{-1}, and the minimum nanofluid viscosity value was 8.565 mPa.s [89].

The impact of temperature and nanoparticle volume concentrations on the viscosity of silica-alumina-MWCNT/water hybrid nanofluid was examined in a study [90]. A non-linear model was developed using MATLAB, with temperature (ranging from 20 to 60 ^{o}C) and nanoparticle volume concentration (ranging from 0.1 to 0.5%) as inputs [90]. It was found that as the volume concentration of nanoparticles increased, the viscosity of the nanofluid also increased. Conversely, as the temperature increased, the viscosity decreased [90]. For instance, at a temperature of 40 ^{o}C, the viscosity of the nanofluid rose from 1.55 to 3.26 cP as the volume concentration increased from 0.1 to 0.5% [90]. However, at a volume concentration of 0.3%, the viscosity of the nanofluid decreased from 3.3 to 1.73 cP as the temperature increased from 20 to 60 ^{o}C [90]. Additionally, it was revealed that the viscosity of the nanofluid showed greater variation at lower temperatures and higher volume concentrations of nanoparticles [90].

2.8 Summary

In this chapter, the review involved discussions about nanofluids, what they are and examples, who started using them first. Then it talks about their preparations – the one – step and two – step methods of preparation. The issues of nanofluid stability were discussed and the different fixes for these issues were explained. Then the applications of nanofluids were discussed from which the need for a model for

predicting which assumption would be best for the simulation of a particular nanofluid since different assumptions give different accuracy for different nanofluid configurations and flow conditions was identified [91-97].

The prediction of nanofluid properties was discussed which led to the need for increasing the accuracy of the single-phase model in simulating single-material nanofluids by developing a temperature-based neural network model as an additional equation to accurately represent the thermal conductivity and viscosity of the single material nanofluid in the single-phase model and a more generalised approach for predicting the thermophysical properties of single-material nanofluids [98-106].

A highlight of the various ways nanofluids can enhance our daily lives was presented and emphasis on relatively new technologies and applications were given. An overview of nanofluids' models was discussed ranging from theoretical, experimental and machine learning models were included [87-90].

The previous machine learning work discussed in 2.7 applies only to direct prediction of the nanofluid properties, not an evaluation of the accuracy or effectiveness of the models presented in 2.5. The literature on nanofluids reveals many gaps and challenges that need to be addressed. Researchers have extensively reviewed nanofluids, including their various nanoparticles, preparation methods, and the impact of these methods on their properties. Additionally, the properties of nanofluids have been explored, and several applications have been highlighted. Theoretical and empirical models for the thermophysical properties of nanofluids have been presented. But there is still the need to accurately model nanofluids and machine learning has shown such promise. In this work, machine learning is applied to accurately model nanofluids thermal and flow characteristics.

Chapter 3 Introduction to the published papers included in the thesis and supporting details

3.1 Introduction

The existing literature on nanofluids reveals several gaps and challenges that need to be addressed. Researchers have extensively reviewed nanofluids, including their various nanoparticles, preparation methods, and the impact of these methods on their properties. Additionally, the properties of nanofluids have been explored, and several applications have been highlighted. Theoretical and empirical models for the thermophysical properties of nanofluids have been presented.

However, due to the abundance of research outputs, there is a lack of consensus on the most suitable simulation treatment for nanofluids. Some researchers argue that single-phase modelling is sufficient, while others propose two-phase simulation. Within the two-phase modelling group, there are differing views on the most accurate models. To address this issue, the current study aims to utilise artificial intelligence and develop an algorithm that can provide an answer. By considering a wide range of nanofluid modelling scenarios, the study analyses numerous nanofluid setups and literature results. Over 200 neural networks were tested, and the best neural network underwent 100 runs to ensure the reliability of its performance [12].

From the analysis of different nanofluid simulation models the single phase model was found to be the model with the least accuracy. Hence this study also improves the single-phase modelling treatment by enhancing the prediction of thermophysical properties. This method is exemplified through its application in COMSOL. Additionally, the study develops a novel feature selection algorithm and applies it to create a machine-learning model of the thermal conductivity of nanofluids [13] and it accurately predicts the thermal conductivity of nanofluids.

In conclusion, the literature on nanofluids reveals gaps regarding simulation treatments, consensus on modelling methods, and the need for improved predictions of thermophysical properties. The current study addresses these gaps by utilising machine learning, developing novel feature selection algorithms, and providing numerical evidence. These contributions improve the simulation and modelling of nanofluids using machine learning.

3.2 Predicting the accuracy of nanofluid heat transfer coefficient's computational fluid dynamics simulations using neural networks [12]

Chapter 4 discusses the development of a neural network algorithm to identify the best modelling and simulation methods for nanofluids. The algorithm is trained using data from previous nanofluid experiments and utilises a multilayer perceptron with one hidden layer. The Python Keras module is used to create the neural network algorithm and data set. The algorithm predicts the average percentage error in the heat transfer coefficient of nanofluid models. The paper considers eight different models for nanofluid simulation, including single-phase, discrete phase, Eulerian, mixture, mixed model of discrete and mixture phases, volume of fluid, dispersion, and Buongiorno's model. The author finds that the dispersion, Buongiorno, and discrete-phase models accurately cover a wide range of nanofluid configurations, including particle sizes, Reynolds numbers, and volume fractions.

The accuracy of the algorithm is evaluated using performance metrics such as root mean square error (RMSE), mean absolute error (MAE), and R^2 value. The algorithm achieves an R^2 value of 0.80, an MAE of 0.77, and an RMSE of 2.6 [12]. The paper highlights the importance of modelling nanofluids accurately to reduce design and operational costs and improve research and technological advancements [12]. It discusses various modelling strategies based on different nanofluid physics and emphasises the computational fluid dynamics (CFD) approach as a means to approximate nanofluid behaviour [12]. The choice of modelling assumptions, such as constant or variable thermophysical properties, plays a crucial role in achieving accurate nanofluid models Rashidi, Akar [107]. The research also mentions the application of artificial intelligence (AI) and machine learning (ML) techniques, particularly artificial neural networks (ANNs), in solving engineering problems. AI has shown great accuracy in identifying patterns and assisting humans in problem-solving [12]. The paper utilises an ANN to develop the neural network algorithm for nanofluid modelling. The different models for simulating nanofluids are discussed, including the conventional single-phase model, discrete-phase model, mixture model, volume of fluid (VOF) model, and the combined model of discrete and mixture phases. The advantages and limitations of these models are presented, and comparisons are made based on their accuracy in predicting heat transfer coefficients.

The author collected data from relevant literature to create a data set for training and testing the neural network algorithm. The variables considered include particle size, volume fraction, Reynolds number, and percentage error in heat transfer coefficient prediction. The data was pre-processed and normalised before training the neural network.

The paper aims to determine the best model for nanofluid representation under common setups and applicative uses. It seeks to harmonise the results from various researchers regarding nanofluid model accuracy and assist in the design process by providing an algorithm to select the optimal model for simulating nanofluids' flow. The research addresses the gap in previous studies and provides recommendations for different case setups and their corresponding accuracy.

Overall, the research paper presents a neural network algorithm for identifying the best modelling and simulation methods for nanofluids. It discusses various nanofluid models, evaluates their accuracy, and utilises artificial intelligence (AI) techniques to develop the algorithm. The paper contributes to improving nanofluid simulations and provides valuable insights for researchers and engineers working with nanofluids.

3.3 Supporting details of the study: Predicting the accuracy of nanofluid heat transfer coefficient's computational fluid dynamics simulations using neural networks

3.3.1 Data collection

The data set was obtained from existing literature. Only data set with high [9, 54, 99, 108-132]. High-fidelity datasets were collected, including data with grid independence. Grid independence involves checking solutions from a simulation study over multiple mesh refinements to select the one with the least change in solution while considering the computational cost. The dataset was split into 70% for training, 15% for validation, and 15% for testing. This split was arbitrarily chosen to have more data for training while ensuring there was enough for testing.

3.3.2 Feature selection

The following features were selected: Particle size (PS), Particle volume fraction (PV), Reynold's number (RE), Wall heat flux (WHC), Property assumption (PA), Model assumptions (BM), Particle type (PT), Base fluid (BF), Flow Geometry (GEO), and Percentage deviation (PD) which was the target variable.

3.3.3 Model training

The machine learning algorithms were trained using MATLAB to make predictions on the data. The default random seed was used in order to ensure exact reproducibility of the results. The results of all algorithms on the dataset were displayed in Table 3-1, with the performance of the algorithms sorted based on the root mean squared error of the validation set, from smallest to largest values. It was observed from

Table 3-1 that the model with the least root mean squared error value was the Ensemble model of Boosted Trees, with a minimum leaf size of 8, number of learners of 30, and learning rate of 0.1. The root mean squared error on the validation dataset was 4.075672, the mean squared error on the validation dataset was 16.61111, the R squared on the validation dataset was 0.600199, the mean absolute error on the validation set was 3.076935, the mean absolute error on the test dataset was 2.38775, the root mean squared root on the test set was 10.98583, the root mean squared error on the test dataset was 3.314488, and the R squared on the test dataset was 0.719096.

3.3.4 Neural network model training

The neural network model was trained with the architecture displayed in Figure 3-1. The architecture consisted of one input layer with nine parameters, one hidden layer with the sigmoid activation, and an output layer with linear activation in a regression problem to save the weighted sum of inputs [133].

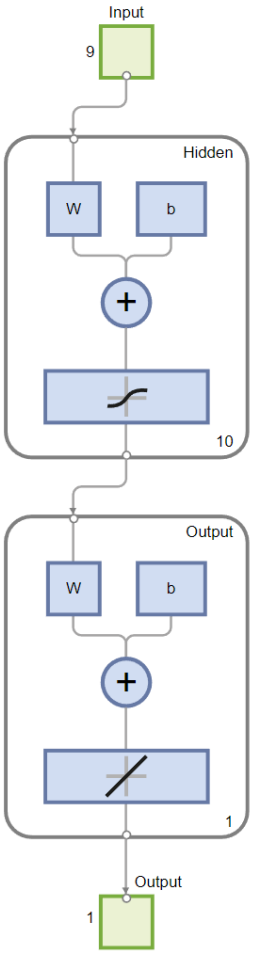

Figure 3-1 Neural network model architecture

The error histogram of the neural network model was shown in Figure 3-2, and it was observed from the figure that there were high instances in other higher error areas. An indication that the neural network did not have a very high accuracy in those instances. However, a very high percentage of the test data fell under the minimum error which showed a good generalization of the neural network model.

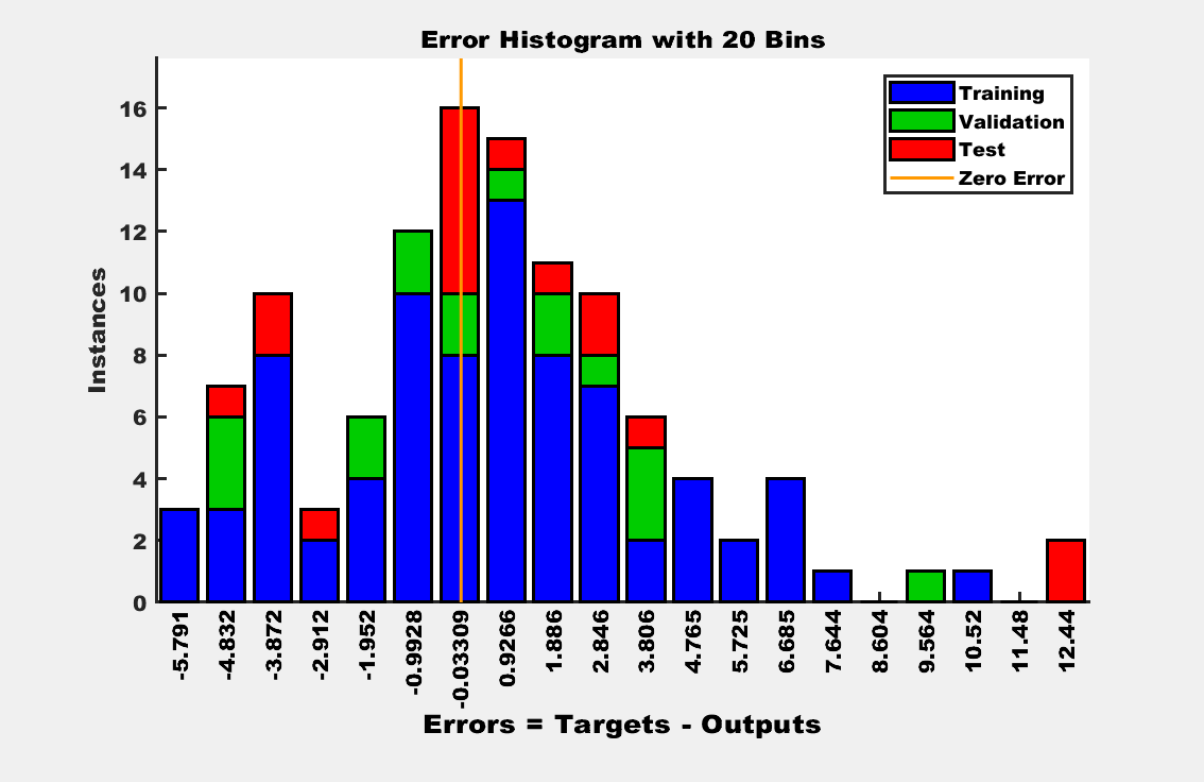

Figure 3-2 Error histogram of the neural network model

The training progress and performance over the total training epochs were shown in Figure 3-3. The learning progress in the training, validation, and test dataset was displayed. It was observed that the neural network's performance on the validation set stopped improving at the 3rd epoch. This led to the training being stopped and that point being selected as the optimal point in the training of the neural network.

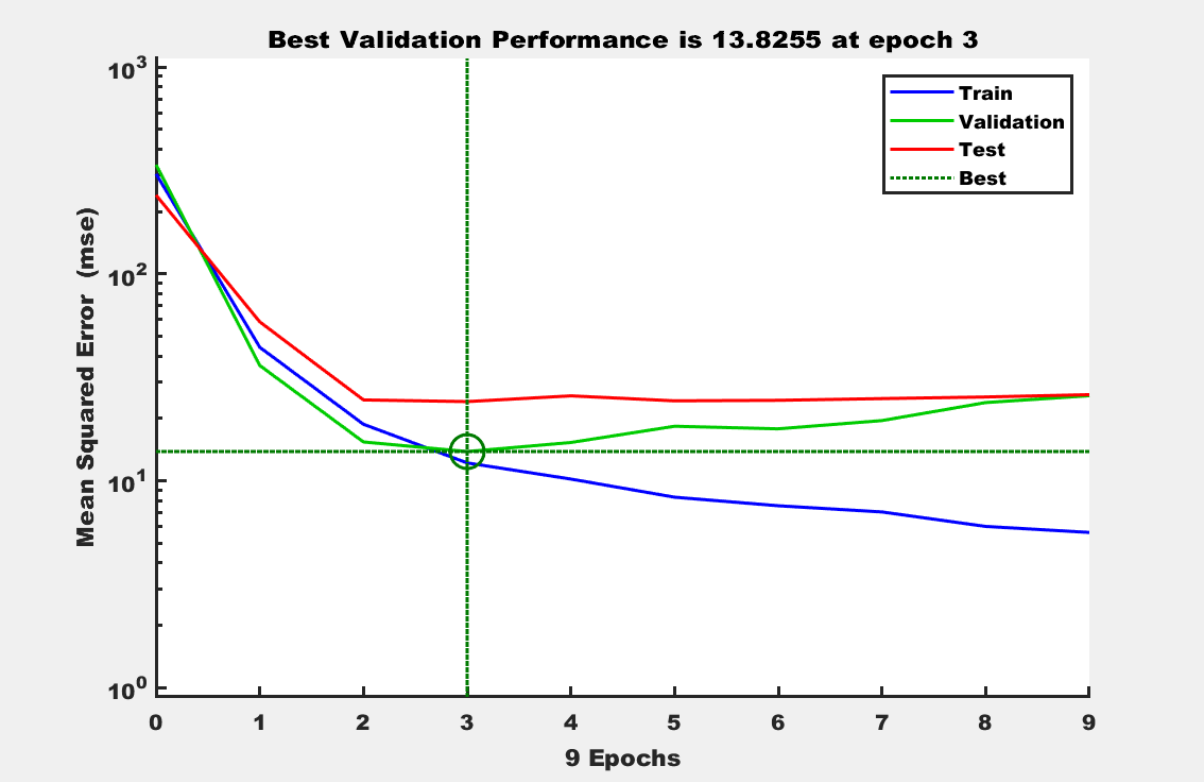

Figure 3-3 Training progress of the neural network model

The gradient, mu, and validation checks of the neural network model were shown in Figure 3-4. It was observed that the gradient was slowly descending over the epochs, while the mu was quite stable over the epoch of the training. Additionally, the validation checks were failed six consecutive times, indicating that the model had finished learning, and further training would not improve its performance but may even deteriorate it. The mu is the parameter used to balance the trade-off between gradient descent (which can be slow near the minimum) and Gauss-Newton (which can overshoot the minimum) and is ultimately used to control neural network learning.

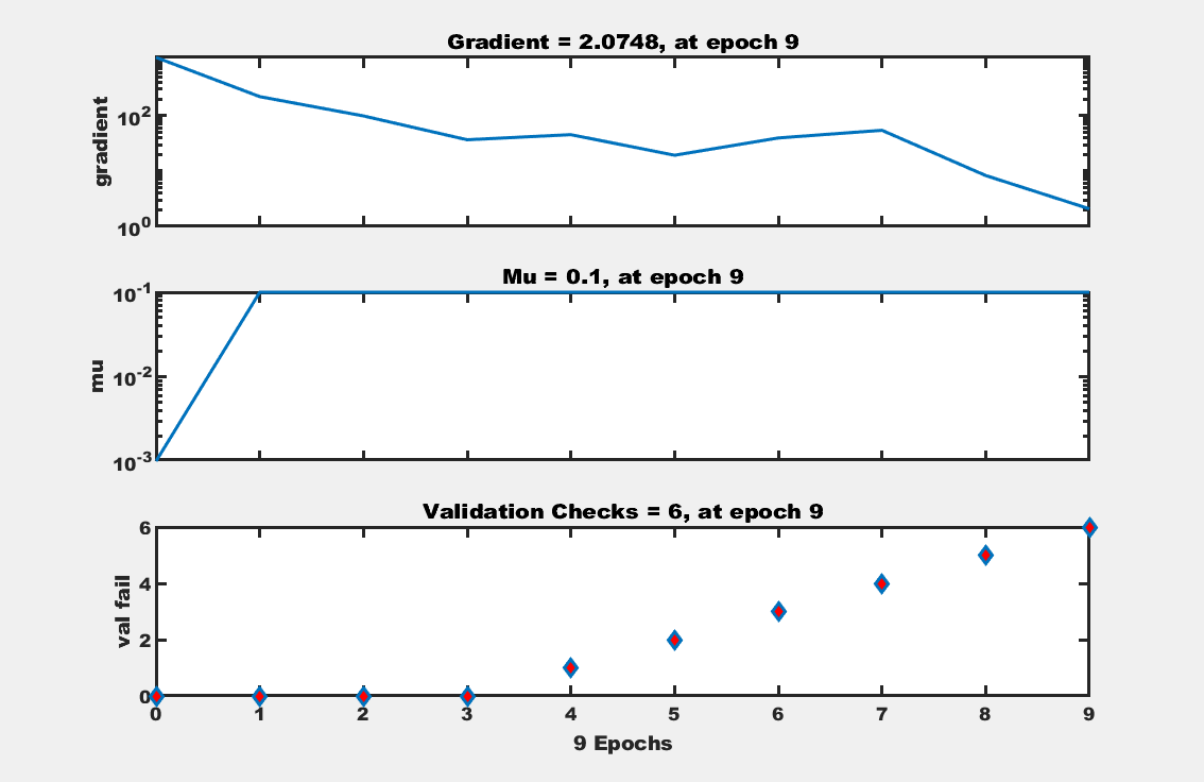

Figure 3-4 Training state of the neural network model

The regression fit of the neural network over the train, test, validation, and combined data set was shown in Figure 3-5. It was demonstrated how well the model (the line) fit the data points. A good fit was observed for all the sets, including the test and validation set.

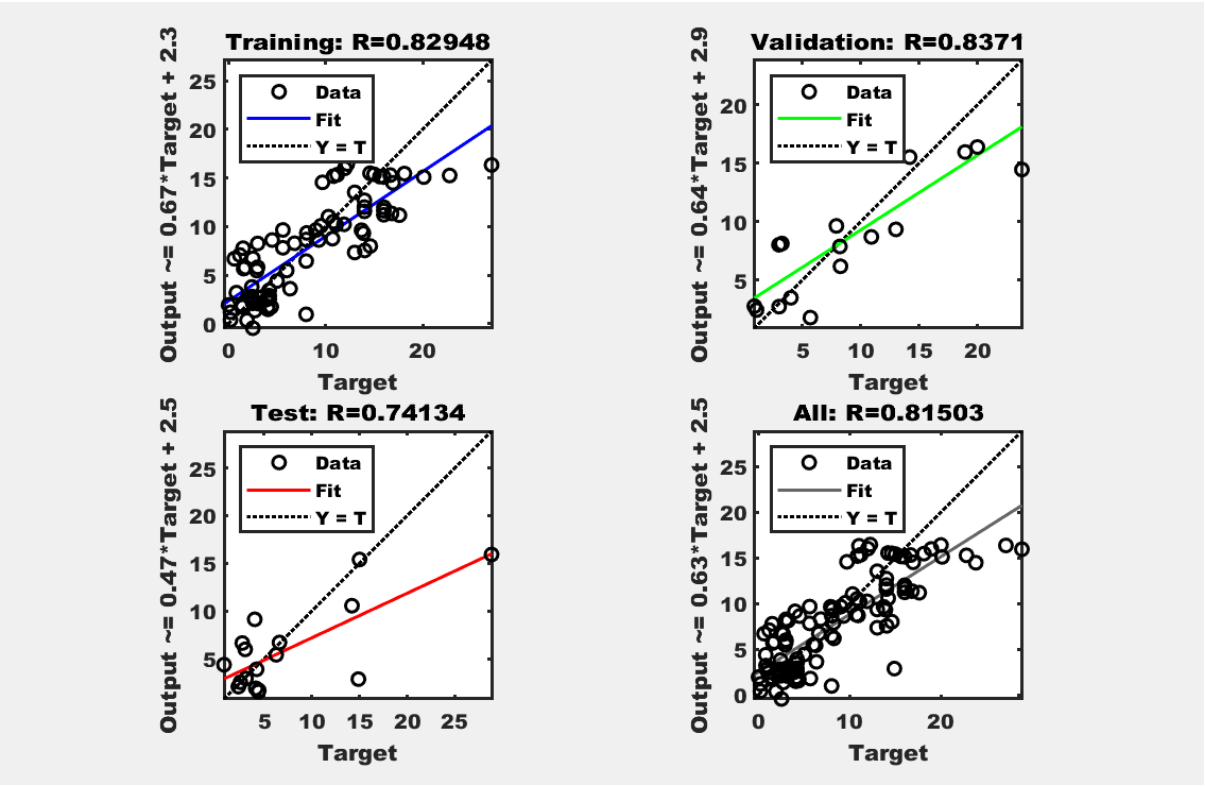

Figure 3-5 Regression fit of the neural network model

3.3.5 The optimized neural network model

The neural network model was optimized using the Bayesian optimization algorithm. As shown in Figure 3-6, the mean squared error was minimized over 30 iterations while attempting to select the best model point over the hyperparameter states with the least mean squared error. The range of the hyperparameters was

1. Number of fully connected layers: 1 – 3
2. First layer size
3. Second layer size
4. Third layer size
5. Activation: None, ReLu, Tanh, Sigmoid
6. Regularization strength: ≥ 0
7. Standardization of data: Yes/No

The best hyperparameter was found to be: 3 Fully connected Layers, Sigmoid activation, No data standardization, regularization strength of 0.022297, First layer size of 2, second layer size of 6, third layer size 0f 276. These gave a minimum mean squared error value of 27.1389.

The optimized model performance was a root mean squared error on the validation data set of 5.784209172, a mean squared error on the validation data set of 33.45707575, R squared on the validation data set of 0.194745517, a mean absolute error on the validation set of 4.698890217, mean absolute error on the test data set of 3.698524723, root mean squared root on the test set of 27.06315792, root mean squared error on the test data set of 5.202226246, R squared on the test data set of 0.308005005.

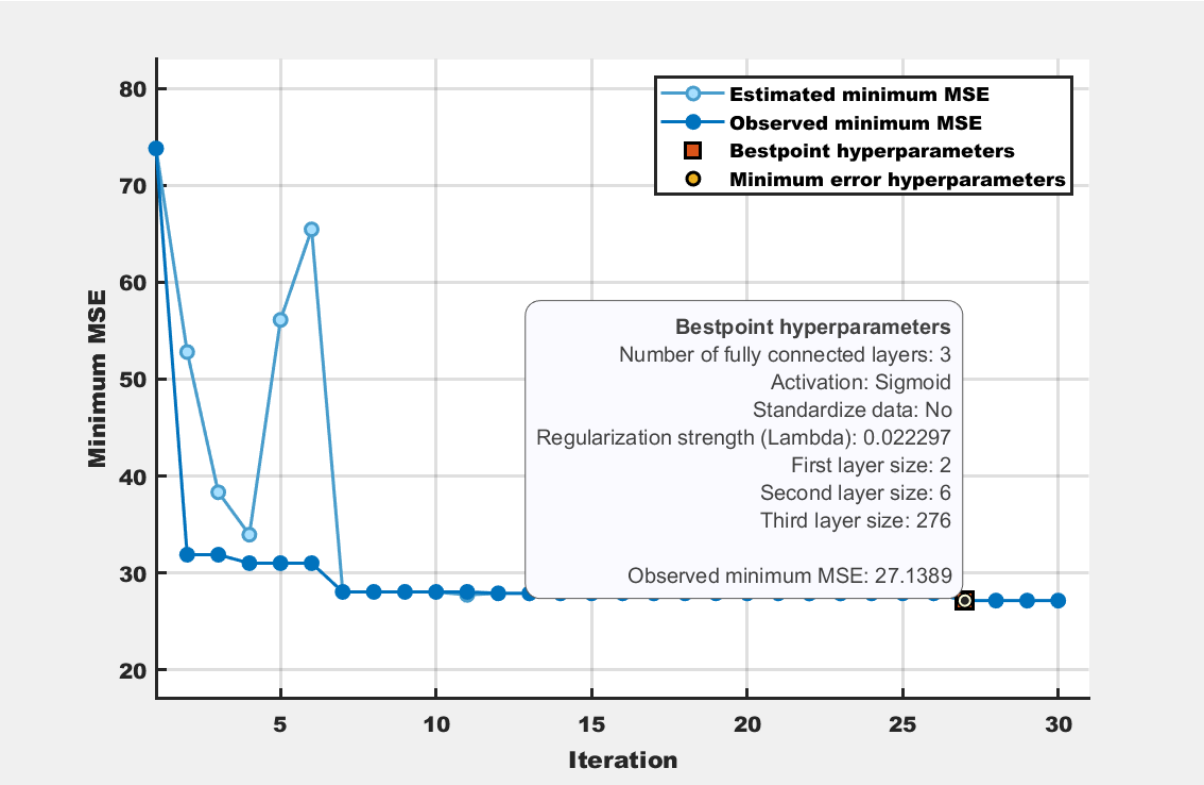

Figure 3-6 Bayesian optimization of the neural network

Table 3-1 Machine learning algorithms result

Model Type	RMSE (Validation)	MSE (Validation)	RSquared (Validation)	MAE (Validation)	MAE (Test)	MSE (Test)	RMSE (Test)	RSquared (Test)	Preset	Hyperparameters
Ensemble	4.075672	16.61111	0.600199	3.076935	2.38775	10.98583	3.314488	0.719096	Boosted Trees	Minimum leaf size: 8; Number of learners: 30; Learning rate: 0.1; Number of predictors to sample: Select All
Gaussian Process Regression	4.315122	18.62028	0.551842	3.219764	1.905293	4.832115	2.198207	0.876445	Squared Exponential GPR	Basis function: Constant; Kernel function: Squared Exponential; Use isotropic kernel: Yes; Kernel scale: Automatic; Signal standard deviation: Automatic; Sigma: Automatic; Standardize data: Yes; Optimize numeric parameters: Yes
Gaussian Process Regression	4.316282	18.63029	0.551601	3.220486	1.905294	4.832124	2.198209	0.876444	Rational Quadratic GPR	Basis function: Constant; Kernel function: Rational Quadratic; Use isotropic kernel: Yes; Kernel scale: Automatic; Signal standard deviation: Automatic; Sigma: Automatic; Standardize data: Yes; Optimize numeric parameters: Yes

Model Type	RMSE (Validation)	MSE (Validation)	RSquared (Validation)	MAE (Validation)	MAE (Test)	MSE (Test)	RMSE (Test)	RSquared (Test)	Preset	Hyperparameters
Gaussian Process Regression	4.359668	19.00671	0.542541	3.261413	1.949561	5.288419	2.299656	0.864777	Matern 5/2 GPR	Basis function: Constant; Kernel function: Matern 5/2; Use isotropic kernel: Yes; Kernel scale: Automatic; Signal standard deviation: Automatic; Sigma: Automatic; Standardize data: Yes; Optimize numeric parameters: Yes
SVM	4.402923	19.38573	0.533419	3.34821	2.306316	7.272227	2.696707	0.814052	Medium Gaussian SVM	Kernel function: Gaussian; Kernel scale: 3; Box constraint: Automatic; Epsilon: Auto; Standardize data: Yes
Ensemble	4.45948	19.88696	0.521355	3.509667	2.401889	9.254971	3.042198	0.763354	Bagged Trees	Minimum leaf size: 8; Number of learners: 30; Number of predictors to sample: Select All
Gaussian Process Regression	4.507748	20.3198	0.510937	3.42511	2.137514	7.124396	2.669156	0.817832	Exponential GPR	Basis function: Constant; Kernel function: Exponential; Use isotropic kernel: Yes; Kernel scale: Automatic; Signal standard deviation: Automatic; Sigma:

Model Type	RMSE (Validation)	MSE (Validation)	RSquared (Validation)	MAE (Validation)	MAE (Test)	MSE (Test)	RMSE (Test)	RSquared (Test)	Preset	Hyperparameters
										Automatic; Standardize data: Yes; Optimize numeric parameters: Yes
Kernel	4.554182	20.74058	0.50081	3.734936	2.777919	11.63807	3.411462	0.702419	Least Squares Regression Kernel	Learner: Least Squares Kernel; Number of expansion dimensions: Auto; Regularization strength (Lambda): Auto; Kernel scale: Auto; Iteration limit: 1000
Tree	4.610658	21.25817	0.488352	3.396103	3.673972	23.86295	4.884972	0.389833	Fine Tree	Minimum leaf size: 4; Surrogate decision splits: Off
SVM	4.725633	22.3316	0.462517	3.496684	3.048478	13.13318	3.623973	0.664189	Fine Gaussian SVM	Kernel function: Gaussian; Kernel scale: 0.75; Box constraint: Automatic; Epsilon: Auto; Standardize data: Yes
Tree	4.823772	23.26878	0.43996	3.674766	2.824131	14.10678	3.7559	0.639295	Medium Tree	Minimum leaf size: 12; Surrogate decision splits: Off
Stepwise Linear Regression	5.102175	26.03219	0.37345	3.749172	2.159175	10.39593	3.224271	0.73418	Stepwise Linear	Initial terms: Linear; Upper bound on terms: Interactions; Maximum number of steps: 1000
Linear Regression	5.404635	29.21008	0.296963	4.362919	4.003006	21.61779	4.649494	0.447241	Linear	Terms: Linear; Robust option: Off

Model Type	RMSE (Validation)	MSE (Validation)	RSquared (Validation)	MAE (Validation)	MAE (Test)	MSE (Test)	RMSE (Test)	RSquared (Test)	Preset	Hyperparameters
SVM	5.428723	29.47103	0.290683	4.226856	4.049306	21.10127	4.593611	0.460448	Coarse Gaussian SVM	Kernel function: Gaussian; Kernel scale: 12; Box constraint: Automatic; Epsilon: Auto; Standardize data: Yes
Linear Regression	5.433459	29.52247	0.289445	4.361878	3.974123	21.08009	4.591306	0.46099	Robust Linear	Terms: Linear; Robust option: On
Kernel	5.689494	32.37034	0.220901	4.547689	3.718486	21.31448	4.616761	0.454997	SVM Kernel	Learner: SVM; Number of expansion dimensions: Auto; Regularization strength (Lambda): Auto; Kernel scale: Auto; Epsilon: Auto; Iteration limit: 1000
Neural Network	5.784209	33.45708	0.194746	4.69889	3.698525	27.06316	5.202226	0.308005	Custom Neural Network	Iteration limit: 1000
SVM	5.823876	33.91753	0.183663	4.590617	3.865962	20.88778	4.570315	0.465907	Linear SVM	Kernel function: Linear; Kernel scale: Automatic; Box constraint: Automatic; Epsilon: Auto; Standardize data: Yes
Tree	6.081731	36.98745	0.109775	5.008809	4.818833	32.02376	5.658954	0.181164	Coarse Tree	Minimum leaf size: 36; Surrogate decision splits: Off
SVM	6.534241	42.69631	-0.02763	4.381311	3.113942	14.85259	3.853906	0.620225	Quadratic SVM	Kernel function: Quadratic; Kernel scale: Automatic; Box

Model Type	RMSE (Validation)	MSE (Validation)	RSquared (Validation)	MAE (Validation)	MAE (Test)	MSE (Test)	RMSE (Test)	RSquared (Test)	Preset	Hyperparameters
										constraint: Automatic; Epsilon: Auto; Standardize data: Yes
Neural Network	6.737435	45.39303	-0.09253	4.250691	4.190116	36.91087	6.075432	0.056203	Narrow Neural Network	Number of fully connected layers: 1; First layer size: 10; Activation: ReLU; Iteration limit: 1000; Regularization strength (Lambda): 0; Standardize data: Yes
SVM	6.916518	47.83822	-0.15138	4.126796	3.917551	45.01089	6.709016	-0.15091	Cubic SVM	Kernel function: Cubic; Kernel scale: Automatic; Box constraint: Automatic; Epsilon: Auto; Standardize data: Yes
Neural Network	7.405403	54.84	-0.3199	4.123469	2.459474	13.21331	3.635011	0.662141	Bilayered Neural Network	Number of fully connected layers: 2; First layer size: 10; Second layer size: 10; Activation: ReLU; Iteration limit: 1000; Regularization strength (Lambda): 0; Standardize data: Yes
Neural Network	7.591617	57.63265	-0.38712	4.164771	2.245157	10.46645	3.235189	0.732377	Trilayered Neural Network	Number of fully connected layers: 3; First layer size: 10; Second layer size: 10; Third layer size: 10;

Model Type	RMSE (Validation)	MSE (Validation)	RSquared (Validation)	MAE (Validation)	MAE (Test)	MSE (Test)	RMSE (Test)	RSquared (Test)	Preset	Hyperparameters
										Activation: ReLU; Iteration limit: 1000; Regularization strength (Lambda): 0; Standardize data: Yes
Neural Network	7.820877	61.16612	-0.47216	4.622032	1.607375	3.958595	1.989622	0.89878	Trilayered Neural Network	Number of fully connected layers: 3; First layer size: 10; Second layer size: 10; Third layer size: 10; Activation: ReLU; Iteration limit: 1000; Regularization strength (Lambda): 0; Standardize data: Yes
Neural Network	14.53701	211.3245	-4.08622	5.253877	8.030686	213.6081	14.61534	-4.46188	Bilayered Neural Network	Number of fully connected layers: 2; First layer size: 10; Second layer size: 10; Activation: ReLU; Iteration limit: 1000; Regularization strength (Lambda): 0; Standardize data: Yes
Neural Network	16.9628	287.7364	-5.92532	7.969194	2.913254	19.1844	4.380001	0.509462	Medium Neural Network	Number of fully connected layers: 1; First layer size: 25; Activation: ReLU; Iteration limit: 1000; Regularization strength

Model Type	RMSE (Validation)	MSE (Validation)	RSquared (Validation)	MAE (Validation)	MAE (Test)	MSE (Test)	RMSE (Test)	RSquared (Test)	Preset	Hyperparameters
										(Lambda): 0; Standardize data: Yes
Linear Regression	17.22954	296.8569	-6.14484	6.170534	2.499591	8.876674	2.979375	0.773027	Interactions Linear	Terms: Interactions; Robust option: Off
Neural Network	17.7706	315.7941	-6.60062	9.33196	9.886356	412.1715	20.30201	-9.53907	Wide Neural Network	Number of fully connected layers: 1; First layer size: 100; Activation: ReLU; Iteration limit: 1000; Regularization strength (Lambda): 0; Standardize data: Yes
Neural Network	20.56061	422.7386	-9.17459	10.24064	5.300163	57.13593	7.558831	-0.46094	Wide Neural Network	Number of fully connected layers: 1; First layer size: 100; Activation: ReLU; Iteration limit: 1000; Regularization strength (Lambda): 0; Standardize data: Yes
Neural Network	23.77434	565.2194	-12.6039	6.337873	6.852535	194.1103	13.93235	-3.96333	Narrow Neural Network	Number of fully connected layers: 1; First layer size: 10; Activation: ReLU; Iteration limit: 1000; Regularization strength (Lambda): 0; Standardize data: Yes
Neural Network	24.29441	590.2185	-13.2055	11.4169	9.869576	298.6496	17.28148	-6.63636	Medium Neural Network	Number of fully connected layers: 1; First layer size: 25;

Model Type	RMSE (Validation)	MSE (Validation)	RSquared (Validation)	MAE (Validation)	MAE (Test)	MSE (Test)	RMSE (Test)	RSquared (Test)	Preset	Hyperparameters
										Activation: ReLU; Iteration limit: 1000; Regularization strength (Lambda): 0; Standardize data: Yes

3.4 Single phase nanofluid thermal conductivity and viscosity prediction using neural networks and its application in a heated pipe of circular cross-section [13]

Chapter 5 investigates the single-phase simulation of nanofluids using a neural network incorporated into the governing equations [13]. The study focuses on the thermophysical properties of nanofluids, specifically viscosity and thermal conductivity, which have been areas of contention in nanofluid research [13]. The neural network is trained using experimental data gathered from the literature, and the simulations are performed using the finite element method. Grid independence analysis is conducted, and the results are validated with experimental data that was not used for training the neural networks.

The study finds that the simulations achieve a minimum average percentage error of 0.679%, indicating that the thermal conductivity and viscosity of most single-material nanofluids can be accurately modelled. This reduced the error in simulations using the single-phase model, which assumes that nanofluids are homogeneous and have enhanced and effective properties.

Numerical studies of nanofluids have posed challenges for researchers, as inconsistent findings and different formulations hinder progress in nanofluid applications. Conducting expensive and repetitive experiments further prolongs the product development process. Previous research by Vajjha, Das [134] focused on the single-phase treatment of nanofluids in a three-dimensional flow geometry, specifically studying heat transfer and laminar flow in nanofluids with ethylene glycol-water mixture as the base fluid and Al_2O_3 and CuO nanoparticles. The study observed an increased heat transfer coefficient and average friction factor with an increase in volume fraction. However, their simulations deviated from the established correlation for the Nusselt number.

To model the viscosity and thermal conductivity of nanofluids, individual neural network models were developed based on data from various studies in the literature. The models considered different nanofluid constituents, such as metals, oxides, nanoparticles, and base fluids. The viscosity data consisted of 885 rows with nine features, while the thermal conductivity data consisted of 489 rows with ten features. The neural network models for viscosity and thermal conductivity each had one hidden layer with 10 neurons and used the Levenberg-Marquardt algorithm for

training. The models took multiple variables as inputs, including nanoparticle-specific heat, density, particle size, volume fraction, temperature of the fluid, and properties of the base fluid. The results showed good convergence and validation performance of the neural network models.

The single-phase assumption for nanofluids replaces the thermophysical properties of the base fluid with those of the nanofluid. The viscosity and thermal conductivity are obtained directly from the trained neural network models, considering the individual properties of the nanoparticles and base fluid, as well as the volume fraction, particle size, and fluid temperature. The study provides the governing equations and details the methodology for incorporating the neural network models into the simulation process.

Several figures are presented to illustrate the performance and accuracy of the models. These figures include mean squared error plots, error histograms, gradient plots, regression plots, and grid convergence plots. The results show good agreement between the simulation results with neural network properties and experimental data for various nanofluids, demonstrating the accuracy and validity of the approach.

In summary, the study develops neural network models for predicting the viscosity and thermal conductivity of nanofluids. These models are integrated into single-phase simulations using the finite element method. The results indicate that the models accurately represent the properties of most single-material nanofluids. The study's findings have implications for improving the accuracy and efficiency of numerical simulations in nanofluid research and development.

3.5 Supporting details of the study: Single phase nanofluid thermal conductivity and viscosity prediction using neural networks and its application in a heated pipe of circular cross-section

The following sections provide extra supporting details for the paper: Single phase nanofluid thermal conductivity and viscosity prediction using neural networks and its application in a heated pipe of circular cross-section.

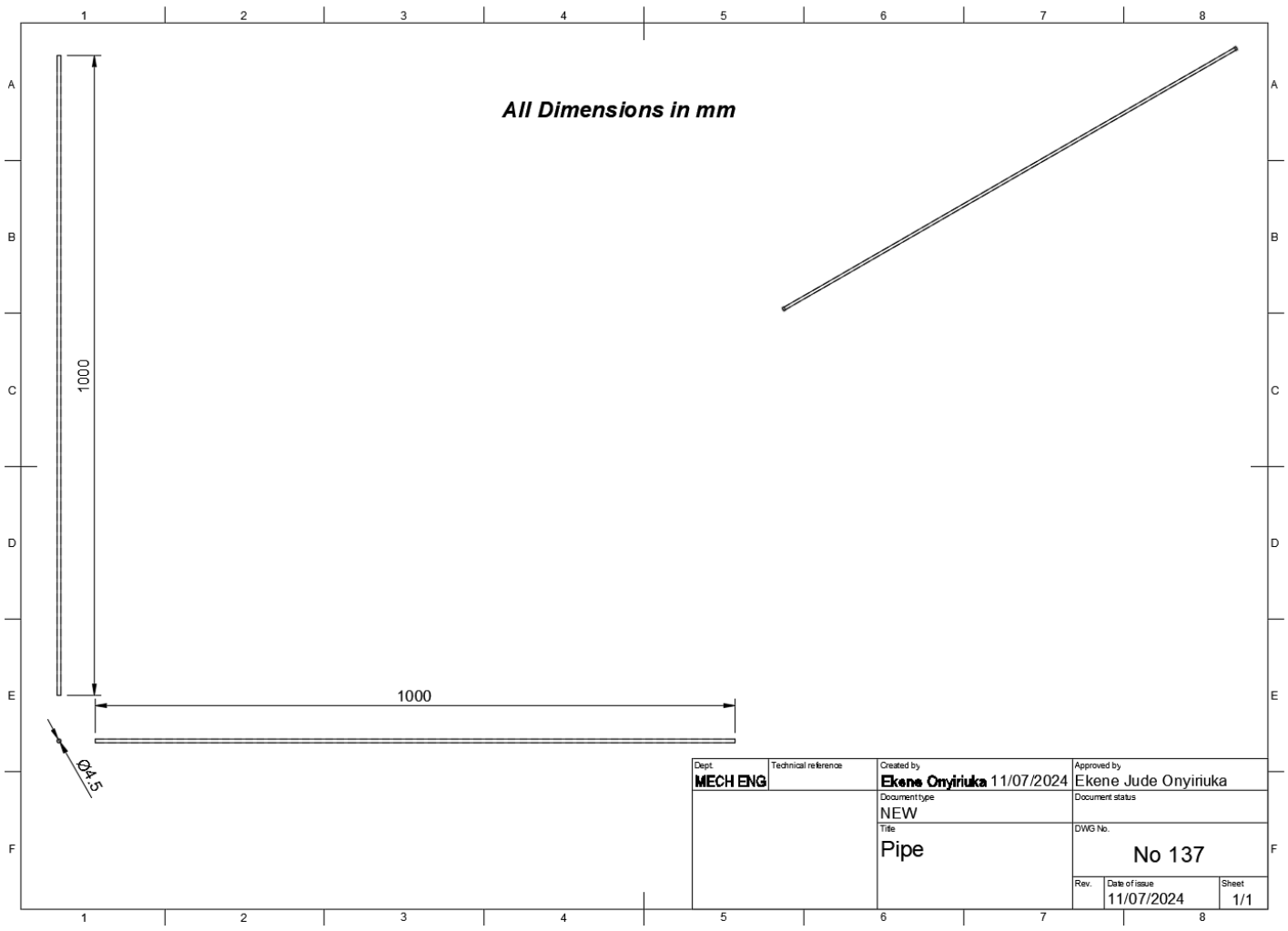

Figure 3-7 Geometry details

Figure 3-7 shows the geometry of the circular pipe. It has a length of 1000 mm and an inner diameter of 4.5 mm.

3.5.1 Meshing of the geometry

The geometry meshing was driven by the physics of the problem. The meshing process automatically established the size and sequence of operations based on the physics of the problem. Once the flow conditions were set for a fluid flow model in COMSOL Multiphysics, physics-controlled meshing sequences were triggered. These sequences were influenced by several factors including the settings of physics properties (such as turbulence models with automatic wall treatment resulting in finer meshes), specific features like walls inducing finer meshes and boundary layer meshes, and the size of the geometry bounding box determining the scale of the mesh elements [135]. An example mesh is shown in Figure 3-8.

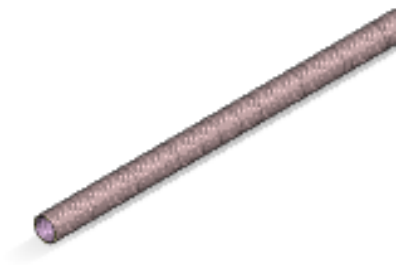

Figure 3-8 Mesh of the geometry

3.5.2 Boundary conditions of the problem

The boundary conditions of the problem were: non-slip condition was imposed on the Wall (Laminar) velocity = 0 m/s (No slip condition). Uniform Inlet velocity of 0.212 m/s was set. The outlet was 1 atm. The inflow heat transfer condition was 295 K, and the wall heat flux was 2000 W/m^2. Similarly, all other cases had the same boundary conditions type.

3.5.3 Linking the neural network model with COMSOL

In COMSOL Desktop®, the workflow is as follows: set up the geometry, set up and couple different physics, assign material properties, mesh, compute, plot, and

evaluate results. In MATLAB, the workflow involves starting Livelink™ for MATLAB®, importing the COMSOL Multiphysics model, performing data fitting/modeling to obtain material parameters, specifying design parameters, updating parameters, and solving the model in a loop. It also involves customizing data extraction and plotting.

3.6 Predictive modelling of thermal conductivity in single material nanofluids: a novel approach [14]

Chapter 6 highlighted the limitations of current modelling techniques of different researchers who model the thermophysical properties of nanofluids, such as their focus on specific nanofluid types and their inability to account for a wide range of nanofluids. The study aims to address these limitations by developing a generalised model that can predict the thermal conductivity of single-material nanofluids

The introduction also mentions the importance of considering various features, including temperature, volume fraction, particle size, nanoparticle material, and base fluid material, in predicting thermal conductivity. It references the need for a shift in the choice of model features to enable accurate predictions for a broader range of nanofluid types. It explains the conceptualisation of the novel method for parameter selection in predicting the thermal conductivity of nanofluids. It introduces the idea of feature engineering to increase the dimensional space of the dataset and create additional information for the model to make distinct predictions. The difference between conventional feature engineering and the approach used in this study is highlighted.

The algorithm for parameter selection is briefly described, involving steps such as identifying relevant features based on the physics of nanofluids related to temperature, volume fraction, particle size, nanoparticle material, and base fluid material and applying statistical methods for feature selection. The main focus of the parameter selection is on enhanced model learning for generalisation while still prioritising accuracy.

The data used in the study is also discussed, which was collected from experimental studies. The experimental setup for measuring thermal conductivity is described, that is, the transient hot wire apparatus. The reliability and accuracy of the measurement technique are emphasised. It also mentions the use of machine learning techniques, such as neural networks, gradient boosting, random forest, support vector machine

(SVM), linear models, and decision trees for analysing and predicting thermal conductivity.

Overall, the published material presents a novel approach for predicting the thermal conductivity of single material nanofluids. It emphasises the importance of feature engineering and parameter selection in developing an accurate and generalised predictive model.

3.6.1 Supporting details of the study: Predictive modelling of thermal conductivity in single material nanofluids: a novel approach

The performance of the various feature selection algorithms was displayed in Figure 3-9. It was observed that the feature algorithm described below had the best performance for both the validation and test sets. It was also shown that the one with different statistical characteristics performed better than the one with similar characteristics. In order of performance, the next was the RReliefF, the Ftest, and the minimum redundancy and maximum relevance methods (MRMR).

NFS-Different was the feature selection algorithm that took the physics of what was to be modelled and used the physics information to model it: First, the fluid of which temperature could be selected was modelled, then the multiphase was modelled, giving volume fraction and particle size as the parameters. Then the nanoparticle material was modelled, in which case, any two intensive properties could be used. Intensive properties are those properties that were independent of size and mass. Similarly, for the base fluid, any two intensive properties could be used. Although many intensive properties exist, the ones with the most different properties statically are the ones selected. Similarly, for the NFS-Similar, this took intensive properties of similar statistical characteristics.

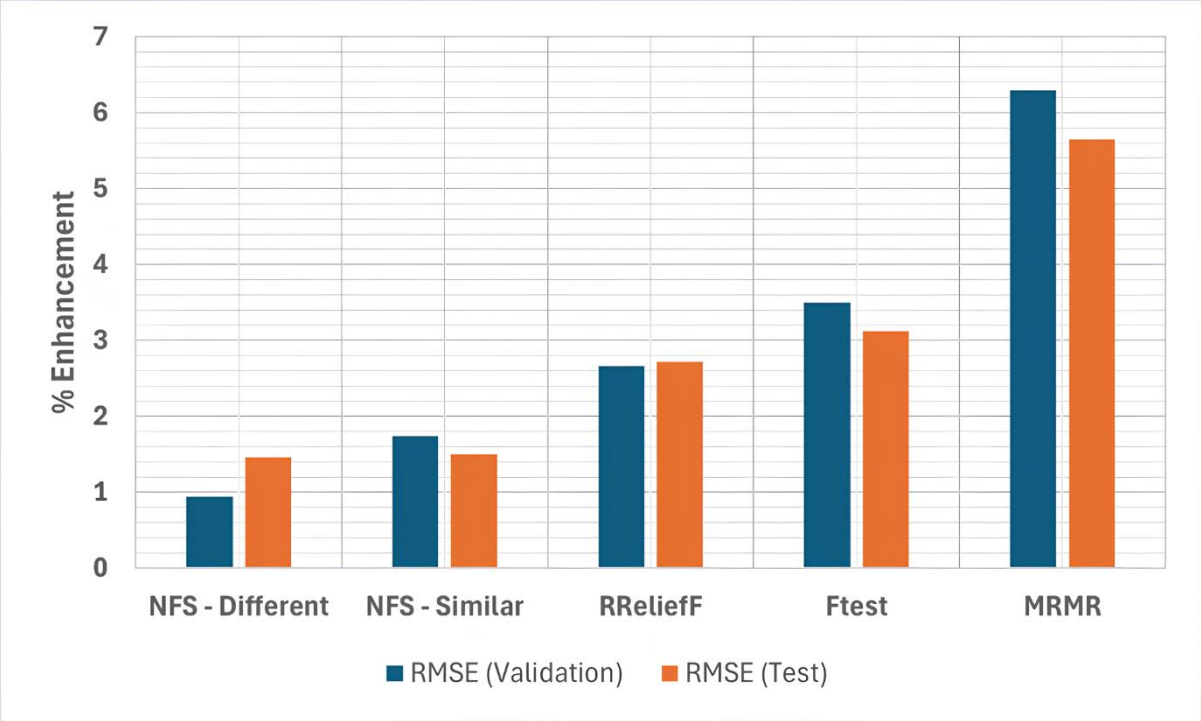

Figure 3-9 The performance of the feature selection algorithms

3.7 Summary

In summary, this chapter presented the three studies and their brief methods, it highlighted the rigorous study of nanofluid modelling and simulation and laid out the proposed solution to the different nanofluid problems identified. The study in Chapter 4 is limited to the data collected, for example, due to experimental limitations only a few geometry types are included in the study and hence the predictions are also limited to those geometries. The study resulted in a model that can reduce cost, research, design and simulation times involved in nanofluid studies, The study in Chapter 5 is limited to only two nanofluid thermophysical properties namely, thermal conductivity and viscosity. The study resulted in a model with a 0.679% average error in temperature solutions. The study in Chapter 6 is limited to single material nanofluids. The study resulted in a novel modelling approach that leads to better models. These studies rigorously examine nanofluid modelling and simulation and provide solutions to accurate modelling of nanofluid thermal and flow characteristics using machine learning.

Chapter 4 Predicting the accuracy of nanofluid heat transfer coefficient's computational fluid dynamics simulations using neural networks

ABSTRACT

This research presents a neural network algorithm to identify the best modelling and simulation methods and assumptions for the most widespread nanofluid combinations. The neural network algorithm is trained using data from earlier nanofluid experiments. A multilayer perceptron with one hidden layer was employed in the investigation. The neural network algorithm and dataset were created using the Python Keras module in order to forecast the average percentage error in the heat transfer coefficient of nanofluid models. Integer encoding was used to encode category variables. 200 trials of different neural networks were taken into consideration. The worst-case error bound for the chosen architecture was then calculated after 100 runs. Among the eight models examined were the single-phase, discrete-phase, Eulerian, mixture, mixed model of discrete and mixture phases, fluid volume, dispersion, and Buongiorno's model. We discover that a broad range of nanofluid configurations are accurately covered by the dispersion, Buongiorno, and discrete phase models. They were accurate for particle sizes (10–100 nm), Reynolds numbers (100–15000), and volume fractions (2%–3.5%). The accuracy of the algorithm was evaluated using the root mean squared error, mean absolute error, and r-squared performance metrics. The algorithm's r-squared value was 0.80, mean absolute error was 0.77, and root mean squared error was 2.6.

Keywords

Neural networks; nanofluid simulation accuracy; error analysis; predicting; keras

1. Introduction

Nanofluids were coined by Choi at Argonne in 1995 [1]. They are colloids of solids in liquids where the size of solids ranges between 5 nm and 200 nm. They are called nanoparticles because of their size and particle form. Examples of nanoparticles

include Al_2O_3, CuO, Cu, SiO_2, TiO_2, ZnO, and carbon nanotubes. These small particles are suspended in fluid, and the fluid is commonly used in industries to transfer heat. Examples of these fluids include water, oils, and ethylene glycol. These fluids, where the nanoparticles are submerged, are called base fluids. These colloids are preferentially suspended stably and uniformly for greater potency of the nanofluids [2-8].

A nanofluid model is a representation of the behaviour of nanofluids. This can be in terms of their flow and heat transfer properties. One of the benefits of developing models is a reduction in the design and operational costs of industries and research groups. Besides, they lead to improvements in carrying out studies and the design of new technology or products. For example, Toyota uses models to generate car designs. The accuracy of this process can lead to good cars, or otherwise, it can be very disastrous [9].

The process of modelling involves analytical methods [10], experimental methods, and/or statistical methods [8, 11-13]. At the heart of nanofluid modelling is the computational fluid dynamics approach, which serves to approximate nanofluid behaviour to a certain accuracy. This accuracy depends on the human factor, the level of discretization of the flow domain, and the underlining numerical scheme. In terms of heat transfer, the best model is one that accurately represents the thermal properties of nanofluid. This is so since we favour accurate models over inaccurate ones. There are different configurations of nanofluid as there are different needs and uses in terms of its heat transfer characteristics. The nanofluids could vary according to the size of the nanoparticles, the volume fraction/concentration, the base fluid type, the nanoparticle types, heat, and the flow conditions of their application. Many researchers have modelled nanofluids using various modelling strategies based on different nanofluid physics. Other researchers just modelled nanofluids based on trial and error. For example, some researchers have modelled nanofluid flow, which has been understood as a particulate flow, using the volume of a fluid model that is based on the mixture of two immiscible fluids [14]. Yet, they reported high accuracy in predicting the volume of a fluid model in terms of predicting the heat transfer coefficient of nanofluid [14], Furthermore, due to the numerous simulation studies that have been conducted for nanofluid flows in different conduits, researchers can now easily identify the best strategy for simulating a nanofluid configuration of interest

Artificial intelligence (AI), which has been recently tied to machine learning (ML), has been applied to solve various engineering problems like self-driving cars, facial recognition, security, and trading in the financial markets. AI has shown extreme accuracy in understanding patterns which humans may or may not notice. Hence, AI is applied to assist humans in solving problems, whether they are everyday problems or specific engineering problems. In the next decade, AI has been said to be in everything and cut through the fibre of human existence and help in predicting the future [15, 16]. Examples of algorithms that are used in AI include neural networks, support vector machines, the k-nearest neighbours, the k-means, decision trees, and ensemble methods. One method in AI is the artificial neural network. In this paper, this artificial neural network method is applied.

2. Models for Simulation of nanofluids

When modelling nanofluids, it is critical to first decide whether the thermophysical properties should be considered constant (CONST) properties that do not change with temperature or variable (VAR) properties that do change with temperature. The following step is to consider the models to be used. Both steps are referred to as the selection of modelling assumptions. The various models for simulating nanofluids are presented in this section.

Firstly, the single phase model is discussed thus: The basic assumption in the conventional single-phase model (SPM) is that the nanofluid is taken as a homogeneous fluid flow with enhanced transport properties. It also assumes that the liquid and particle phases move together with the same flow velocity and are in thermal equilibrium. Bianco et al. [17] studied the developing laminar flow of nanofluid under forced convection numerically. They applied the common single-phase model in their study. The nanofluid they studied was the Al_2O_3-water nanofluid in a cylindrical pipe with constant (CONST) wall heat flux boundary conditions. The results they obtained were then compared with a two-phase (discrete phase) model. They reported in their paper that there was a maximum deviation of 11% from each other and that the heat transfer coefficient was higher for the cases where the transport properties were assumed to vary with the fluids' temperature. Besides, they stated that the single-phase with constant transport property assumption deviated from the experimental data by 17% of the maximum value. Although the experimental data was carried out with constant wall temperature settings, they gave a correction of a 20% increase in the Nusselt number concerning the constant wall heat flux boundary condition [18]. Rostamani et al [19] were interested in the turbulent flow characteristics of nanofluids. They studied different nanoparticles such as alumina, cupric oxide, and titania with various nanoparticle concentrations. The

cylindrical pipe configuration was used in their geometric setup. The control volume approach was applied to solve the governing equations with varying transport properties, and constant wall heat flux was set up as the wall thermal boundary condition. They discovered that the resulting Nusselt number from their studies agreed with the results of the correlations presented by [20, 21]. The limitations of the common single-phase model are the reliance on selecting the correct thermophysical properties' correlations, which makes this model dependent. Hence, using the common single-phase model comes with the need to have accurate correlations to represent the nanofluids' transport properties [18, 22] Secondly, in the dispersion model, it is assumed that sedimentation and dispersion exist together in a nanofluid flow. This is coupled with the Brownian force, the friction force, and the gravity force on the base fluid and nanoparticles. These bring about a difference in velocities between the nanoparticle and the host fluid, which is assumed to be a non-negligible quantity. Again, the nanoparticle random motion enhances the thermal dispersion in nanofluids. This leads to higher heat flow. Mojarra et al.[23] used the control volume approach to study the heat transfer of a nanofluid made from alpha-alumina nanoparticles with water as the host fluid. Their interest was in the rounded pipe's entrance region. They compared the results they got with experimental data in the open literature. They concluded that the dispersion model does well to predict the heat transfer of nanofluid despite its simplicity. Other researchers [24, 25] also agree with these findings [18].

Next two phase flows are discussed, several factors are involved in this, including forces due to Brownian motion, friction, thermophoresis (a force due to temperature gradient), and gravity, lead some researchers to classify and treat nanofluids as two-phase flows [26, 27]. This has led to analytical and empirical equations for representing mixtures of solids and liquids. Furthermore, governing equations have been developed to accommodate this kind of model: the most common two-phase models used in nanofluid studies are the Eulerian, Eulerian-Lagrangian, the volume of a fluid, a combined model of the mixture, and Eulerian-Lagrangian, and the simplified Eulerian model (known as the mixture model) [26, 27]. All these two-phase models have the inherent drawback of high computational cost. Hence, as we are treating the flow with two different phases, we have at least one extra equation to solve for the second phase/particulate phase, which then updates the continuous phase. It is worth noting that all the two-phase assumptions technically do not require the effective property models of nanofluids to be known [18].

From the two phase flows considered in this study the Eulerian-Lagrangian is presented first; In this model the dispersed phase or particulate phase is tracked in the Lagrangian frame, and the fluid phase is updated in terms of interaction with the particles represented as a source term in both momentum and energy equations. This model has a limit of a 10% concentration of nanoparticles since any value above that threshold will lead to particle-particle interactions and hence void the model's make-up. But nanofluids never really get up to that volume fraction in practise due to the diminishing effect it has on the fluid's potential as the volume fraction increases above a 5-6% concentration. It was also noted by Xu et al [28] and Safaei et al [29] that the model takes a large amount of time to solve and is best at a volume fraction of less than 1%. Behroyan et al. [30] were interested in the turbulent flow regime (Reynolds' number of 10,000 to 25,000) and a 0 to 2% concentration of copper nanoparticles. They found that the discrete phase model (DPM)—also known as the Lagrangian-Eulerian model—was more accurate than the other two models studied, namely the Eulerian and mixture models. The Eulerian model was found to give incorrect results, excluding volume fraction (ϕ) = 0.5%. A maximum error of 15% was observed for the mixture model. The Newtonian single-phase model and the discrete phase model were the suggested models for future investigations [18].

Secondly, the Eulerian-Eulerian model is considered. In this model, the governing equations are solved for each phase while pressure is assumed to be equal for all the phases. Chen et al. [31] were interested in forced convection in the laminar and turbulent flow regimes. They studied the flow using both the mixture and Eulerian models. Their finding was that the mixture model led to a better agreement with the experimental results [18].

Thirdly, the mixture model is presented. This model assumes that all phases share a single pressure, that the dispersed phase interactions are negligible, and that the phase slip is used to solve the dispersed phase equation. This model is popular for its simplicity and low cost of computation. Niphon and Nakharintr [32] studied nanofluid flow in a 3-dimensional mini-channel heat sink under laminar convection heat transfer. Coupled with this, they also carried out experiments to validate their model. They observed that the mixture model was in better agreement with experimental outcomes than the single-phase model [18].

Fourthly, the volume of fluid is discussed here. In this model, the continuity equation for the second phase is solved to get the volume fraction of all phases for the complete flow domain. To obtain the components of velocity, one momentum equation set is solved for all the phases. Average weighting is used to calculate the physical properties of the different phases in line with their volume fraction in each

control volume. A study was carried out by Naphon and Nakharintr [32] where they employed the single-phase model, mixture model, and volume of fluid models along with the k-epsilon turbulence model. They also carried out experiments to complement the study. It was discovered that the two-phase models agreed with the experimental studies, but the single-phase model could not predict the Nusselt number as well as the others. And they attributed this to the Brownian motion and disordered distribution of the nanoparticles in their host fluid not captured by the single-phase model. They carried out a grid independence search and had the highest percentage deviation of 1.02% from other grids. This means their numerical set-up was not a function of the grid chosen [18].

Lastly, the combined model of discrete phase and mixture phase is presented. This model involves the combination of the discrete phase model and mixture models where the flow and energy equations are solved for the host fluid and then the Brownian force and particle heat transfer are implemented, and the discrete phase is solved for only one iteration after which the particle concentration is stored, the temperature gradient is calculated, fluid properties are evaluated, and the energy equation source terms are implemented. The mixture model step is then completed [33]. Mahdavi et al. [33] had a 10% error in pressure drop by using this model. They also reported good agreement with heat transfer data from experiments.

There are a lot of other models applied to multiphase studies. Some of the important ones as applied to nanofluids are presented here.

Firstly, the Lattice-Boltzmann method was used to study nanofluids, replacing microscopic and macroscopic views with molecular dynamics. The assumption in this model is that nanoparticles are microscopically located at the lattice site and are treated according to Boltzmann's method. The advantages of the model are first the use of uniform algorithms to solve multiphase flows and second, the ability to deal with complex boundaries. This model is applied to free, mixed, and forced convection of nanofluid. Karimipour et al. [34] used the double population thermal lattice Boltzmann model (TLBM) method for a 100 nm diameter and a 2–4% concentration of Cu-water nanofluid flow in a microchannel with heat flux boundary condition. Their results showed the applicability of the lattice Boltzmann model (LBM) in the microflow of nanofluid. The Nusselt number increases as the slip coefficient increases and the solid volume fraction decreases, and this increase is found to be more significant as the Reynolds number increases. With published literature, they had an error of 0.2 and 1.9% [34]. They also carried out grid independence, which means their results did not vary with the grid size chosen and gave stable results [18].

Secondly, the non-homogeneous two component model (Buongiorno et al's transport model) is presented here. In Buongiorno et al.[35], seven slip mechanisms, including gravity, Brownian, thermophoresis, Magnus effect, inertia, diffusiophoresis, and fluid drainage, are studied. He discovered by dimensionless analysis that the most important ones in terms of flow and heat transfer were the Brownian and thermophoresis mechanisms. The governing equations were based on the following assumptions: negligible external forces, incompressible flow, no chemical reactions, negligible viscous dissipation, a dilute mixture (a volume fraction far less than 1%), neglecting radiative heat transfer, a local thermal equilibrium of the nanoparticles, and the base fluid. Sheikhzadeh et al. [36] studied the natural convection of an Al_2O_3-water nanofluid in a square cavity and made comparisons between predictions of this transport model and the homogenous model. This comparison revealed that the transport model was more in agreement with the experimental results in contrast to the homogeneous model [18].

Thirdly, the Optimal homotopy analysis method (OHAM) is presented. This method involves the conversion of the non-linear partial differential equations (PDEs) into non-linear ordinary differential equations (ODEs) and is solved analytically using OHAM. In some cases [37], in just one iteration, OHAM gives the exact solutions but depends upon selecting a forcing function, whether in full or in part. Furthermore, numerical solutions are returned in good congruency with the exact solutions. Besides, small perturbations, discretization, and linearization are not needed for OHM. Hence, the computations required are greatly reduced, as detailed in [37], [18]. As a way of summary, the work of Hanafizadeh et al [38] is cited. In their study, they compared the single-phase and two-phase models using the Fe_3O_4-water nanofluid flowing in a circular constant wall heat flux pipe. They studied both the developed and developing regions for 0.5-2 % volume concentration in the laminar flow regime. They observed that for an increase in the Reynolds number and volume concentration of the fluid, the heat transfer coefficient averaged over the length of the geometry was enhanced. Further, they observed that increasing the number of dispersed nanoparticles in the host fluid in the developed region reduces the error of the applied numerical schemes. For low Reynolds numbers in the developing region, the increase in volume concentration of the nanofluid led to decreased accuracy of the applied numerical schemes. The reverse was the case for moderate and high Reynolds numbers. Further, the mixture model was found to have the least deviation from experimental studies within the studied volume fraction, and they suggested that the mixture model can estimate the average heat transfer coefficient in all Reynolds numbers, ranging from 300 to 1200. The paper, however, did not provide any grid independence studies [18].

Vaferi et al. [39] presented the prediction of the heat transfer coefficient using artificial neural networks (ANN). They considered a circular tube from experimental data with different wall conditions under different flow regimes. They compared the performance of the proposed approach with reliable correlations given in different studies. They stated that their model was better in performance than the other published works [40-42]. Their study was focused on predicting the heat transfer coefficient of nanofluids flowing through circular conduits. This study is focused on predicting the best model to apply in order to accurately simulate nanofluid flow in various flow geometries, including circular tubes. Furthermore, this study shifts the focus from predicting the thermal behaviour of nanofluids to focusing on deciding the best assumptions to make about the physics of the flow and heat characteristics of nanofluids of different types. The resulting algorithm can therefore be used to select the best model for simulating nanofluids' flow. By this, the accuracy of nanofluids simulation is increased. The artificial neural network (ANN) is a tool that has been shown by researchers to be highly effective in making predictions.

This study aims to come up with an algorithm that determines the best model for nanofluid representation under the most common setups and applicative uses. To the best of our knowledge, no researcher has carried out this study [39, 43, 44]. There exist disagreements among various researchers in the literature regarding which model is best for nanofluids. Hence, this paper also aims to harmonise the results of researchers regarding the accuracy of nanofluid models for different cases. It also seeks to aid in the design process of nanofluids by making an exhaustive search of optimal nanofluid parameters and models possible. By coming up with a neural network algorithm created from data gotten from researchers' reports on eight different models, the most suitable model for the most configurations of nanofluid, conventional setups, and applicative uses is determined. It is worthwhile to state that the paper is focused on the error in predicting the heat transfer coefficient by the different models. A recommendation of the models for different case setups to be used and their corresponding accuracy will also be available from this work.

3. Methodology

3.1. Method

The algorithm that determines the suitable modelling assumption, which produces the least prediction error, for carrying out computational fluid dynamics (CFD) simulations of nanofluids for different nanofluid configurations and flow geometry has been developed. The most common conduits in the literature will be used as case studies along with the most common models for CFD simulations of multiphase flows

being considered. Data on models, nanofluid configurations, and percentage error in predicting heat transfer coefficients will be collected. The input to the algorithm will be the model types, nanofluid configurations, and the geometry of flow. The output of the algorithm is the percentage error in predicting the heat transfer coefficient for each model (the percentage error is the difference between the simulation heat transfer coefficient and its corresponding experimental heat transfer coefficient gotten from the literature that used any of the models covered in this study). Specifically, an artificial neural network is designed to predict the model that will have the least error for a particular nanofluid simulation. The objectives of this chapter are as follows: Firstly, collect relevant data from the literature; secondly, preprocess the data into a form useful for neural network development; and thirdly, train, evaluate, and verify the neural network algorithm prediction using an unseen test data set. Finally, we present the results for commonly encountered scenarios in nanofluid simulations.

3.2. Data collection

The dataset (102 rows and 10 columns) is summarised in Table 1(a) and was collected from the literature [17, 19, 21, 30, 31, 33, 41, 44-64]. These pieces of literature were chosen because they used any of the various models that were of interest in this study. This study was interested in commonly used models. Each row in the dataset represents a given record in the dataset. And it reflects the nanofluid configuration, flow regime, experimental setup, and nanofluid models along with their corresponding percentage error between the model prediction and the experimental results. From Fig. 1 (a - d), we can notice the values for chosen variables of the dataset. The figure illustrates the range of values of each data along with the distribution of the data. The chosen variables were: The particle size (PS(nm)), the volume fraction (PV(%)), the Reynolds number (RE), and the percentage error (PD (%)). The rest of the data had similar dimensions. The predictors were normalised to 0 and 1. This was done to control the gradients in the neural network computations so that we could obtain an optimal solution [65].

Table 1 shows the correlation plot of each variable. We can observe that the highest correlation with the percentage deviation was a positive correlation of 0.5, obtained for the property assumption variable. The others were the particle size and Reynolds number, which had a negative correlation of 0.4 each. This also implies that these variables have the most impact on the accuracy of different models in modelling nanofluid flows. The neural network was chosen due to its ability to handle these kinds of problems where the correlations of variables are low [65].

The collected data had the following features as shown in Table 2(a). Furthermore, the complexity of the problem we have set out to solve requires that we consider the computational schemes used in obtaining the solutions for the different models. Hence, we present Table 2(b). Table 2(b) shows the different computational schemes used for each model. From this table, we can observe the model with a different computational scheme was the VOLUME OF FLUID model, which has a Pressure-Implicit with Splitting of Operators (PISO). We can assume that, in terms of the computational schemes used, the models have been properly adjusted such that the numerical error is not a dominant part of the model's prediction. We also point out that we collected simulation results from authors that used grid independence methods to show their results were not dependent on the mesh.

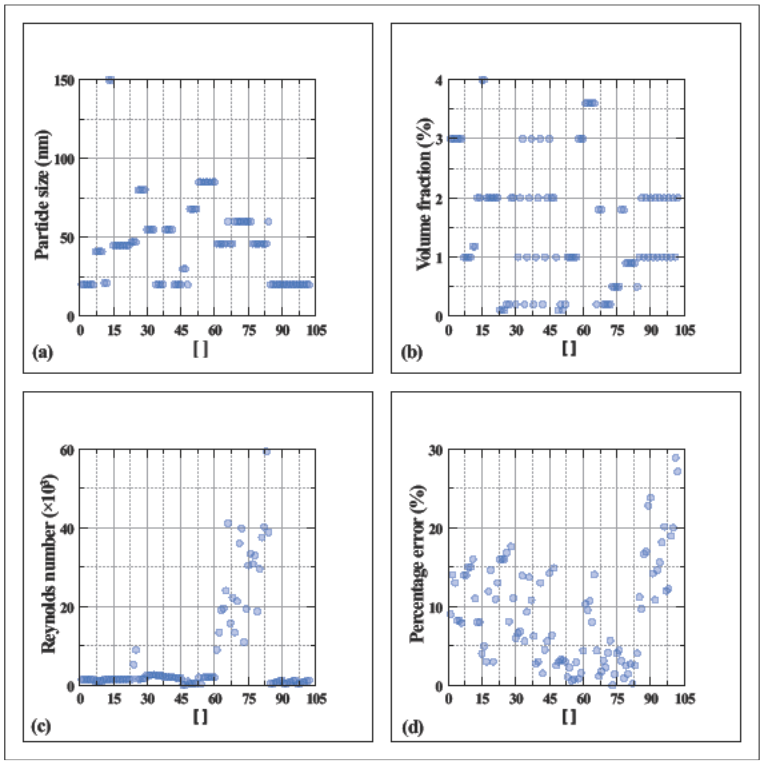

Fig. 1(a). A presentation dataset collected from literature

Table 1

The correlation plot of the dataset collected from literature

	PS (nm)	PV (%)	RE	WHC	PA	BM	PT	BF	GEO	PD (%)
PS (nm)	1.0	-0.1	0.1	0.1	-0.4	-0.1	-0.3	-0.1	-0.1	-0.4
PV (%)	-0.1	1.0	-0.2	-0.2	0.1	-0.3	-0.3	0.1	-0.3	0.2
RE	0.1	-0.2	1.0	-0.3	-0.3	0.3	0.3	-0.1	0.2	-0.4
WHC	0.1	-0.2	-0.3	1.0	-0.4	-0.1	-0.2	-0.1	0.5	-0.1
PA	-0.4	0.1	-0.3	-0.4	1.0	-0.1	0.4	-0.1	-0.1	0.5
BM	-0.1	-0.3	0.3	-0.1	-0.1	1.0	0.2	0.0	0.2	-0.1
PT	-0.3	-0.3	0.3	-0.2	0.4	0.2	1.0	0.1	0.6	0.2
BF	-0.1	0.1	-0.1	-0.1	-0.1	0.0	0.1	1.0	0.1	0.0
GEO	-0.1	-0.3	0.2	0.5	-0.1	0.2	0.6	0.1	1.0	0.0
PD (%)	-0.4	0.2	-0.4	-0.1	0.5	-0.1	0.2	0.0	0.0	1.0

Table 2(a)

The definition and meaning of each variable and their corresponding encoding.

Column name	Meaning	Encoding (Integer)	Units
PS	Particle size: Represents the	-	nm

	average size of the nanoparticle		
PV	Particle volume fraction: Represents the concentration of the particles in the host fluid	-	%
RE	Reynolds number: Represents the flow condition	-	-
WHC	Wall thermal flux condition: Represents the thermal boundary condition imposed on the wall of the conduit	Constant heat flux [1], constant wall temperature [2]	-
PA	Thermophysical property assumption: Represents whether we are considering properties that change with temperature - variable (VAR) or remains constant with temperature constant -(CONST)	constant properties [1], variable properties [2]	-
BM	Model: This represents the model applied to simulate nanofluids	SINGLE PHASE MODEL [1], DISCRETE PHASE MODEL [2], EULERIAN	-

		(EUL) MODEL [3], MIXTURE MODEL [4], COMBINED MODEL OF DISCRETE AND MIXTURE PHASES (CDM) [5], VOLUME OF FLUID (VOF) [6], DISPERSION MODEL (DIS) [7], TRANSPORT MODEL/ BUONGIORNO (BUO) [8]	
PT	Particle type: Represents the constituents of the nanoparticles	Al_2O_3[1], Cu [2], CuO [3], Graphite [4], ZrO [5], Fe_3O_4 [6]	-
BF	Host fluid: Represents the base fluid/conventional fluid which buoys the nanoparticles.	Water [1], Oil[2]	-
GEO	Geometry: Represents the flow conduit	2D axisymmetric pipe [1], 3D circular pipe [2], Helical pipe [3]	-
PD	Average percentage error: Represents the deviation of the numerical studies from experimental reports		%

Table 2(b)

A table of the models and their computational schemes considered

Model	Computational scheme considered
SINGLE PHASE MODEL	Semi-Implicit Method for Pressure-Linked Equation (SIMPLE)
DISCRETE PHASE MODEL	Semi-Implicit Method for Pressure-Linked Equation (SIMPLE)
EULERIAN	Semi-Implicit Method for Pressure-Linked Equation (SIMPLE)
MIXTURE	Semi-Implicit Method for Pressure-Linked Equation (SIMPLE)
COMBINED MODEL OF DISCRETE AND MIXTURE PHASES	Semi-Implicit Method for Pressure-Linked Equation (SIMPLE)
VOLUME OF FLUID	Pressure-Implicit with Splitting of Operators (PISO)
DISPERSION	Semi-Implicit Method for Pressure-Linked Equation (SIMPLE)
TRANSPORT MODEL/ BUONGIORNO	Semi-Implicit Method for Pressure-Linked Equation (SIMPLE)

3.3. Method - Artificial neural network (ANN)

ANN has been shown to handle difficult problems like handwriting recognition, facial recognition, currency trading, and self-driving cars. Although it is a very simple concept, it is based on the way the human brain functions. The basic neural network is made of neurons. For example, in the multilayer perceptron architecture, layers of neurons are typical, with input and output layers where information flows in one direction (feed-forward). That is, one node receives data from other nodes in the

layer under it and sends data to nodes in the layers above. A detailed description of the multilayer perceptron is discussed in the paper by [66].

3.4. The neural network learning process

Vafaei et al. [67] studied the steam distillation process using neural networks. They used ANN and an adaptive neuro-fuzzy interference system (ANFIS) to investigate the distillate recoveries using a collection of data. The models were able to estimate with a minimum error the yield of the distillates. While Salehi et al [68] successfully designed a neural network by genetic algorithm for nanofluid in a closed thermosyphon, in their study, they also made a multilayer perceptron (MLP) network (a backpropagation network). As stated in their paper, the MLP is termed a Universal Approximation because, with its simple structure, it can map any non-linear input/output interaction. It is made up of an input layer, a hidden layer, and an output layer. They found the MLP to correctly predict the experimental data, likewise the genetic algorithm neural network. Bahiraei et al. [44] reviewed the algorithms of AI applied to study nanofluids and the potential of nanofluids with the challenges ahead in the field of nanofluids and its applications. However, they did not mention the use of AI or machine learning-related tools to determine the best model for nanofluid simulation, which is lacking in the literature. They probably did not mention it because there was no paper on the subject. It can, therefore, be concluded that this application is new and novel. Also, they mentioned the most commonly used algorithms for nanofluids studies, listed as MLP, RBF (Radial Basis Function), FUZZY LOGIC, and optimization methods like genetic algorithm, particle swarm optimization, artificial bee algorithm, and ANFIS. They also mentioned the various activation functions for AI in nanofluids studies, listed as Sigmoid, hyperbolic tangent, inverse tangent, threshold, Gaussian radial basis, and linear functions. In their paper, they pointed out that for thermal conductivity and viscosity predictions, the Levenberg-Marquardt approach and the Bayesian-based regularisation were the best.

The MLP networks are made up of three different layers: the input, hidden, and output layers. Information from the predictor variables is fed into the input layer according to a mathematical procedure. They are then sent to the hidden layer where they are processed and sent to the output layer. The output neuron gives the value of the target variable. The output value of each neuron can be calculated by Eq. (1):

$$n_j = f\left(\sum_{r=1}^{N} w_{jr} x_r + b_j\right) \quad (1)$$

Eq. (1) shows that the b_j (which represents the biases) is summed with the results from the product of the information (x_r) and their corresponding weight coefficient (w_{jr}). The transfer function f is the function that receives the output of each neuron. They include various types of transfer functions, including the hyperbolic tangent sigmoid, radial basis functions, rectified linear units, logarithmic sigmoids, and linear. But in this study, the rectified linear unit (ReLU) has been used for the input, hidden layer. The output layer is left without activation with a single unit, and it is a linear layer since this is a regression problem and we are trying to predict a single continuous value. Its formulation is given in Eq. (2):

$$f(x) = \max(0, n_j) \tag{2}$$

4. Neural network algorithm

4.1. Description of the ANN model

The ANN model is developed from the following inputs: These inputs represent the main determinants in the modelling of nanofluids. The inputs are particle size, particle volume fraction, wall thermal condition, thermophysical property assumption, model, particle type, host fluid, and geometry. The output variable is the average percentage error of the heat transfer coefficient (h) predicted by the model used for simulation. The lack of literature data that considers nanoparticle shape to be an important factor in nanofluid simulation prevents it from being considered.

The ANN model consists of nine input variables and one target variable. It consists of one hidden layer, as Hornik et al [69] have shown that the MLPs with only one hidden layer are universal approximators and that they do well even for small data, meaning they can accurately estimate any multivariate function if its hidden units have a non-linear transfer function. This single hidden layer consists of 170 neurons. This number was selected based on the lowest root mean squared error and R-squared value after 200 runs of different networks with different numbers of neurons, as shown in Fig. 2(a) and (b). However, other researchers use the formula Eq. (3), Between the size of the input layer and the size of the output layer, there should be an appropriate number of hidden neurons. Heaton [70] stated that 2/3 the size of the input layer plus the size of the output layer should be the number of hidden neurons or Less than twice as many hidden neurons as input layer should be present.

$$N_{\text{hidden neurons}} = \left(\frac{N_{\text{samples}}}{[\alpha\{N_{\text{input neurons}} + N_{\text{output neurons}}\}]}\right) \tag{3}$$

where,

N = the number of

α = a random scaling factor, usually between 2-10.

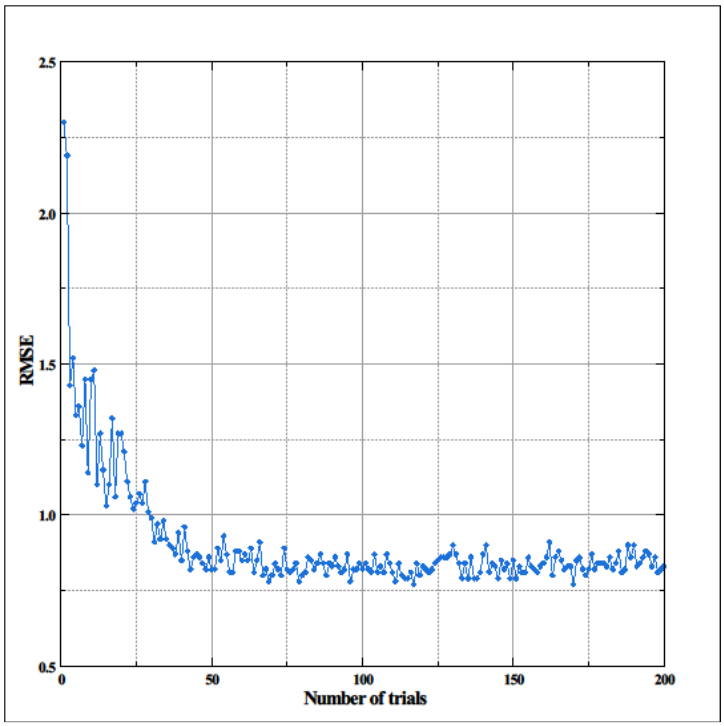

Fig. 2(a). A plot of root mean squared error for 200 trials of the different neural network architectures varied in terms of number of neurons

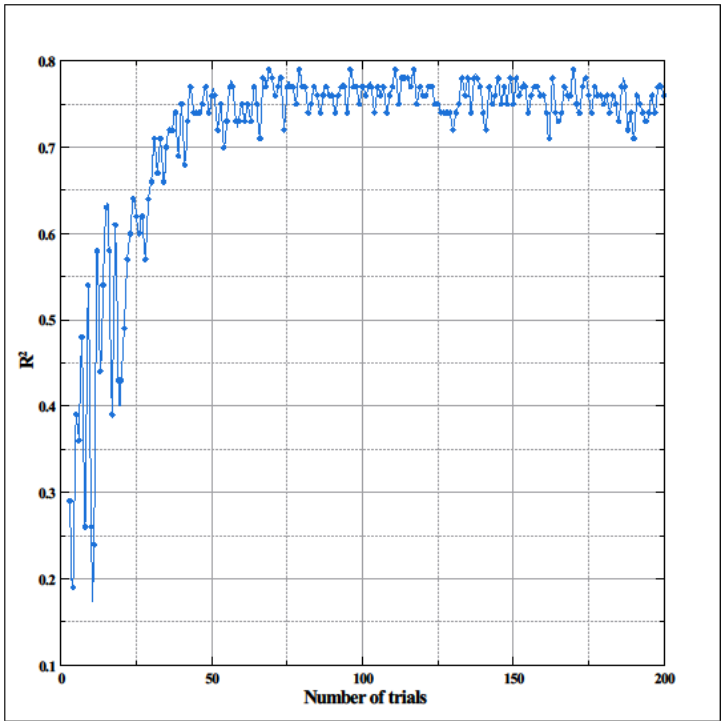

Fig. 2 (b). A plot of R-squared for 200 trials of the different neural network architectures varied in terms of the number of neurons.

The RMSprop algorithm [71, 72] is used as the optimizer in this ANN model. These settings were implemented in Python using the Keras module. The schematic of a simple ANN model and the Keras neural network algorithm created is shown in Fig. 3 for clarity. The neural network in Keras shown in Fig. 1(b) was run for 1000 epochs with a learning rate reduced to a plateau and with batch normalization. The loss function was the mean squared error, while the error metric was the mean absolute error. A loss function is a mathematical formula that converts an event or the values of several variables to a real number that, inferentially, represents some "cost" related to the occurrence. When mean squared error (MSE) is employed as a loss function, this has the effect of "punishing" models more for higher errors. Similarly, when the root mean squared error (RMSE) is used, it has the same effect since they both have the square of the error. The mean absolute error (MAE) has a neutral effect when used as a loss function. An error score is the discrepancy between a person's measured or scored results and their anticipated results. It can be represented by mean squared error (MSE), root mean squared error (RMSE), mean absolute error (MAE), R-squared (R^2), mean absolute deviation (MAD), mean absolute percentage error (MAPE), and standard error (SE). The mean absolute error (MAE) measures the average error between the predicted error and the true error in heat transfer coefficients of nanofluids. The root mean squared error (RMSE) measures the square root of the average value of the square of the error between the true error and the predicted error in the heat transfer coefficient of nanofluids. While the R-squared quantified the degree of fit between the predicted error and the true error of the heat transfer coefficient of nanofluids, The mean absolute deviation (MAD) represents the average of the collected data’s absolute departures from its mean. A mean absolute percentage error (MAPE) is a statistic that measures how well a modelling approach predicts the future. While for error standard deviation, the standard error (SE) is a statistical model that assesses how accurately a sample distribution represents a population. In this study, the following error score criteria were applied: Mean absolute error (MAE), Root mean squared error (RMSE), and R-squared (R2). This mix of performance criteria accesses different characteristics of the performance of the model in this study, as highlighted above.

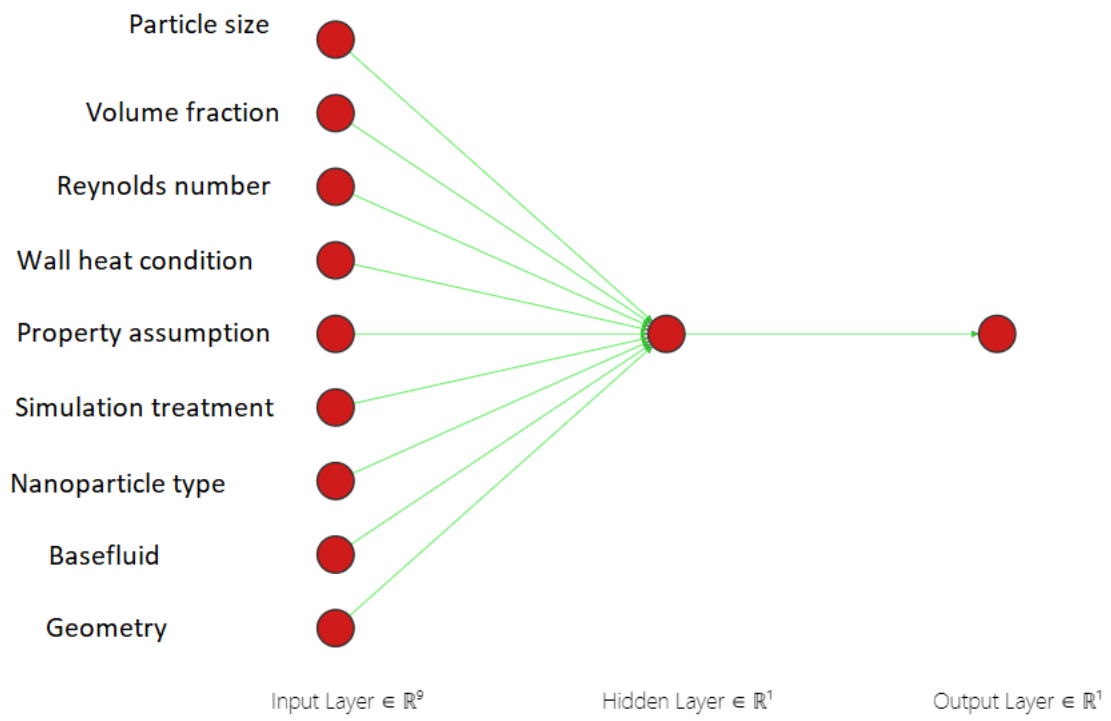

Fig. 3. A simple one-layer neural network

4.2. Performance of the ANN Model

The dataset was split into training, validation, and testing sets by a 70%:15%:15% split, that is, 71 of them were used for training, 15 for validation, and 16 for testing. The subset for training was used for determining the unknown weights and biases and finding the best network. The ability of the ANN model to predict the heat transfer coefficient is examined and validated by the testing dataset, and this can be evaluated statistically using the mean squared error (MSE) and the R-squared (R^2) values. Eq. (4–9) [39] depicts the statistical definition of these quantities.

.

$$MSE = \frac{1}{n}\sum_{i=1}^{n}(h_i - {h_i}^{pred})^2 \quad (4)$$

$$\bar{h} = \frac{1}{n}\sum_{i=1}^{n} h_i \quad (5)$$

$$SS_{reg} = \sum_i({h_i}^{pred} - \bar{h})^2 \quad (6)$$

$$SS_{tot} = \sum_i\left(h_i - \bar{h}\right)^2 \quad (7)$$

$$R^2 = \frac{SS_{reg}}{SS_{tot}} \quad (8)$$

$$RMSE = \sqrt{\frac{1}{n}\sum_{i=1}^{n}(h_i - h_i{}^{pred})^2} \quad (9)$$

n is the number of samples, h_i is the observed heat transfer coefficient in the data, and $h_i{}^{pred}$ is the predicted heat transfer coefficient by the ANN model. The MAE and RMSE of this model were found to be 2.6 and 0.77, while the R2 was 0.80. Because the root mean squared error gives the root of the squared error, a value of 2.6 is acceptable. The mean absolute error also gives the mean of the difference between real and predicted values, so this is also an acceptable value for the range of error seen throughout this study. An r-squared of 0.80 indicates that the true error and predicted error are well fit.

4.3. Results and discussion of the resulting model

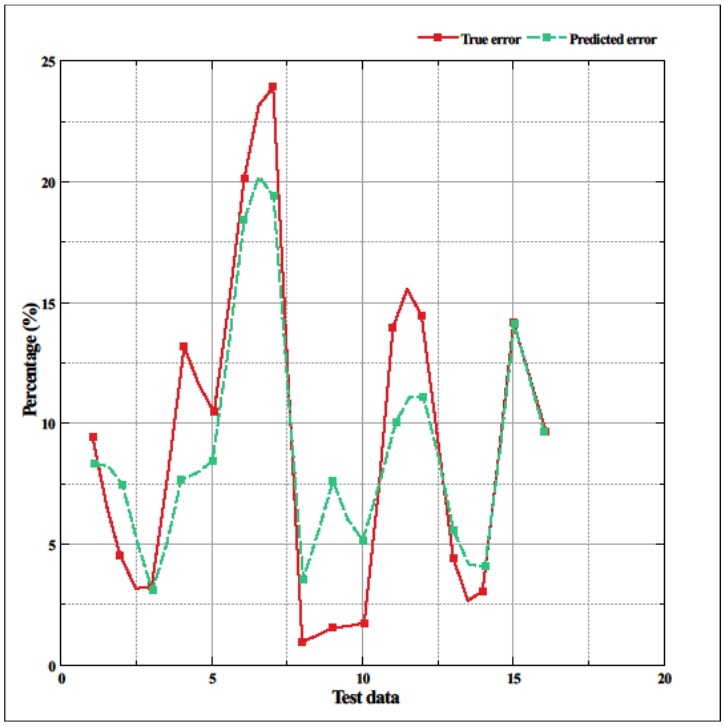

Figure 4a: A plot of validation of the algorithm with the test data points

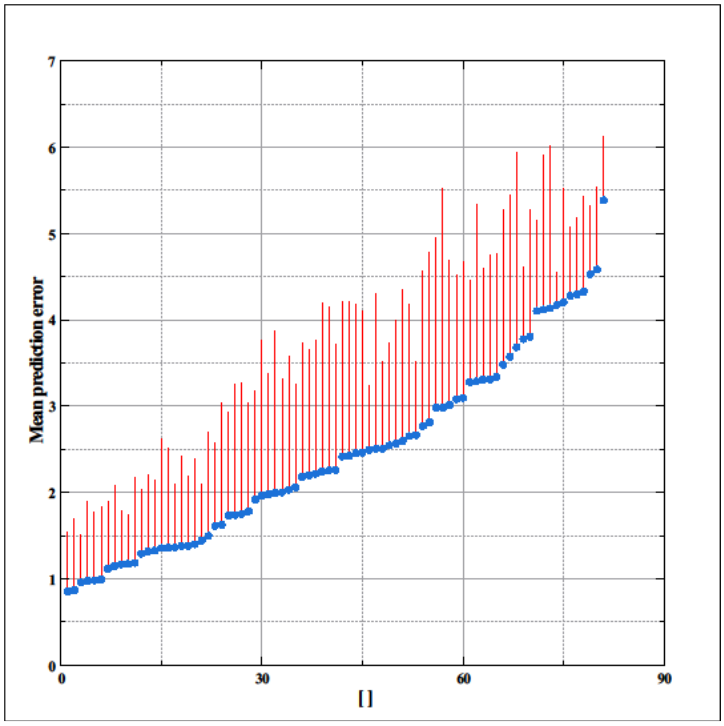

Figure 4b shows a plot of the worse case bound based on 1σ of the mean absolute error of prediction for each test dataset over the model trained with randomly selected training data.

For the 16 test data which serve as the verification set to verify the neural network, the true percentage error of the models in predicting the heat transfer coefficient is the red solid line in Fig. 4a. The green dashed line is the prediction of the neural network for each model. A good correlation can be observed, and this verifies the R2 value of 0.80. This value implies that the algorithm can explain the variance in the dataset. However, the areas of mismatch in Fig. 4a indicate the algorithm prediction error. The lowest error encountered in the test data was 0.4%, which was for the combined model of discrete and mixture phases of nanofluid with a volume fraction of 1% and a 41 nm particle size in the laminar flow regime, while the largest error was 5.9% for the mixture model in the laminar flow regime for a nanofluid of 0.2% volume fraction and 20 nm particle size.

To validate the performance of the prediction with the data, the same training procedure is performed with a different division of the data into the training, the validating, and the testing, and the overall error for the trained neural network is calculated with the variance. This is repeated 81 times. The prediction performance is shown in Fig. 4b.

Fig. 4b shows the plot of mean absolute error for each test data set over the model trained with different randomly selected training data. It illustrates that for a 1σ , the

maximum error in the worst case was 6%. This also shows that the modelling technique is valid and is suitable for the problem to which it has been applied. From the plot, the errors ranged from high values to lower values.

The model prediction percentage error is examined concerning different Reynolds Numbers. 16 different models, whose specific definitions can be found in the abbreviation section, are considered in Figures 5i(a – d) and 5ii(a - d).

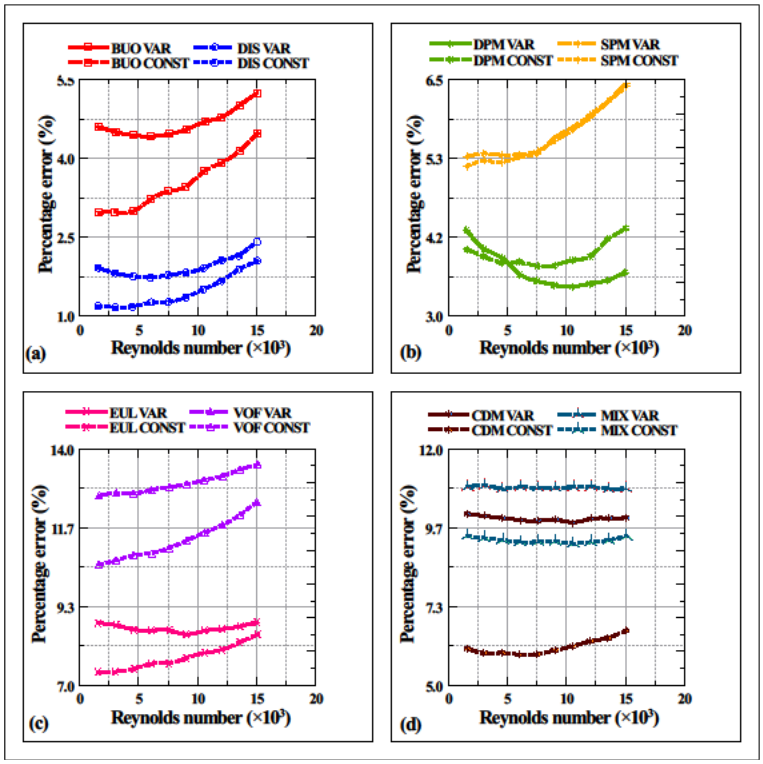

Figure 5i(a –d) shows a plot of percentage error versus Reynolds number for all three (3) dimensional pipe flow models with constant wall heat flux.

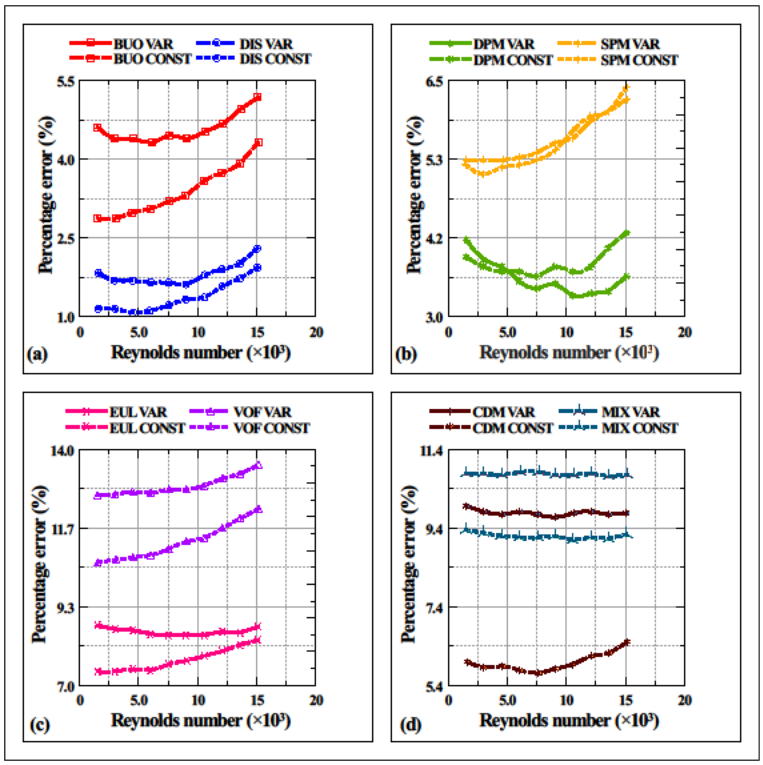

Figure 5ii(a – d) shows a plot of percentage error versus Reynolds number for all three (3) dimensional pipe flow models with constant wall temperature.

Fig. 5i(a-d) shows the plot of percentage error for various models under all flow regimes with a constant heat flux boundary condition on the walls. It can be observed from the figure that the accuracy of the models decreases with an increase in Reynolds number. This means that modelling nanofluid flow is more difficult in a turbulent flow regime. Furthermore, for all models, there is a significant difference between the results obtained under the constant properties assumption and the variable or temperature-dependent properties assumption. The constant properties assumption is best for all the models concerning the simulation of nanofluids. This observation, is because the temperature is always changing in the variable properties case and hence the values of the related variables change during the generation of the solution for the different field variables. These changes may not be properly handled by the numerical solver, resulting in a loss of solution accuracy. There are some highly accurate models; they are dispersion, Buongiorno, and DPM. They all have an accuracy within 5%, with the dispersion model being the best for both constant and temperature-dependent property assumptions. The DPM model seems to do better in turbulent flow than in laminar flow, while the Buongiorno models do better under laminar flow conditions. This is because the DPM model caters to turbulent eddies while Buongiorno's model makes assumptions and does

not agree that all turbulent features are important for nanofluid modelling.

Similarly, Fig. 5ii(a – d) shows no significant difference from Fig. 5i(a – d). This is because the wall boundary conditions have no real difference under fully developed flows. That is, regardless of the wall boundary condition, constant heat flux, or constant wall temperature, the results of heat transfer are the same for fully developed flow. So, henceforth, only constant wall heat flux calculation is considered.

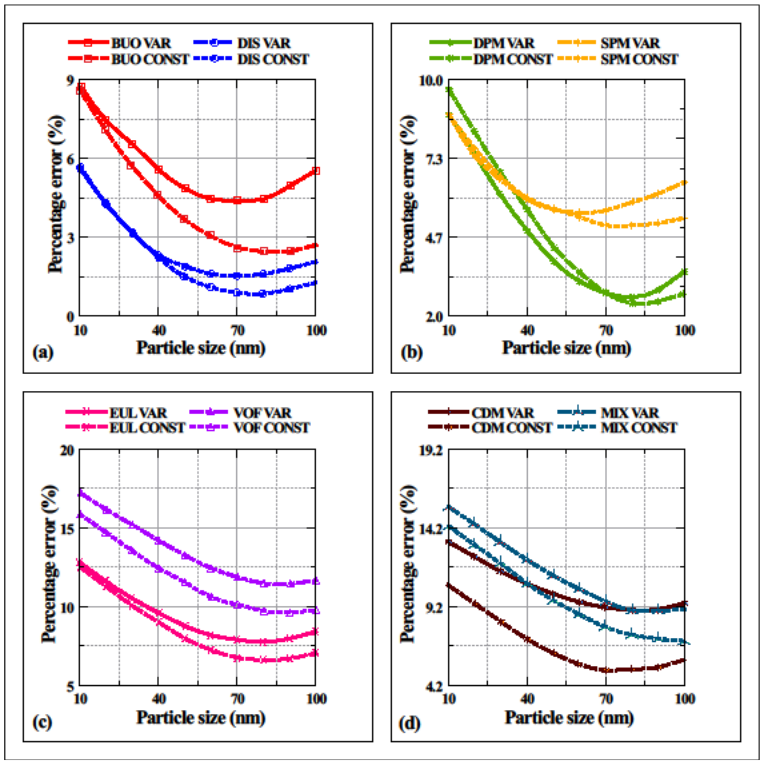

Figure 6(a-d) shows a plot of percentage error versus particle size for all three-dimensional pipe flow models with constant heat temperature.

Fig. 6(a-d) shows the plot of percentage error with particle size for all models under a range of particle sizes. As the particle size increases, all the models give acceptable accuracies. This agrees with the fact that the bigger the size of the particles, the

easier it is for the models to capture the underlining physics. As the sizes grow bigger, they enter the micrometer range that has been comfortably modelled. The dispersion, Buongiorno, and DPM models do well for all particle sizes considered. They also maintain high accuracy for constant property assumptions, as shown in Fig. 5i (a-d), and Fig 5ii (a-d).

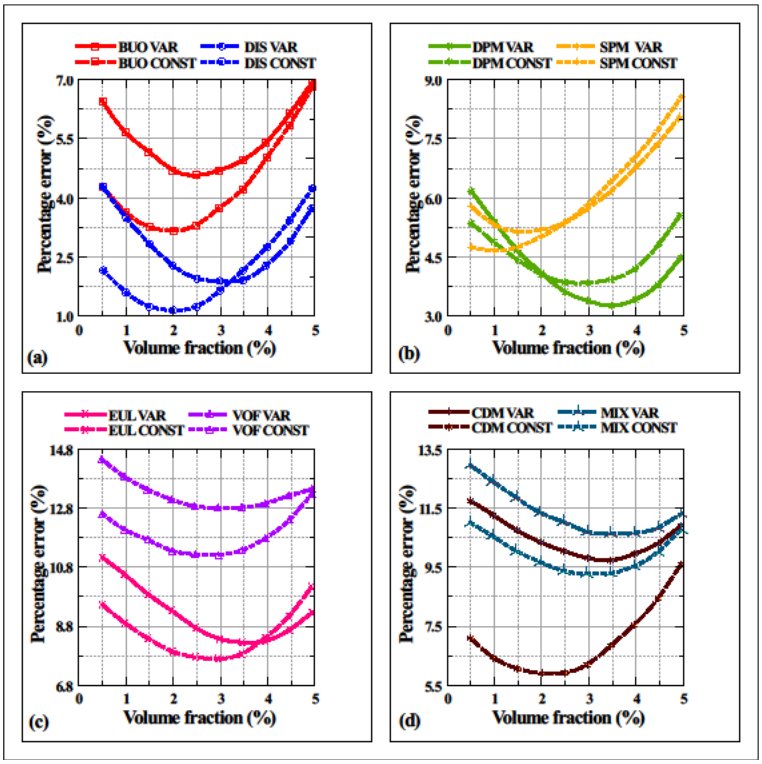

Fig. 7(a-d). A plot of percentage error with volume fraction for all the models with the constant heat temperature for three-dimensional pipe flow

Fig. 7(a-d) shows the plot of percentage error with volume fraction for all models under a range of volume fractions. It can be observed that there exists an optimal volume fraction that gives the best results for all models. This range can be observed to be the 2% to 3.5% volume fraction. The too-low volume fraction is as difficult to model as the too-high volume fraction. This is because the physics of the particle interactions is better captured by these models at this range than at other ranges for nanofluid modelling. The dispersion, Buongiorno, and DPM models do well for all volume fractions considered. They also maintain high accuracy for constant property assumptions, as shown in Fig. 5i (a-d), and Fig 5ii (a-d).

5. Conclusion

The objective of this study was to find the best model to simulate nanofluids under different conditions and give a summary of their strengths and weaknesses regarding nanofluid representation. And, to come up with an algorithm to quickly test out the best models and assumptions out of the plethora of models that should be applied for a particular nanofluid simulation set-up. The neural network algorithm showed a good fit. It was observed from study that the algorithm had a 80% fit between true error and predicted error.

From this study, the major findings are that the dispersion, Buongiorno, and discrete phase models can simulate a very wide coverage of nanofluid configurations with high accuracy. They were found to be accurate for all Reynolds numbers (60 – 59300) considered in this study; all particle sizes (20 – 150) and volume fractions ranged from 2% to 3.5%. The SPM is not a good model for nanofluids and should only be used where there is no other option. It is the suggestion from this work that the mixture model and the single-phase model should be improved by incorporating accurate nanofluid properties into the model.

Nomenclature

b	Biases
D	Diameter (m)
$\bar{h}$	Mean value of observed heat transfer coefficient
N	Number
n	Output
Nu	Nusselt's number
R^2	R-squared value
Re	Reynold's number
SS_{reg}	explained sum of squares
SS_{tot}	total sum of squares
w	weights
x	input

Greek letters

α	arbitrary scaling factor

ϕ	Volume fraction
Superscript	
$pred$	Prediction
Abbreviation	
ANFIS	Adaptive Neuro-Fuzzy Interference System
ANN	Artificial Neural Network
BUO	Buongiorno's Model
CDM	Combined model of discrete phase and mixture phase
CONST	Constant thermophysical properties assumption
DIS	Dispersion Model
DPM	Discrete Phase Model
EUL	Eulerian-Eulerian Model
MIX	Mixture Model
MLP	Multi-layered Perceptron
MSE	Mean Square Error
RBF	Radial Basis Function
SPM	Single-Phase Model
VAR	Variable thermophysical properties assumption
VOF	Volume of Fluid

Acknowledgements

Funding: This work was funded by the Tertiary Education Trust Fund (TETF/ES/UNIV/EDO STATE/TSAS/2019/VOL. I).

Declarations

Funding: This work was funded by the Tertiary Education Trust Fund (TETF/ES/UNIV/EDO STATE/TSAS/2019/VOL. I).

Conflicts of interest/Competing interests: The authors declare that there is NO conflict of interest.

Availability of data and material: All data used were sourced from the open literature and there are references in this material anywhere they appear.

Code availability: Not applicable.

References

[1] S.U. Choi, J.A. Eastman, Enhancing thermal conductivity of fluids with nanoparticles, in, Argonne National Lab., IL (United States), 1995.
[2] M. Gupta, V. Singh, R. Kumar, Z. Said, A review on thermophysical properties of nanofluids and heat transfer applications, Renewable and Sustainable Energy Reviews, 74 (2017) 638-670.
[3] E. Onyiriuka, E. Ikponmwoba, A numerical investigation of mango leaves-water nanofluid under laminar flow regime, Nigerian Journal of Technology, 38 (2019) 348-354.
[4] E. Onyiriuka, O. Ighodaro, A. Adelaja, D. Ewim, S.J.H. Bhattacharyya, A numerical investigation of the heat transfer characteristics of water-based mango bark nanofluid flowing in a double-pipe heat exchanger, 5 (2019) e02416.
[5] T.O. Scott, D.R. Ewim, A.C. Eloka-Eboka, Experimental investigation of natural convection Al2O3-MWCNT/water hybrid nanofluids inside a square cavity, Experimental Heat Transfer, (2022) 1-19.
[6] O.G. Fadodun, D.R.E. Ewim, S.M. Abolarin, Investigation of turbulent entropy production rate with SWCNT/H2O nanofluid flowing in various inwardly corrugated pipes, Heat Transfer.
[7] T.O. Scott, D.R. Ewim, A.C. Eloka-Eboka, Hybrid nanofluids flow and heat transfer in cavities: a technological review, International Journal of Low-Carbon Technologies, 17 (2022) 1104-1123.
[8] D.R.E. Ewim, M.O. Okwu, E.J. Onyiriuka, A.S. Abiodun, S.M. Abolarin, A. Kaood, A quick review of the applications of artificial neural networks (ANN) in the modelling of thermal systems, Engineering and Applied Science Research, 49 (2022) 444-458.
[9] J. Muller, Toyota: Computer-Addled Design?, in, 2010.
[10] A. Dogonchi, D. Ganji, Analytical solution and heat transfer of two-phase nanofluid flow between non-parallel walls considering Joule heating effect, J Powder Technology, 318 (2017) 390-400.
[11] D. Wen, Y. Ding, Experimental investigation into convective heat transfer of nanofluids at the entrance region under laminar flow conditions, International journal of heat and mass transfer, 47 (2004) 5181-5188.
[12] C. Ho, W. Chen, W. Yan, Correlations of heat transfer effectiveness in a minichannel heat sink with water-based suspensions of Al2O3 nanoparticles and/or MEPCM particles, International Journal of Heat and Mass Transfer, 69 (2014) 293-299.
[13] A.E. Taiwo, A.I. Okoji, A.C. Eloka-Eboka, P. Musonge, The role of artificial neural networks in bioproduct development: a case of modeling and optimization studies, in: Current Trends and Advances in Computer-Aided Intelligent Environmental Data Engineering, Elsevier, 2022, pp. 417-431.
[14] S. Rashidi, S. Akar, M. Bovand, R. Ellahi, Volume of fluid model to simulate the nanofluid flow and entropy generation in a single slope solar still, Renewable Energy, 115 (2018) 400-410.

[15] I. Arel, D.C. Rose, T.P. Karnowski, Deep machine learning-a new frontier in artificial intelligence research, IEEE computational intelligence magazine, 5 (2010) 13-18.
[16] D. Ewim, A. Adelaja, E. Onyiriuka, J. Meyer, Z. Huan, Modelling of heat transfer coefficients during condensation inside an enhanced inclined tube, Journal of Thermal Analysis Calorimetry, (2020) 1-13.
[17] V. Bianco, F. Chiacchio, O. Manca, S. Nardini, Numerical investigation of nanofluids forced convection in circular tubes, Applied Thermal Engineering, 29 (2009) 3632-3642.
[18] M.R. Safaei, A. Jahanbin, A. Kianifar, S. Gharehkhani, A.S. Kherbeet, M. Goodarzi, M.J.M. Dahari, s.i.e. sciences, Mathematical modeling for nanofluids simulation: a review of the latest works, (2016).
[19] M. Rostamani, S. Hosseinizadeh, M. Gorji, J. Khodadadi, Numerical study of turbulent forced convection flow of nanofluids in a long horizontal duct considering variable properties, J International Journal of Heat Mass Transfer, 37 (2010) 1426-1431.
[20] B.C. Pak, Y.I. Cho, Hydrodynamic and heat transfer study of dispersed fluids with submicron metallic oxide particles, Experimental Heat Transfer an International Journal, 11 (1998) 151-170.
[21] S.E.B. Maiga, S.J. Palm, C.T. Nguyen, G. Roy, N. Galanis, Heat transfer enhancement by using nanofluids in forced convection flows, International journal of heat and fluid flow, 26 (2005) 530-546.
[22] E. Onyiriuka, A. Obanor, M. Mahdavi, D.R.E. Ewim, Evaluation of single-phase, discrete, mixture and combined model of discrete and mixture phases in predicting nanofluid heat transfer characteristics for laminar and turbulent flow regimes, Advanced Powder Technology, (2018).
[23] M.S. Mojarrad, A. Keshavarz, A. Shokouhi, Nanofluids thermal behavior analysis using a new dispersion model along with single-phase, Heat and Mass Transfer, 49 (2013) 1333-1343.
[24] S.Z. Heris, M.N. Esfahany, S.G. Etemad, Experimental investigation of convective heat transfer of Al2O3/water nanofluid in circular tube, International Journal of Heat and Fluid Flow, 28 (2007) 203-210.
[25] S. Kumar, S.K. Prasad, J. Banerjee, Analysis of flow and thermal field in nanofluid using a single phase thermal dispersion model, J Applied Mathematical Modelling, 34 (2010) 573-592.
[26] A. Albojamal, K. Vafai, Analysis of single phase, discrete and mixture models, in predicting nanofluid transport, J International Journal of Heat Mass Transfer, 114 (2017) 225-237.
[27] O. Mahian, L. Kolsi, M. Amani, P. Estellé, G. Ahmadi, C. Kleinstreuer, J.S. Marshall, M. Siavashi, R.A. Taylor, H. Niazmand, Recent advances in modeling and simulation of nanofluid flows-Part I: Fundamentals and theory, Physics reports, 790 (2019) 1-48.
[28] P. Xu, Z. Wu, A. Mujumdar, B. Yu, Innovative hydrocyclone inlet designs to reduce erosion-induced wear in mineral dewatering processes, J Drying Technology, 27 (2009) 201-211.
[29] M. Safaei, O. Mahian, F. Garoosi, K. Hooman, A. Karimipour, S. Kazi, S.J.T.s.w.j. Gharehkhani, Investigation of micro-and nanosized particle erosion in a 90 pipe bend using a two-phase discrete phase model, 2014 (2014).

[30] I. Behroyan, P. Ganesan, S. He, S. Sivasankaran, M. Transfer, Turbulent forced convection of Cu–water nanofluid: CFD model comparison, J International Communications in Heat, 67 (2015) 163-172.
[31] Y. Chen, Y. Li, Z. Liu, Numerical simulations of forced convection heat transfer and flow characteristics of nanofluids in small tubes using two-phase models, J International Journal of Heat Mass Transfer, 78 (2014) 993-1003.
[32] P. Naphon, L. Nakharintr, Numerical investigation of laminar heat transfer of nanofluid-cooled mini-rectangular fin heat sinks, J Journal of Engineering Physics Thermophysics, 88 (2015) 666-675.
[33] M. Mahdavi, M. Sharifpur, J.P. Meyer, A novel combined model of discrete and mixture phases for nanoparticles in convective turbulent flow, Physics of Fluids, 29 (2017) 082005.
[34] A. Karimipour, M.H. Esfe, M.R. Safaei, D.T. Semiromi, S. Jafari, S.J.P.A.S.M. Kazi, i. Applications, Mixed convection of copper–water nanofluid in a shallow inclined lid driven cavity using the lattice Boltzmann method, 402 (2014) 150-168.
[35] J. Buongiorno, Convective transport in nanofluids, Journal of heat transfer, 128 (2006) 240-250.
[36] G.A. Sheikhzadeh, M. Dastmalchi, H. Khorasanizadeh, Effects of nanoparticles transport mechanisms on Al2O3–water nanofluid natural convection in a square enclosure, J International Journal of Thermal Sciences, 66 (2013) 51-62.
[37] M.R. Mufti, M.I. Qureshi, S. Alkhalaf, S. Iqbal, An Algorithm: Optimal Homotopy Asymptotic Method for Solutions of Systems of Second-Order Boundary Value Problems, J Mathematical Problems in Engineering, 2017 (2017).
[38] P. Hanafizadeh, M. Ashjaee, M. Goharkhah, K. Montazeri, M. Akram, The comparative study of single and two-phase models for magnetite nanofluid forced convection in a tube, J International Communications in Heat Mass Transfer, 65 (2015) 58-70.
[39] B. Vaferi, F. Samimi, E. Pakgohar, D. Mowla, Artificial neural network approach for prediction of thermal behavior of nanofluids flowing through circular tubes, J Powder technology, 267 (2014) 1-10.
[40] Y. Xuan, Q. Li, Investigation on convective heat transfer and flow features of nanofluids, Journal of Heat transfer, 125 (2003) 151-155.
[41] X. Wang, A.S. Mujumdar, Heat transfer characteristics of nanofluids: a review, International journal of thermal sciences, 46 (2007) 1-19.
[42] M. Heyhat, F. Kowsary, A. Rashidi, S.A.V. Esfehani, A. Amrollahi, Experimental investigation of turbulent flow and convective heat transfer characteristics of alumina water nanofluids in fully developed flow regime, International Communications in Heat and Mass Transfer, 39 (2012) 1272-1278.
[43] M. Bahiraei, S. Heshmatian, H. Moayedi, Artificial intelligence in the field of nanofluids: A review on applications and potential future directions, J Powder Technology, (2019).
[44] M. Bahiraei, A comprehensive review on different numerical approaches for simulation in nanofluids: traditional and novel techniques, J Journal of dispersion science technology, 35 (2014) 984-996.
[45] M. Akbari, A. Behzadmehr, F. Shahraki, Fully developed mixed convection in horizontal and inclined tubes with uniform heat flux using nanofluid, International Journal of Heat and Fluid Flow, 29 (2008) 545-556.
[46] M. Akbari, N. Galanis, A. Behzadmehr, Comparative assessment of single and two-phase models for numerical studies of nanofluid turbulent forced convection, International Journal of Heat and Fluid Flow, 37 (2012) 136-146.

[47] A. Albojamal, K. Vafai, Analysis of single phase, discrete and mixture models, in predicting nanofluid transport, International Journal of Heat and Mass Transfer, 114 (2017) 225-237.
[48] K. Anoop, T. Sundararajan, S.K. Das, Effect of particle size on the convective heat transfer in nanofluid in the developing region, International journal of heat and mass transfer, 52 (2009) 2189-2195.
[49] A. Akbarinia, A. Behzadmehr, Numerical study of laminar mixed convection of a nanofluid in horizontal curved tubes, Applied Thermal Engineering, 27 (2007) 1327-1337.
[50] V. Bianco, O. Manca, S. Nardini, Numerical investigation on nanofluids turbulent convection heat transfer inside a circular tube, International Journal of Thermal Sciences, 50 (2011) 341-349.
[51] M. Ghanbarpour, R. Khodabandeh, K. Vafai, An investigation of thermal performance improvement of a cylindrical heat pipe using Al 2 O 3 nanofluid, Heat and Mass Transfer, 53 (2017) 973-983.
[52] L. Godson, B. Raja, D.M. Lal, S. Wongwises, Enhancement of heat transfer using nanofluids—an overview, Renewable and sustainable energy reviews, 14 (2010) 629-641.
[53] Y. He, Y. Men, Y. Zhao, H. Lu, Y. Ding, Numerical investigation into the convective heat transfer of TiO2 nanofluids flowing through a straight tube under the laminar flow conditions, Applied Thermal Engineering, 29 (2009) 1965-1972.
[54] M. Hejazian, M.K. Moraveji, A. Beheshti, Comparative study of Euler and mixture models for turbulent flow of Al2O3 nanofluid inside a horizontal tube, International Communications in Heat and Mass Transfer, 52 (2014) 152-158.
[55] S.Z. Heris, M.N. Esfahany, G. Etemad, Numerical investigation of nanofluid laminar convective heat transfer through a circular tube, Numerical Heat Transfer, Part A: Applications, 52 (2007) 1043-1058.
[56] S.Z. Heris, M.N. Esfahany, G. Etemad, Investigation of CuO/water nanofluid laminar convective heat transfer through a circular tube, Journal of Enhanced Heat Transfer, 13 (2006).
[57] M.K. Moraveji, M. Darabi, S.M.H. Haddad, R. Davarnejad, Modeling of convective heat transfer of a nanofluid in the developing region of tube flow with computational fluid dynamics, International communications in heat and mass transfer, 38 (2011) 1291-1295.
[58] R. Lotfi, Y. Saboohi, A. Rashidi, Numerical study of forced convective heat transfer of nanofluids: comparison of different approaches, International Communications in Heat and Mass Transfer, 37 (2010) 74-78.
[59] S.M. Vanaki, P. Ganesan, H.J.R. Mohammed, S.E. Reviews, Numerical study of convective heat transfer of nanofluids: a review, 54 (2016) 1212-1239.
[60] A.T. Utomo, E.B. Haghighi, A.I. Zavareh, M. Ghanbarpourgeravi, H. Poth, R. Khodabandeh, B. Palm, A.W. Pacek, The effect of nanoparticles on laminar heat transfer in a horizontal tube, International Journal of Heat and Mass Transfer, 69 (2014) 77-91.
[61] M. Saberi, M. Kalbasi, A. Alipourzade, Numerical study of forced convective heat transfer of nanofluids inside a vertical tube, International Journal of Thermal Technologies, 3 (2013) 10-15.
[62] G. Saha, Heat transfer performance investigation of nanofluids flow in pipe, in, University of Glasgow, 2016.

[63] S. Özerinç, A. Yazıcıoğlu, S. Kakaç, Numerical analysis of laminar forced convection with temperature-dependent thermal conductivity of nanofluids and thermal dispersion, International Journal of Thermal Sciences, 62 (2012) 138-148.
[64] A. D'Orazio, Z. Nikkhah, A. Karimipour, Simulation of copper–water nanofluid in a microchannel in slip flow regime using the lattice Boltzmann method with heat flux boundary condition, in: Journal of Physics: Conference Series, IOP Publishing, 2015, pp. 012029.
[65] G. Yang, J. Pennington, V. Rao, J. Sohl-Dickstein, S.S. Schoenholz, A mean field theory of batch normalization, arXiv preprint arXiv:1902.08129, (2019).
[66] N. Tangri, D. Ansell, D. Naimark, Predicting technique survival in peritoneal dialysis patients: comparing artificial neural networks and logistic regression, J Nephrology Dialysis Transplantation, 23 (2008) 2972-2981.
[67] M. Vafaei, R. Eslamloueyan, S. Ayatollahi, Simulation of steam distillation process using neural networks, J Chemical Engineering Research Design, 87 (2009) 997-1002.
[68] H. Salehi, S. Zeinali Heris, M. Koolivand Salooki, S.J.B.J.o.C.E. Noei, Designing a neural network for closed thermosyphon with nanofluid using a genetic algorithm, 28 (2011) 157-168.
[69] K. Hornik, M. Stinchcombe, H.J.N.n. White, Multilayer feedforward networks are universal approximators, 2 (1989) 359-366.
[70] J. Heaton, The Number of Hidden Layers in, 2017.
[71] T. Tieleman, G. Hinton, Lecture 6.5-rmsprop: Divide the gradient by a running average of its recent magnitude, J COURSERA: Neural networks for machine learning, 4 (2012) 26-31.
[72] F. Zou, L. Shen, Z. Jie, W. Zhang, W. Liu, A sufficient condition for convergences of adam and rmsprop, in: Proceedings of the IEEE conference on computer vision and pattern recognition, 2019, pp. 11127-11135.

Chapter 5 Single phase nanofluid thermal conductivity and viscosity prediction using neural networks and its application in a heated pipe

Abstract

This study investigates the single-phase simulation of nanofluid with neural network incorporated into the thermophysical properties in governing equations for the single phase treatment. The thermophysical properties effected are the viscosity and the thermal conductivity as both properties has been the area of contention in the study of nanofluid. The neural network is trained from experimental data gleaned from available literature. The single phase and neural network are setup and solved using finite element method in available commercial code. Grid independence was carried out and the results were validated with experimental data that the neural networks was not trained with. It was observed that the lowest accuracy from the several simulations was 0.679% average percentage error. The results obtained agreed that nanofluids' thermal conductivity and viscosity can be accurately modelled for most single material nanofluids and hence reducing the error in the simulations of nanofluids using the single-phase model which assumes the nanofluids is homogeneous and its properties are enhanced and effective.

Keywords: Nanofluid, Neural network, Modelling, Single-phase model, Thermal conductivity, Viscosity

1. Introduction

1.1. Nanofluid modeling challenge

Numerical studies of nanofluids pose a serious challenge to nanotechnology researchers, this challenge has hampered progress in nanofluids applications by limiting the number of trusted and verified simulation results. Although numerical studies are very important in the product development process. The inconsistent numerical findings by different researchers are also a challenge. Since they use different formulations to represent nanofluid and hence obtain differing results. To overcome these challenges costly experiments must be carried out and repeated many times. This greatly increase the product development time.

Vajjha et al [1] carried out a single phase treatment of nanofluids. Their numerical study was carried out on a three-dimensional flow geometry. The three-dimensional

geometry was flat tubes of an automobile radiator. They studied the heat transfer and laminar flow of two nanofluids: ethylene glycol-water mixture as basefluid and Al_2O_3 and CuO nanoparticles. They accessed the advantage of nanofluids over the base fluid. They observed that the heat transfer coefficient and average friction factor increased whenever the volume fraction was increased. However. Their simulations had a maximum and average deviation of 3.1 % and 1.1 % from the Shah and London correlation in Nusselt number.

Ahmed et al [2] numerically investigated Al_2O_3 -water nanofluid convective heat transfer under laminar flow over tube banks with constant wall temperature conditions. They considered staggered arrangement of circular-tube banks. They observed that the best results were obtained at a transverse pitch ratio of 2.5 and longitudinal pitch ratio of 1.5, nanoparticles volume fraction of 5% over a Reynolds number range. Their results had an 18 % maximum deviation from previous numerical studies.

Moraveji et al [3] in an article, presented the results of a computational fluid dynamics study of the single phase convective heat transfer effect on the nanofluid flow in the developing region of a tube with constant heat flux. They used Al_2O_3-water nanofluid with particle sizes of 45 and 150 nm and particle volume fractions of 1, 2, 4 and 6 wt.%. They studied a range of Reynolds number and obtained a Nusselt number equation in terms of dimensionless numbers. They obtained a maximum error of 10%.

Namburu et al [4] numerically studied CuO, Al_2O_3 and SiO_2 in ethylene glycol and water mixture in turbulent flow. They used a circular tube with constant heat flux condition. They developed and validated new correlations for viscosity that depends on volume fraction and temperature from experimental data. However, their study showed a maximum and average deviation of 3.2 % and 1.9 % from the Blasius theoretical equation.

Özerinç et al [5] in an article stated that “In order to utilize nanofluids in practical applications, accurate prediction of forced convection heat transfer of nanofluids is necessary”. They used the nanofluid thermophysical properties to apply the classical correlations of forced convection heat transfer developed for the flow of pure fluids to nanofluids. They compared their results with experimental data and observed that their method underestimates the heat transfer enhancement. Furthermore, they studied the thermal dispersion by using single-phase and temperature dependent thermal conductivity and observed that the single-phase treatment with temperature dependent thermal conductivity and thermal dispersion was an accurate way of

capturing the heat transfer enhancement. However, they obtained a numerical result with an 11 % deviation from the experimental data.

From the above review we can observe high discrepancies in similar simulation studies. Furthermore, nanofluids can technically be applied in situations where increase in heat transfer is desirable for product development. Some main applications of nanofluid are given in Saidur et al [6]: Space, defense and ships, nuclear reactor, medical application, antibacterial activities, grinding, cooling electronics, chillers, domestic refrigerator, engine cooling/vehicle thermal management, detection of knock occurrence in a gas spark ignition engine, coolant in machining, cooling of diesel electric generator, diesel combustion, boiler flue gas temperature reduction, solar water heating, cooling and heating in buildings, transformers use, heat exchangers, drilling, new sensors for improving exploration, application of nanofluids in thermal absorption system, application in fuel cell.

In conclusion, accurate simulation for nanofluids is critical in product development, and the simplicity of the simulation improves the process even more. A simulation that is less computationally expensive will ensure that results are generated quickly. Furthermore, no model exists that accurately accounts for a large number of nanofluids with only the properties of the basefluid and the nanoparticle known; the resulting model from this study has been designed and proven to be effective in doing so - making accurate predictions of the thermal conductivity and viscosity of all single material nanofluids. It has also been demonstrated that the simulations are more accurate in predicting temperature profiles of flows in circular cross-sectional pipes.

The procedure presented in this study provides a method that eliminates the need for correlations. It is also applicable to most nanofluids containing a single type of nanoparticle as well as a basefluid.

2. Thermophysical properties of nanofluids

When solid particles of small size (1-100 nm) are added to a conventional fluid the property of the new fluid is enhanced. Researchers have suggested several correlations for representing these new properties but there are still problems with regards to the proper correlations for viscosity and thermal conductivity for many nanofluids with an acceptable accuracy [7].

2.1. Nanofluid density and specific heat

The following equations are used for determining the density and specific heat of nanofluids [7].

$$\rho_{nf} = (1 - \phi)\rho_{bf} + \phi\rho_p \qquad 1$$

ρ_{nf} represents the density of the nanofluid, ϕ represents the volume fraction of the nanoparticles, ρ_{bf} represents the density of the basefluid, and ρ_p represents the density of the nanoparticle.

$$Cp_{nf} = \frac{(1-\phi)Cp_{bf}\rho_{bf}+\phi Cp_p\rho_p}{\rho_{nf}} \quad 2$$

Cp_{nf} represents the specific heat of the nanofluid, Cp_{bf} represents the specific heat of the basefluid and the Cp_p represents the specific heat of the nanoparticles.

2.2. Nanofluid viscosity and thermal conductivity

For the nanofluid viscosity and thermal conductivity individual neural network models were developed. Data was gleaned from experimental studies in open literature. The data of thermal conductivity gleaned included information of the following nanofluids: Al – transformer oil [8], CuO – transformer oil [8], CNT – engine oil [9], Al – engine oil [9], $Mg(OH)_2$ – ethylene glycol [10], Al_2O_3 - ethylene glycol [11], ZnO - ethylene glycol [12], TiO_2 - ethylene glycol [9], SiC - ethylene glycol [13], CuO - ethylene glycol [8], Al - ethylene glycol [9], Al_2Cu - ethylene glycol [14], Ag_2Al - ethylene glycol [14], SiC – water [13], Al_2O_3 – water [15], TiO_2 – water [16], Al – water [8], CuO – water [8], Ag_2Al – water[14], Ag_2Cu – water[14], SiO_2 – water [17].

The data of viscosity gleaned included information of the following nanofluids: TiO_2 – water [9], CuO – ethylene glycol [18], Al_2O_3 – ethylene glycol [18], CeO_2 – ethylene glycol [18], $Mg(OH)_2$ – ethylene glycol [10], Al_2O_3 – water [19], SiO_2 – water [17], CuO – water [20], ZnO – ethylene glycol [12].

The data for viscosity was 885 rows and each having 9 properties. The data for thermal conductivity was 489 rows and each having 10 properties.

Table 1

Table 1

Variable selected as inputs and outputs in this study.

Column name	Meaning	Units
d_p	Particle size: Represents the average size of the nanoparticle	nm
ϕ	Particle volume fraction: Represents the concentration of the particles in the host fluid	%
Cp_p	Specific heat capacity of the nanoparticles	J/kgK
k_p	Thermal conductivity of the nanoparticles	W/mK
T	Temperature of fluid	K
ρ_p	density of the nanoparticles	kg/m^3
Cp_{bf}	Specific heat capacity of the basefluid	J/kgK
k_{nf}	Thermal conductivity of the nanofluid	W/mK
μ_{bf}	Viscosity of the basefluid	Pa. s
μ_{nf}	Viscosity of the nanofluid	Pa. s

k_{bf}	Thermal conductivity of the basefluid	W/mK
ρ_{bf}	density of the basefluid	kg/m^3

Table 1, shows the definition, meaning and units of each variable selected as inputs and outputs in this study.

3. Neural network architecture

3.1. Viscosity modeling

The neural network model as shown in Fig. 1 consists of one hidden layer with 10 neurons and the Log-Sigmoid transfer function, the output layer consisted of the linear transfer function. The network takes eight variables as inputs. They are nanoparticle specific heat, density, particle size, volume fraction, Temperature of the fluid, density, specific heat capacity, and viscosity of the basefluid. The training algorithm is the Levenberg-Marquardt algorithm. This algorithm utilizes more memory however takes lesser time.

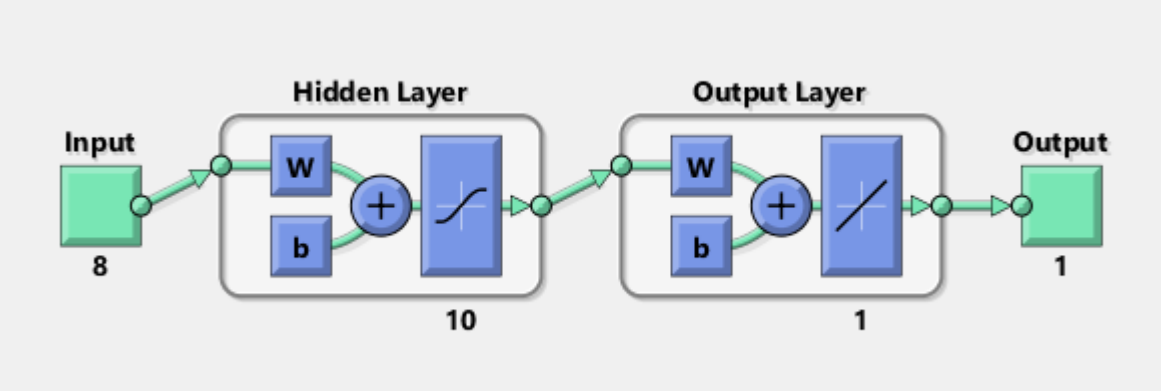

Figure 1 Neural network architecture for the nanofluid viscosity

3.2. Thermal conductivity modeling

The neural network model as shown in Fig. 2 consists of one hidden layer with 10 neurons and the Log-Sigmoid transfer function, the output layer consisted of the linear transfer function. The network takes nine variables as inputs. They are nanoparticle specific heat, density, thermal conductivity, particle size, volume fraction, Temperature of the fluid, density, specific heat capacity, and thermal conductivity of the basefluid. The training algorithm is the Levenberg-Marquardt algorithm. This algorithm uses more memory but less time. When generalization has plateaued (this is shown by the increase of the validation samples' mean squared error) the training automatically stops.

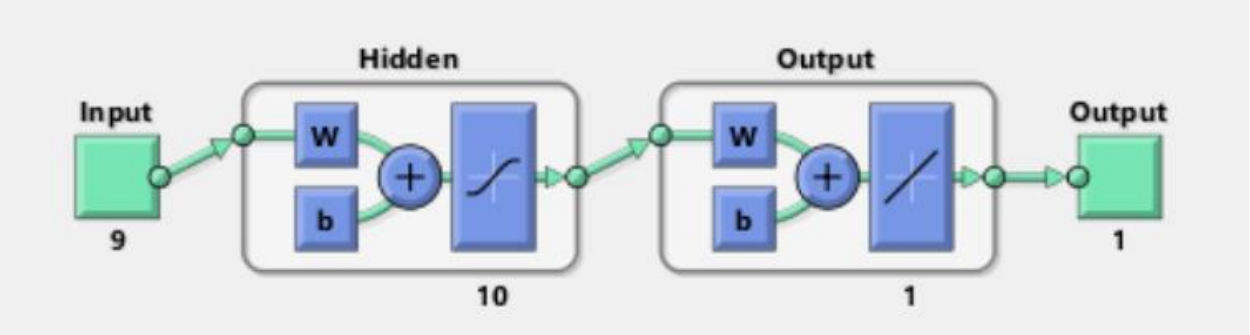

Figure 2 Neural network architecture for the nanofluid thermal conductivity

3.3. Governing equations

The following equations represents the single phase assumption for nanofluids [21]. In this formulation the thermophysical property of the fluid (the density, viscosity, specific heat capacity and thermal conductivity) is replaced with those of the nanofluid. The viscosity and thermal conductivity of the nanofluid are obtained directly from the neural network model given the individual properties of the nanoparticles and the basefluid along with the volume fraction, particle size and fluid temperature. However, the specific heat capacity and density of the nanofluids are computed from Equations 1 and 2.

Continuity

$$\nabla.\left(\rho_{nf}\vec{\boldsymbol{v}}\right) = 0 \qquad 3$$

$\nabla.$ represents the divergence of the velocity vector $\vec{\boldsymbol{v}}$ (m/s) and it results in a scalar, $\vec{\boldsymbol{v}}$ represents the velocity of flow through the pipe.

Momentum

$$\nabla.\left(\rho_{nf}\vec{\boldsymbol{v}}\vec{\boldsymbol{v}}\right) = -\nabla P + \nabla.\left(\mu_{nf}\nabla\vec{\boldsymbol{v}}\right) \qquad 4$$

The P (Pa. s) is the pressure of the fluid through the pipe.

Energy

$$\nabla.\left(\rho_{nf}\vec{v}\,Cp_{nf}\,T\right)=\nabla.\left(k_{nf}\nabla\,T\right) \quad 5$$

T (K) represents the temperature of the nanofluid flow in the pipe and k_{nf}(W/mK) is the thermal conductivity of the nanofluid.

3.4. Simulation Setup

The different components of the simulation are presented here:

Table 2

The numerical simulation values for the nanofluids considered.

Nanoparticle type	**Al_2O_3**	**CuO**	**TiO_2**	**ZrO_2**
Cp_p **(J/kgK)**	680	551	710	418
ρ_p **(kg/m³)**	3970	6000	4170	5600
d_p **(nm)**	40	40	21	50
ϕ **(%)**	0.25	0.003	1.18	1.32
ρ_{bf} **(kg/m³)**	998.2	998.2	998.2	998.2
Cp_{bf} **(J/kgK)**	4182	4182	4182	4182
μ_{bf} **(Pa. s)**	0.001003	0.001003	0.001003	0.001003
k_p **(W/mK)**	40	33	13.7	2
k_{bf} **(W/mK)**	0.6	0.6	0.6	0.6

Table 2, shows the specific numerical values of 4 water based nanofluids used in this study namely: Al_2O_3, CuO, TiO_2, ZrO_2 – water.

Table 3

Boundary conditions and geometrical configuration from unseen data gotten from literature.

Nanofluid	**Al_2O_3**	**CuO**	**TiO_2**	**ZrO_2**
Geometry (Diameter, Length)	4.5 mm, 1 m	8 mm, 1.5 m	5 mm, 2 m	4.5 mm, 1.01 m

Wall (Laminar)	Velocity = 0 m/s (No slip condition)	Velocity = 0 m/s (No slip condition)	Velocity = 0 m/s (No slip condition)	Velocity = 0 m/s (No slip condition)
Inlet	Velocity = 0.212 m/s	Velocity = 0.17 m/s	Velocity = 0.315 m/s	Velocity = 0.062 m/s
Outlet	Pressure = 1 atm	Pressure = 1 atm	Pressure = 1 atm	Pressure = 1 atm
Inflow (Heat transfer)	295 K	290 K	295 K	295.24 K
Wall (Heat flux)	2000 W/m2	7960 W/m2	4000 W/m2	16308 W/m2

Table 3 shows the four scenarios and nanofluids settings that were considered in this study, they were obtained from available literature [22-26].

Table 4.

Mesh settings

Mesh No	**Mesh 1**	**Mesh 2**	**Mesh 3**
Maximum element size	2.49 E -04	3.2 E -04	9.25 E -05
Minimum element size	7.12 E -06	1.42 E -05	1.07 E -06
Curvature factor	0.3	0.3	0.25
Maximum element growth rate	1.13	1.15	1.08
Predefined size	Fine	Finer	Extra fine
No of elements	92828	243777	653509

Table 4, shows the three mesh sizes that were investigated.

3.4.1. COMSOL solver settings

The constant Newton non-linear method with a maximum iteration of 1000 and termination by solution was applied along with the Parallel Direct Solver for handling

a large system of sparse linear equations on multicore architectures that are using a shared-memory, a pivoting perturbation of 1E-13.

4. Results and discussion

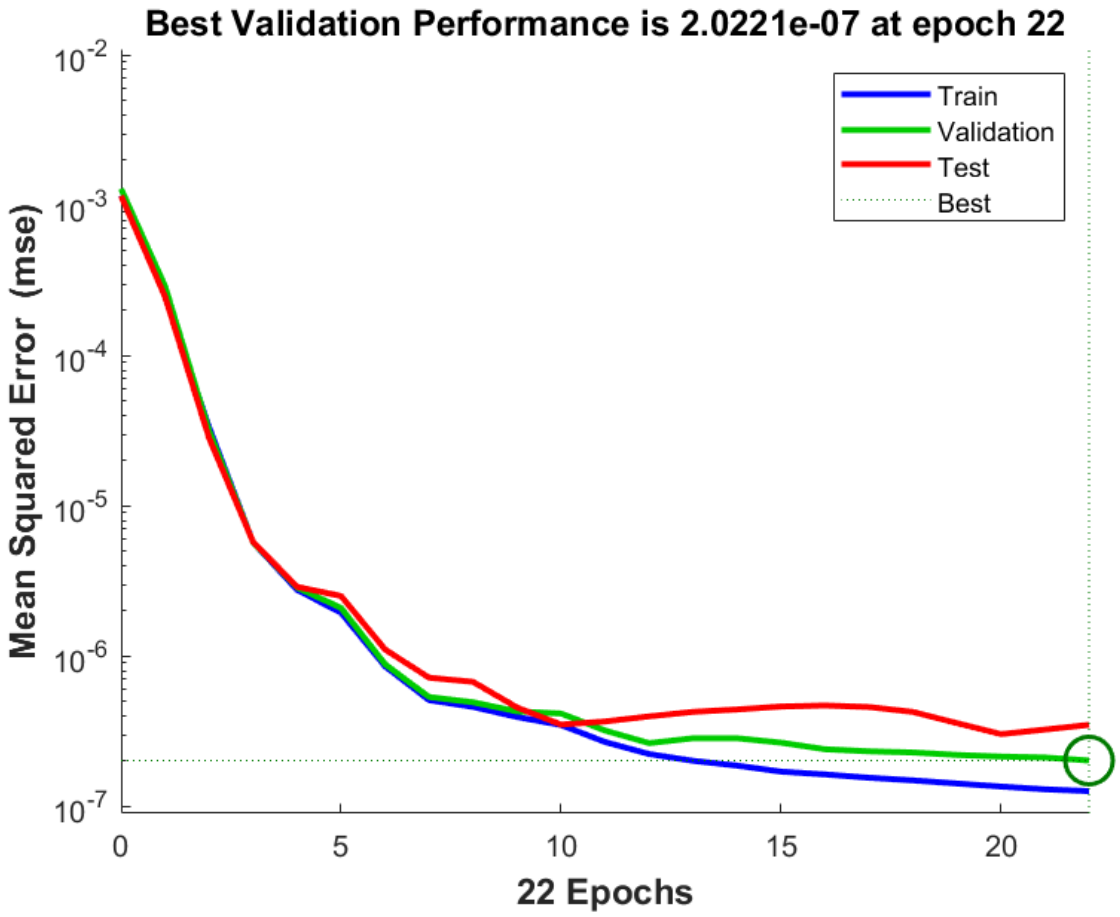

Figure 3 Neural network performance plot for nanofluid viscosity

Fig.3 shows the plot of mean squared error with epochs, an epoch represents the number of times all the training vectors are used to update the weights. The mean squared error is the computation of the square of the mean error between the observations and predictions. The best performance was gotten at the 22nd epoch.

We can observe the network converge smoothly implying that the network was able to find an optimal solution and that the network had a possibly ideal configuration. We can also observe that all the curves converge to the same point. It shows that the network performs equally well in both training and validation. A model that is under fit will have a high training and testing error, while one that overfits will have extremely low training error but high testing error. But in this case the errors are about the same range and relatively low.

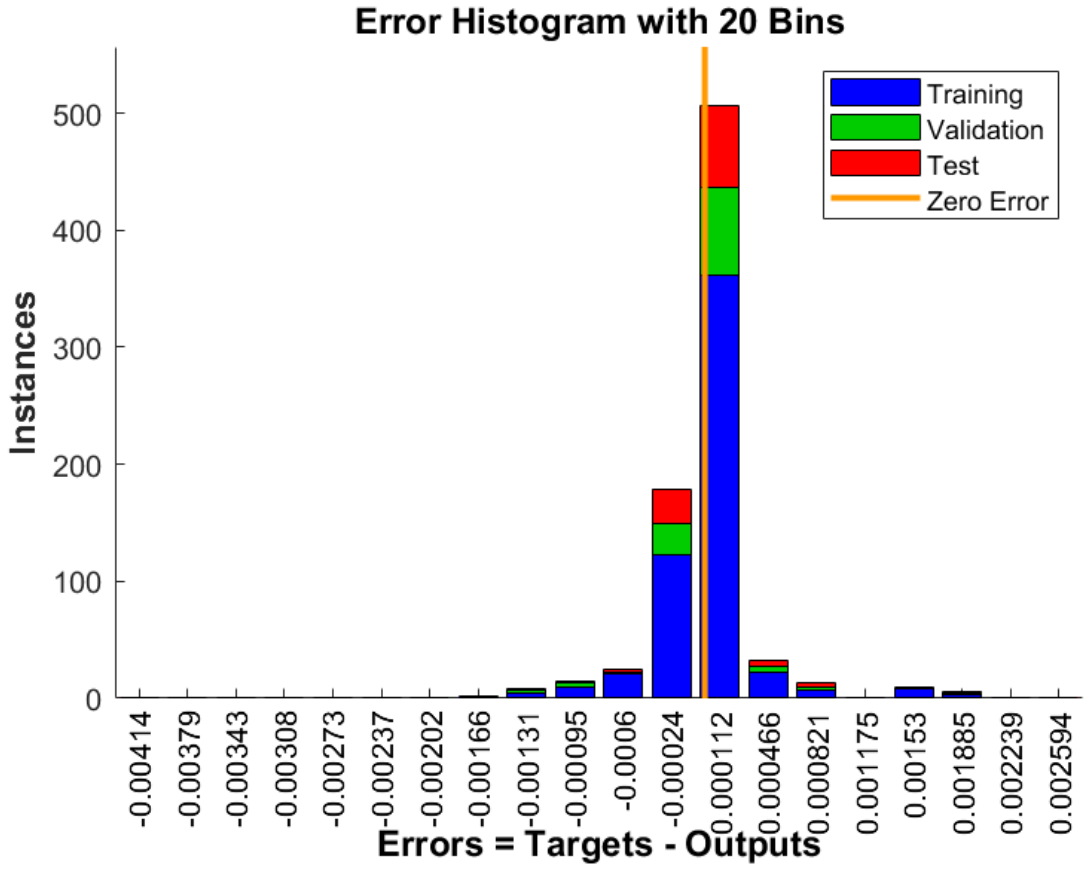

Figure 4 Neural network error histogram plot for nanofluid viscosity

Fig.4 shows the error histogram with 20 bins. It is the plot of the error and the corresponding instances in the data for training, validation, and testing. Bins are the number of vertical bars being observed on the graph. The total error ranges from the leftmost (-0.00414) to the rightmost (0.002594). A large part of the data (training, validation, and test data) falls into the 0.000112 error bin which is within the zero-error range.

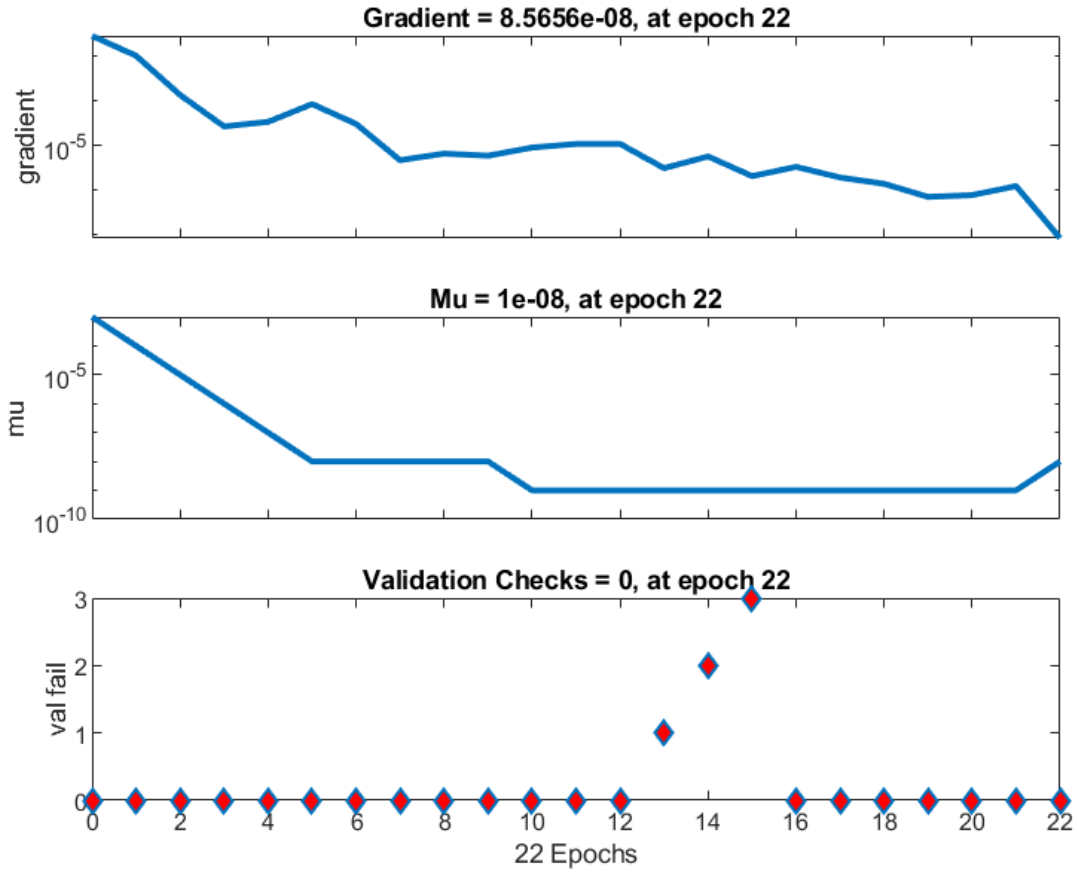

Figure 5 Neural network train state plot for nanofluid viscosity

Fig.5 shows the change of gradient, mu, validation fail with epochs. At epoch 22, the gradient is 8.5656e-08, which is relatively small, this means the training and testing of the network is good. It can also be observed that the gradient decreases with epoch. The validation check is zero at the 22nd epoch.

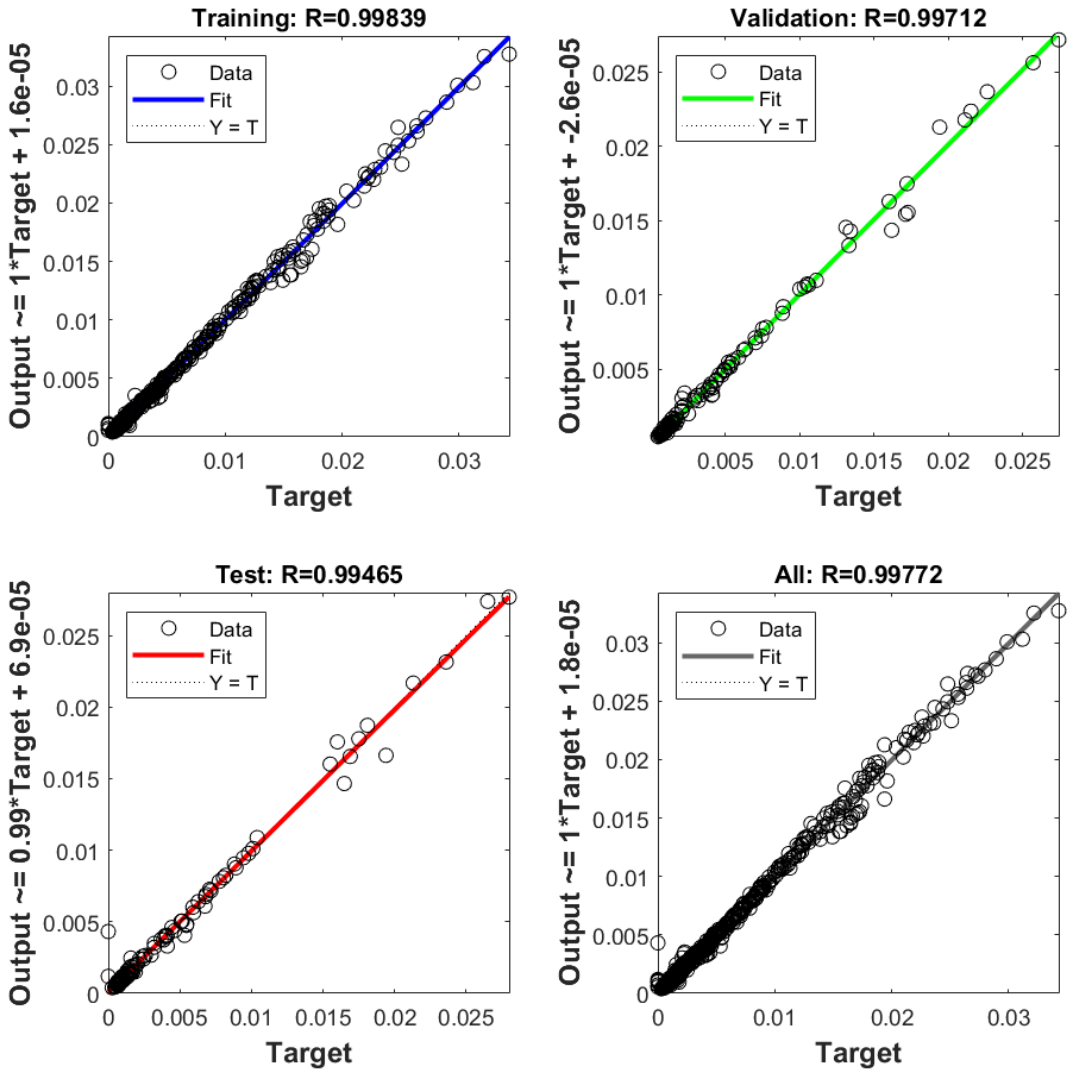

Figure 6 Neural network regression plot for nanofluid viscosity

Fig. 6 shows the regression plot for the training, validation, test, and all of them together. The training set has an R-square of 0.99839, the validation set had an R-square of 0.99712, the test set had an R-square of 0.99465, while when all the datasets are considered as a whole, we have an R square of 0.99772. The R-square value is very close to 1, showing a good fit of the neural network to all the data combinations from training, validation, test, and all.

4.1. Thermal conductivity

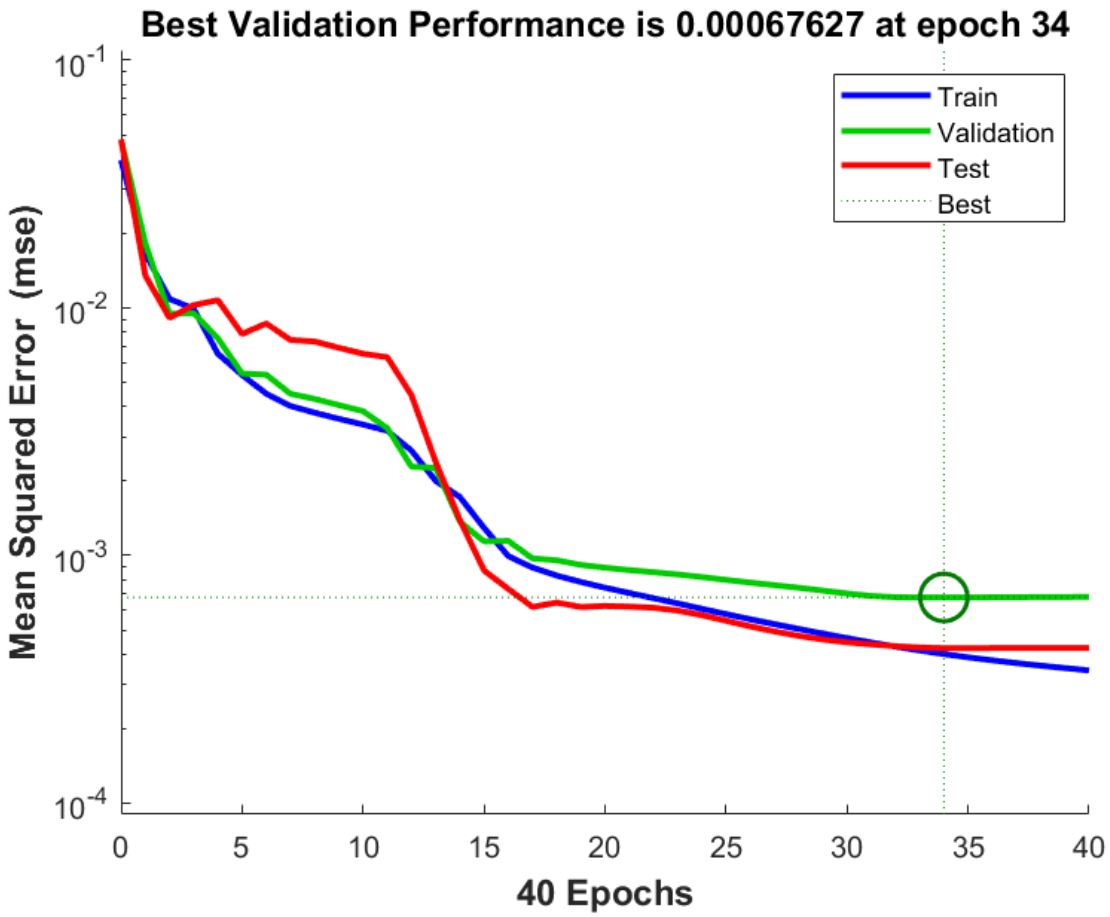

Figure 7 Neural network performance plot for nanofluid thermal conductivity

Fig. 7 shows the performance plot of the neural network for nanofluid thermal conductivity. From the plot the generalization stops improving at epoch 34 and hence the training is stopped. The convergence of the neural network can be observed. The best validation performance was found to be 0.00067627 at the 34th epoch.

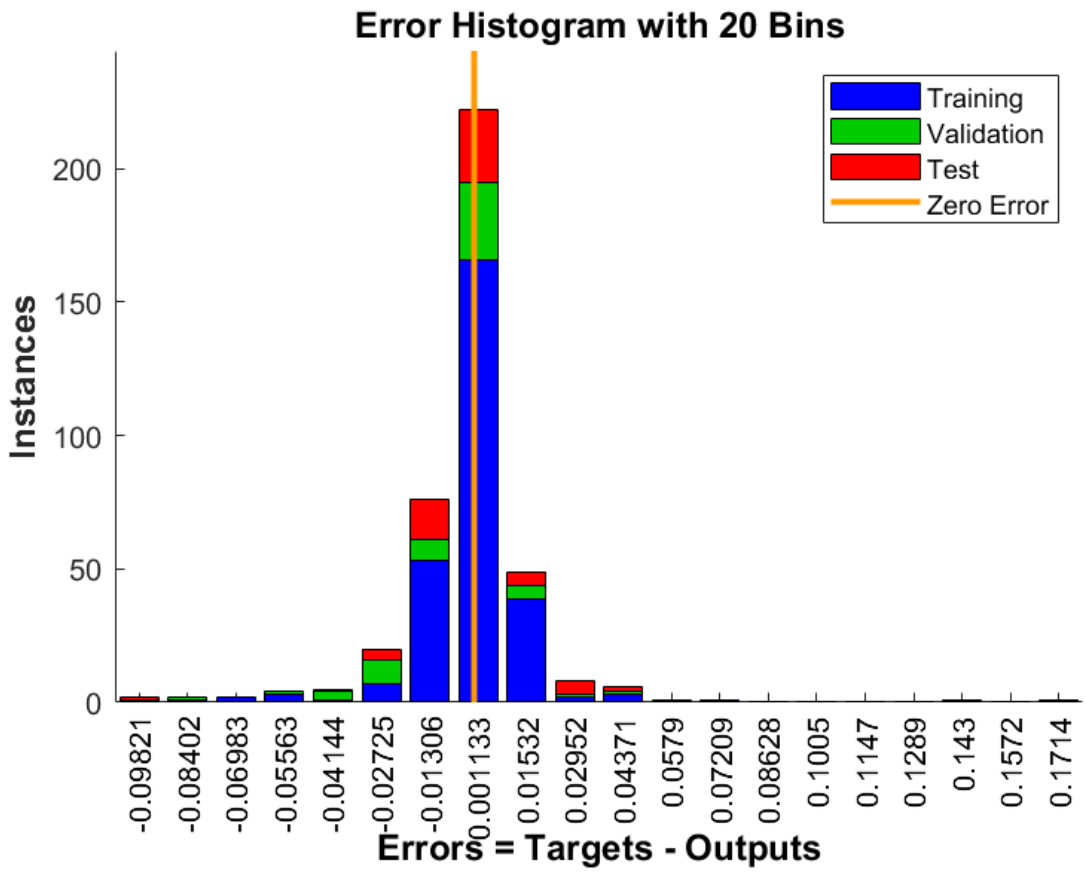

Figure 8 Neural network error histogram plot for nanofluid thermal conductivity

Fig. 8 shows the error histogram plot for the nanofluid thermal conductivity. It can be observed that most of the dataset fell within the error of 0.001133 close to the zero error. The error in all datasets falls within -0.09821 (leftmost) and 0.1714 (rightmost).

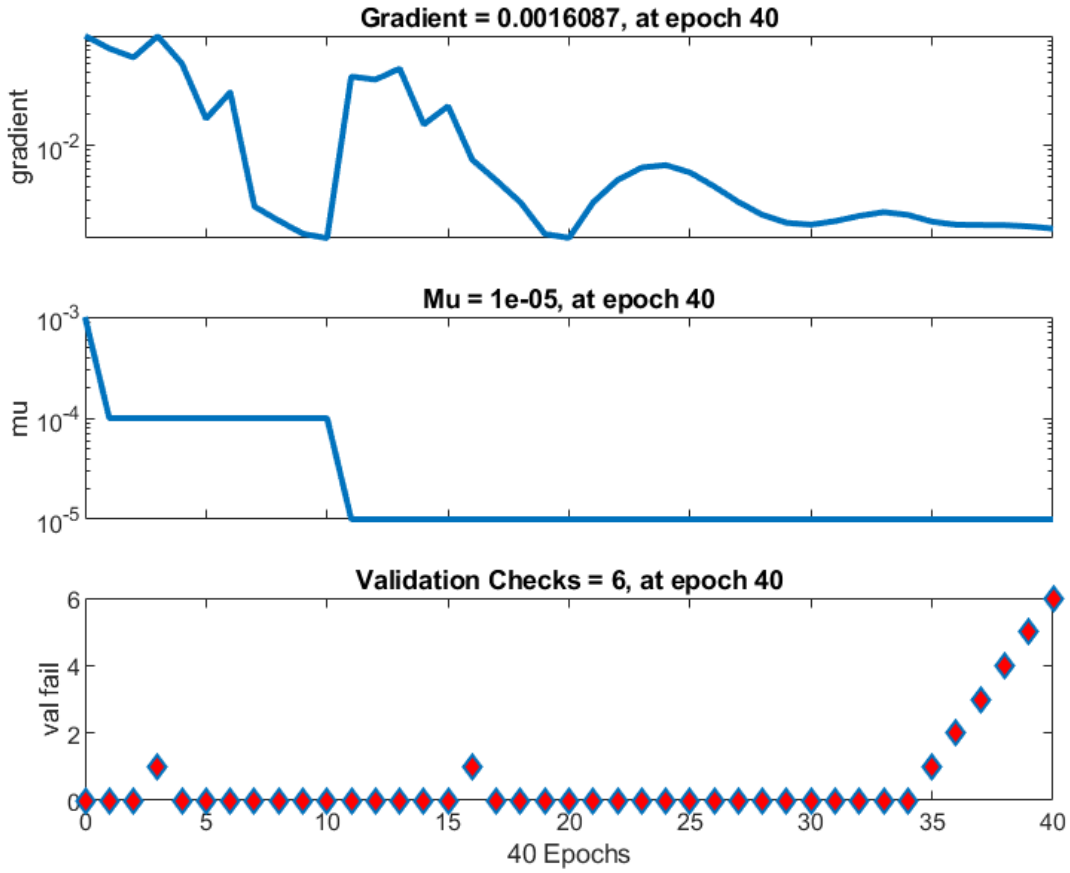

Figure 9 Neural network train state plot for nanofluid thermal conductivity

Fig. 9 shows the train state for the nanofluid thermal conductivity. It can be observed that the gradient decreased with epoch. The mu also decreased with epoch. The validation checks had six consecutive failures from the 34th epoch. Which indicates that the network had stopped generalizing.

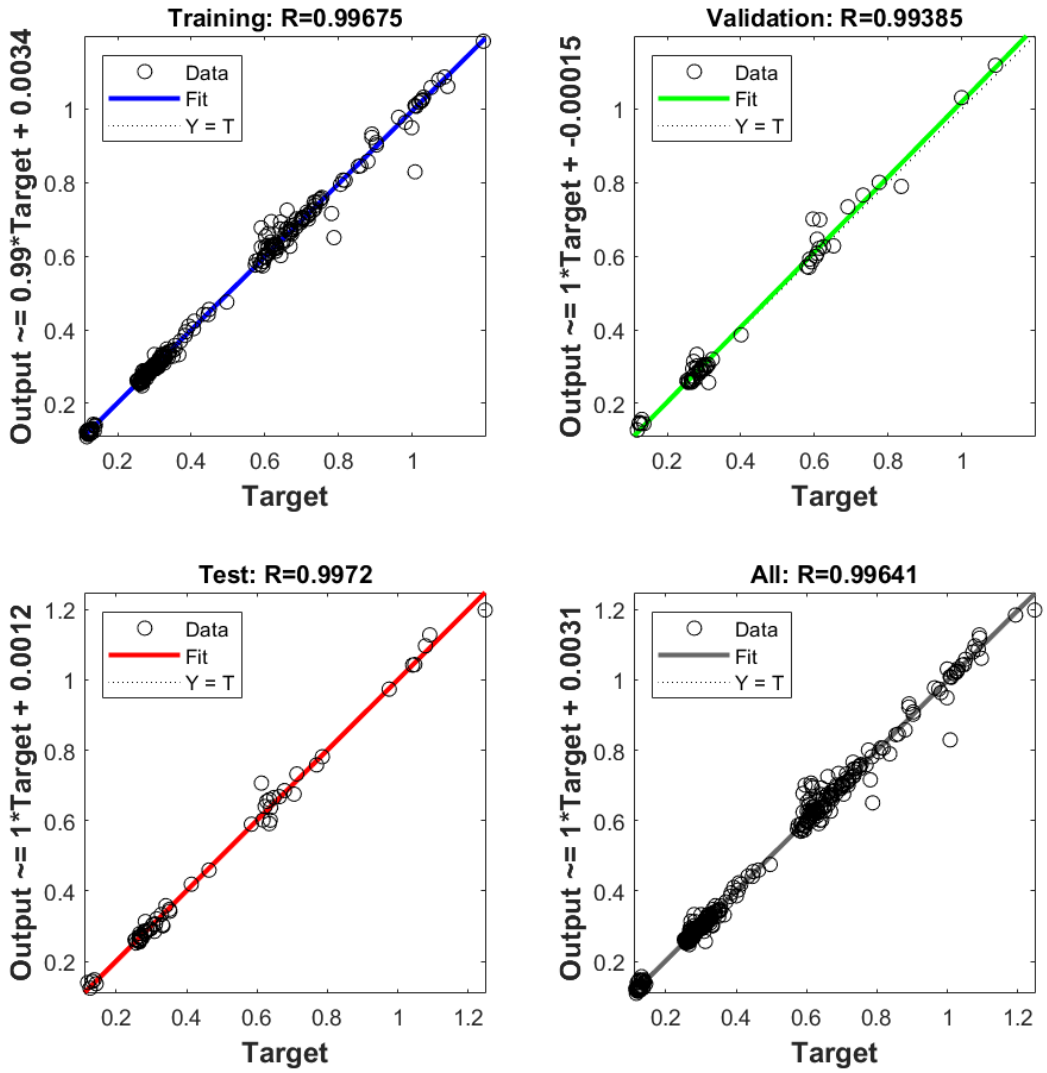

Figure 10 Neural network regression plot for nanofluid thermal conductivity

Fig. 10 shows the regression plot of the neural network for nanofluid thermal conductivity. It captures the R-square for all data combinations: the training set had an R-square of 0.99675, the validation set had R-square of 0.99385, the test set had an R-square of 0.9972, while the whole data set had an R-square of 0.99641. It is worthy of note that the R-squared for all dataset combination was close to 1 indicating a good fit of the neural network with the data sets.

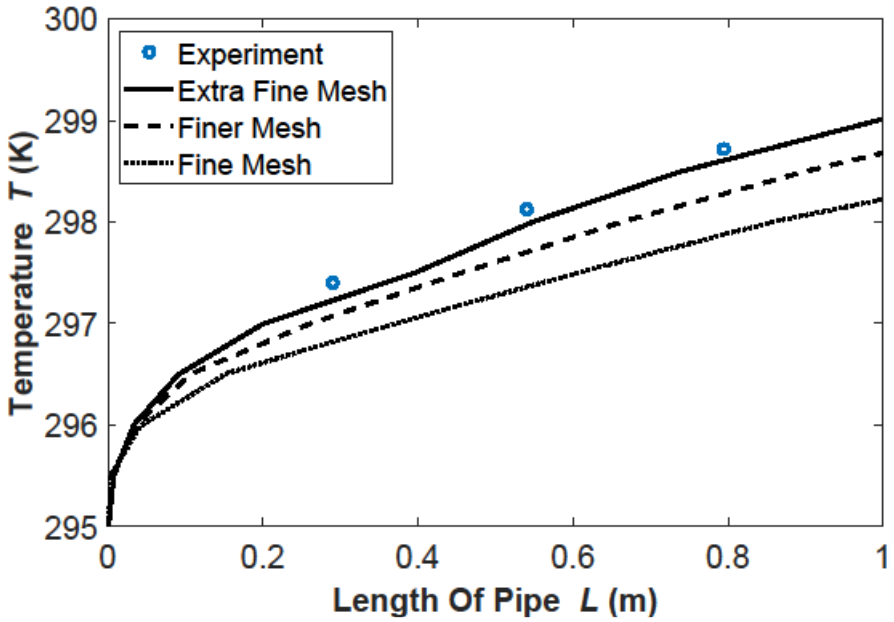

Figure 11 Grid convergence

Fig. 11 shows the grid convergence. The plot of pipe wall temperature with length of pipe was used. The temperature was shown to increase with pipe length as expected physically when there is a heat flux boundary condition on the walls of the pipe. The grid converges to the experimental results. The experimental data was gotten from the work of Kim et al [27] with Al_2O_3-water nanofluid. Three mesh sizes (fine mesh, finer mesh, and extra fine mesh) were tested, and the test stopped at the mesh that gave the most accurate results. The average percentage deviations of the meshes from the experimental data are fine mesh (0.0224%), finer mesh (0.0165%), extra fine mesh (~0%). It also shows the grid independence as the mesh deviation from each other is very less than 1%) meaning the results will not change with the mesh sizes studied. It also shows that the nanofluid thermal characteristics was accurately resolved.

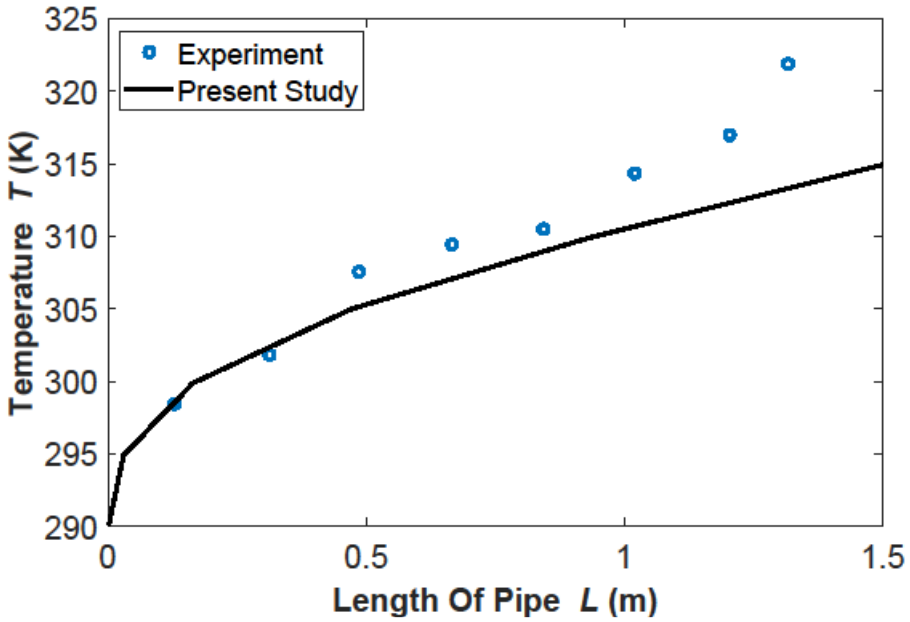

Figure 12 Plot of temperature with length of pipe for CuO-water nanofluid

Fig. 12 shows the plot of temperature with the length of pipe for experimental data of Asirvatham et al [23]. The CuO-water nanofluid was used for the test. A good fit of the experimental results and the simulation with neural network properties can be observed. The average percentage error was found to be 0.679%. This implies an accurate resolution of the nanofluid thermal flow. We can also observe the maximum deviation from the experimental work occurs at tail end of the pipe.

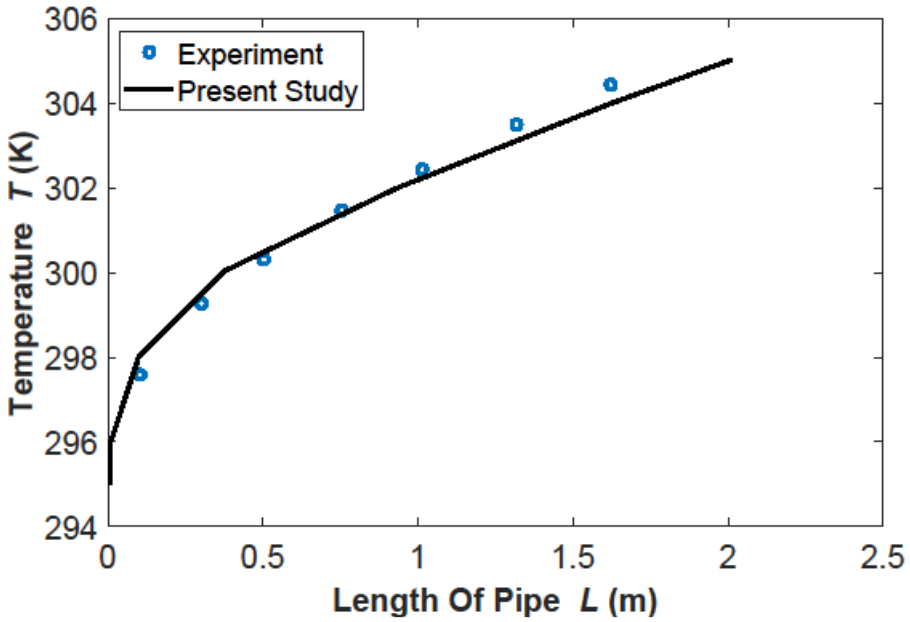

Figure 13 Plot of temperature with length of pipe for TiO2-water nanofluid

Fig. 13 shows the plot of temperature with the length of pipe for experimental data of Murshed et al [24]. The TiO_2-water nanofluid was used for the test. A good fit of the experimental results and the simulation with neural network properties can be observed. The average percentage error was found to be ~0%. This shows that the nanofluid thermal flow was accurately resolved.

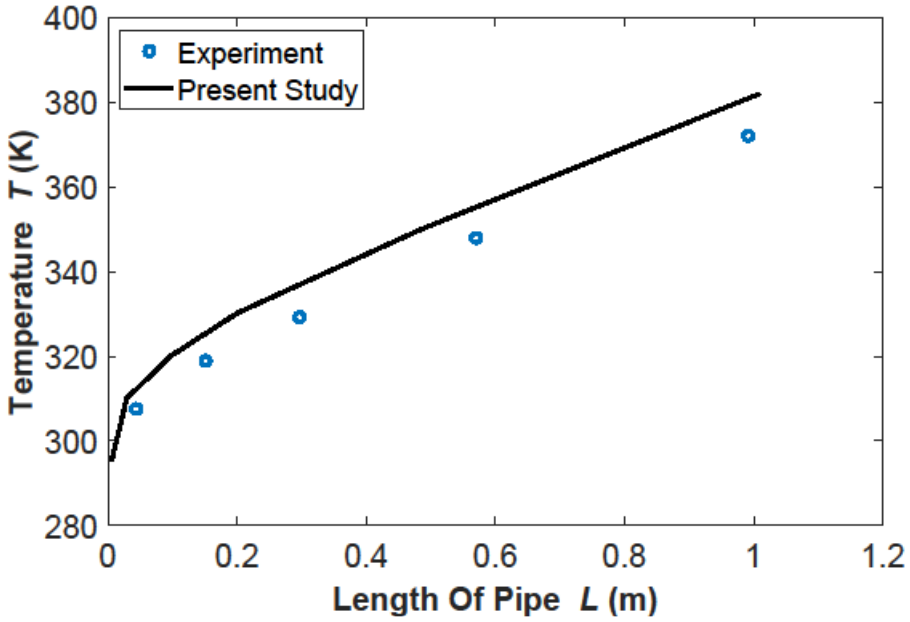

Figure 14 Plot of temperature with length of pipe for ZrO2-water nanofluid

Fig. 14 shows the plot of temperature with the length of pipe for experimental data of Rea et al [25]. The ZrO_2-water nanofluid was used for the test. A good fit of the experimental results and the simulation with neural network properties can be

observed. The average percentage error was found to be ~0.067%. This shows that the nanofluid thermal flow was accurately resolved. Additionally, this nanofluid was not even part of the dataset. This goes to show the procedure is fully verified and validated since the neural network can generalize for even a sample that its properties were not captured in the data collection step.

4.2. Summary of Results

First, Fig. 11 illustrated the grid convergence. The pipe's length was shown on the X-axis in meters (m), while the temperature was shown on the Y-axis in Kelvin (K). Three mesh sizes—fine, finer, and extra fine—were presented, and their solutions were contrasted with the findings of Kim et al's experimental work [27]. An observed convergence to the solution led to the selection of a mesh. The temperature versus pipe length plot for the nanofluids CuO-water, TiO_2-water, and ZrO_2-water was then shown in Figs. 12–14. These plots were displayed to demonstrate how the neural network can be generalized. The last listed nanofluid in these graphs were not present when the neural network was being trained. These charts demonstrate how well the neural network model fits the experimental data.

Thus, we are able to confirm that this strategy of choosing characteristics specific to nanofluid samples can result in generalized models.

4.3. Use of the study’s model

The resulting models are two models that read the temperature from the simulation as well as the other input parameters that were used as inputs to the model and return the thermal conductivity and viscosity of the nanofluid as inputs to the single phase model.

In this study, for example, the models were two MATLAB functions that read the temperature from the COMSOL simulation process as well as other input parameters that the models were trained with. It then returns the thermal conductivity and viscosity of the nanofluid as inputs to COMSOL’s single phase solver, which computes accurate solutions for the single phase model.

The thermal conductivity and viscosity of a single material nanofluid of interest are predicted by this model. It includes the majority of the regularly used single material nanofluids and provides more accurate predictions of thermal conductivity and viscosity of nanofluids than other models [28-33].

It employs freely available data as input, therefore no precomputation of attributes is required. Furthermore, the model is a straightforward model with a straightforward regression neural network architecture. It also returns a prediction quickly when the inputs are passed to it. A approach for validating the model's efficacy was used. The method utilized involved testing the model using out-of-sample data that had not been viewed by the neural network during training and was organized to represent different nanofluid types that had not been used in training the model.

The model is simple to implement in a commercial computational fluid dynamics tool such as COMSOL.

The model was created in such a way that a general model could be derived. The inputs were carefully chosen so that it could uniquely represent many different types of nanofluids. Other models primarily choose aspects that are not unique to nanofluids.

Usage Instructions (A MATLAB and COMSOL Scenario)

Step 1: Collect data

Similar information might be obtained from the books or other sources.

Step 2: Choose a feature

Features can be chosen based on the model's ability to be unique to each nanofluid type.

Step 3: Model development

The model is trained using appropriate activation functions, such as the Log-Sigmoid function and a architecture.

Step 4: Model testing 1

This is the first round of accuracy testing for the model. Only 15% of the data available is utilized.

Step 5: Model testing 2

This is where the model is evaluated against previously unseen nanofluid kinds during training and testing 1.

Step 6: Deploy the model.

Firstly, configure the pipe geometry, then set up and connect various physics (Single phase model)

At this point, two COMSOL functions with the identical names as in MATLAB are created.

The names are then passed as values for the thermal conductivity and viscosity of the COMSOL and MATLAB LiveLink setup.

Other material properties should be assigned.

Use the computational fluid dynamics solver to compute the results.

Plot and assess the results

4.4. Present Study limitations

The goal of this research was not to be able to foretell the thermophysical characteristics of hybrid nanofluids. The harnessing of the physical behavior of single material nanofluid was a direct byproduct of the process even though this was not the focus because model generalization was the procedure's main objective.

5. Conclusion

This study has demonstrated that single-phase models and neural networks are both capable of providing accurate simulations of nanofluid characteristics. The viscosity and thermal conductivity of the nanofluid in question are predicted by a neural network that is called in real time and to which the temperature of the fluid is passed along with other parameters. The neural network replaces the thermophysical properties (viscosity and thermal conductivity) in the single-phase governing equations. The model formulation became nonlinear as a result of this. Additional work can be done to create a standalone programme for particulate fluids that has the particle and the base fluid as its two main components. Furthermore, the neural network was developed for non-hybrids. It may not be strictly physical to consider hybrids.

Nomenclature

Cp	Specific heat capacity (kJ/kgK)
d	Diameter (m)
L	Length of pipe (m)
k	Thermal conductivity (W/mK)
T	Temperature (K)

$\vec{v}$	Velocity (m/s)

Greek letters

μ	Viscosity (Pa. s)
ρ	Density (kg/m^3)
ϕ	Volume fraction

Subscripts

bf	Basefluid
nf	Nanofluid
p	Particle

Acknowledgements

Funding: This work was funded by Tertiary Education Trust Fund (TETFund).

Declarations

Funding: This work was funded by Tertiary Education Trust Fund (TETFund).

Conflicts of interest/Competing interests: The authors declare that there is NO conflict of Interest

Availability of data and material: All data used were sourced the open literature and there are so referenced in this material anywhere they appear.

Code availability: Not applicable

References

[1] R.S. Vajjha, D.K. Das, P.K. Namburu, Numerical study of fluid dynamic and heat transfer performance of Al2O3 and CuO nanofluids in the flat tubes of a radiator, J International Journal of Heat fluid flow, 31 (2010) 613-621.
[2] A. Albojamal, K. Vafai, Analysis of single phase, discrete and mixture models, in predicting nanofluid transport, International Journal of Heat and Mass Transfer, 114 (2017) 225-237.
[3] M.K. Moraveji, M. Darabi, S.M.H. Haddad, R. Davarnejad, Modeling of convective heat transfer of a nanofluid in the developing region of tube flow with computational fluid dynamics, J International communications in heat mass transfer, 38 (2011) 1291-1295.
[4] P.K. Namburu, D.K. Das, K.M. Tanguturi, R.S. Vajjha, Numerical study of turbulent flow and heat transfer characteristics of nanofluids considering variable properties, J International journal of thermal sciences, 48 (2009) 290.

[5] S. Özerinç, A. Yazıcıoğlu, S. Kakaç, Numerical analysis of laminar forced convection with temperature-dependent thermal conductivity of nanofluids and thermal dispersion, J International journal of thermal sciences, 62 (2012) 138-148.
[6] R. Saidur, K. Leong, H.A. Mohammed, A review on applications and challenges of nanofluids, J Renewable sustainable energy reviews, 15 (2011) 1646-1668.
[7] K. Khanafer, K. Vafai, A critical synthesis of thermophysical characteristics of nanofluids, J International journal of heat mass transfer, 54 (2011) 4410-4428.
[8] H.E. Patel, T. Sundararajan, S.K. Das, An experimental investigation into the thermal conductivity enhancement in oxide and metallic nanofluids, Journal of Nanoparticle Research, 12 (2010) 1015-1031.
[9] S. Murshed, K. Leong, C. Yang, Investigations of thermal conductivity and viscosity of nanofluids, International journal of thermal sciences, 47 (2008) 560-568.
[10] M. Esfandiary, B. Mehmandoust, A. Karimipour, H.A. Pakravan, Natural convection of Al2O3–water nanofluid in an inclined enclosure with the effects of slip velocity mechanisms: Brownian motion and thermophoresis phenomenon, International Journal of Thermal Sciences, 105 (2016) 137-158.
[11] M.H. Esfe, A. Karimipour, W.-M. Yan, M. Akbari, M.R. Safaei, M. Dahari, Experimental study on thermal conductivity of ethylene glycol based nanofluids containing Al2O3 nanoparticles, International Journal of Heat and Mass Transfer, 88 (2015) 728-734.
[12] G.-J. Lee, C.K. Kim, M.K. Lee, C.K. Rhee, S. Kim, C. Kim, Thermal conductivity enhancement of ZnO nanofluid using a one-step physical method, Thermochimica acta, 542 (2012) 24-27.
[13] X. Li, C. Zou, X. Lei, W. Li, Stability and enhanced thermal conductivity of ethylene glycol-based SiC nanofluids, International Journal of Heat and Mass Transfer, 89 (2015) 613-619.
[14] M. Chopkar, S. Sudarshan, P. Das, I. Manna, Effect of particle size on thermal conductivity of nanofluid, Metallurgical and materials transactions A, 39 (2008) 1535-1542.
[15] E. Lee, viscosities and thermal conductivities of aqueous nanofluids containing low volume concentrations of Al2O3 nanoparticles, Int. J. Heat Mass Transf, 2651.
[16] S. Murshed, K. Leong, C. Yang, Enhanced thermal conductivity of TiO2—water based nanofluids, J International Journal of thermal sciences, 44 (2005) 367-373.
[17] I. Tavman, A. Turgut, M. Chirtoc, H. Schuchmann, S. Tavman, Experimental investigation of viscosity and thermal conductivity of suspensions containing nanosized ceramic particles, Archives of Materials Science, 100 (2008) 99-104.
[18] D. Yadav, P. Dansena, S.K. Ghosh, P.K. Singh, A unique multilayer perceptron model (ANN) for different oxide/EG nanofluid's viscosity from the experimental study, Physica A: Statistical Mechanics and its Applications, 549 (2020) 124030.
[19] C. Nguyen, F. Desgranges, N. Galanis, G. Roy, T. Maré, S. Boucher, H.A. Mintsa, Viscosity data for Al2O3–water nanofluid—hysteresis: is heat transfer enhancement using nanofluids reliable?, International Journal of Thermal Sciences, 47 (2008) 103-111.
[20] M.J. Pastoriza-Gallego, C. Casanova, J.a. Legido, M.M. Piñeiro, CuO in water nanofluid: influence of particle size and polydispersity on volumetric behaviour and viscosity, Fluid phase equilibria, 300 (2011) 188-196.
[21] A. Albojamal, K. Vafai, Analysis of single phase, discrete and mixture models, in predicting nanofluid transport, J International Journal of Heat Mass Transfer, 114 (2017) 225-237.

[22] Z. Ying, B. He, D. He, Y. Kuang, J. Ren, B. Song, Comparisons of single-phase and two-phase models for numerical predictions of Al2O3/water nanofluids convective heat transfer, Advanced Powder Technology, 31 (2020) 3050-3061.
[23] L.G. Asirvatham, N. Vishal, S.K. Gangatharan, D.M.J.E. Lal, Experimental study on forced convective heat transfer with low volume fraction of CuO/water nanofluid, 2 (2009) 97-119.
[24] B. Kristiawan, B. Santoso, A.T. Wijayanta, M. Aziz, T.J.E. Miyazaki, Heat transfer enhancement of TiO2/water nanofluid at laminar and turbulent flows: A numerical approach for evaluating the effect of nanoparticle loadings, 11 (2018) 1584.
[25] U. Rea, T. McKrell, L.-w. Hu, J. Buongiorno, Laminar convective heat transfer and viscous pressure loss of alumina–water and zirconia–water nanofluids, International Journal of Heat and Mass Transfer, 52 (2009) 2042-2048.
[26] M. Mahdavi, M. Sharifpur, J.P. Meyer, CFD modelling of heat transfer and pressure drops for nanofluids through vertical tubes in laminar flow by Lagrangian and Eulerian approaches, International Journal of Heat and Mass Transfer, 88 (2015) 803-813.
[27] D. Kim, Y. Kwon, Y. Cho, C. Li, S. Cheong, Y. Hwang, J. Lee, D. Hong, S. Moon, Convective heat transfer characteristics of nanofluids under laminar and turbulent flow conditions, Current Applied Physics, 9 (2009) e119-e123.
[28] C. Kamsuwan, X. Wang, P. Piumsomboon, Y. Pratumwal, S. Otarawanna, B. Chalermsinsuwan, Artificial neural network prediction models for nanofluid properties and their applications with heat exchanger design and rating simulation, International Journal of Thermal Sciences, 184 (2023) 107995.
[29] M. Jamei, Z. Said, Recent advances in the prediction of thermophysical properties of nanofluids using artificial intelligence, Hybrid Nanofluids, (2022) 203-232.
[30] M. Gholizadeh, M. Jamei, I. Ahmadianfar, R. Pourrajab, Prediction of nanofluids viscosity using random forest (RF) approach, Chemometrics and Intelligent Laboratory Systems, 201 (2020) 104010.
[31] P. Sharma, K. Ramesh, R. Parameshwaran, S.S. Deshmukh, Thermal conductivity prediction of titania-water nanofluid: A case study using different machine learning algorithms, Case Studies in Thermal Engineering, 30 (2022) 101658.
[32] K.X. Tan, S.U. Ilyas, R. Pendyala, M.R. Shamsuddin, Assessment of thermal conductivity and viscosity of alumina-based engine coolant nanofluids using random forest approach, in: AIP Conference Proceedings, AIP Publishing LLC, 2022, pp. 030002.
[33] W. Ajeeb, S.S. Murshed, Comparisons of Numerical and Experimental Investigations of the Thermal Performance of Al2O3 and TiO2 Nanofluids in a Compact Plate Heat Exchanger, Nanomaterials, 12 (2022) 3634.

Chapter 6 Predictive modelling of thermal conductivity in single-material nanofluids: a novel approach

Abstract:

Background: This research introduces a novel approach for modelling single-material nanofluids, considering the constituents and characteristics of the fluids under investigation. The primary focus of this study was to develop models for predicting the thermal conductivity of nanofluids using a range of machine learning algorithms, including ensembles, trees, neural networks, linear regression, Gaussian process regressors, and support vector machines.

The main body of the abstract: To identify the most relevant features for accurate thermal conductivity prediction, the study compared the performance of established feature selection algorithms, such as minimum redundancy maximum relevance, Ftest, and RReliefF, a newly proposed feature selection algorithm. The novel algorithm eliminated features lacking direct implications for fluid thermal conductivity. The selected features included temperature as a thermal property of the fluid itself, multiphase features such as volume fraction and particle size, and material features including nanoparticle material and base fluid material, which could be fixed based on any two intensive properties. Statistical methods were employed to select the features accordingly.

Results: The results demonstrated that the novel feature selection algorithm outperformed the established approaches in predicting the thermal conductivity of nanofluids. The models were evaluated using 5-fold cross-validation, and the best model was the model based on the proposed feature selection algorithm exhibited a root mean squared error of validation of 1.83 and an R-squared value of 0.94 on validation set. The model achieved a root mean squared error of 1.46 and an R-squared value of 0.97 for the test set.

Conclusions: The developed predictive model holds practical significance by enabling nanofluids' numerical study and optimisation before their creation. This model facilitates the customisation of conventional fluids to attain desired fluid properties, particularly their thermal properties. Additionally, the model permits the exploration of numerous nanofluid variations based on permutations of their features. Consequently, this research contributes valuable insights to the design and optimisation of nanofluid systems, advancing our understanding and application of thermal conductivity in

nanofluids and introducing a novel and methodological approach for feature selection in machine learning.

Keywords: Single material, nanofluids, modelling, predict, thermal conductivity, feature selection.

Background

This research introduces a novel method for modelling nanofluid thermophysical properties (thermal conductivity of single material nanofluid). It uses the physics of the fluid to select its features. Using this approach ensures a generalised physical model. The implication of such an approach is creating a model that meets the needs of many cases of single-material nanofluids. This is so because the feature selection was physics based.

This approach is unusual as much research depends on statistical tools to select its learning features (MathWorks, 2022).

Literature review

The prediction of the thermal conductivity of nanofluids has been studied extensively. The following reviews give the state of the art on this topic as given by various researchers, beginning with some historical studies to present works.

Xie et al. (2002) studied the thermal conductivity measurement of SiC suspension in water and ethylene glycol and the effect of the size and shape of the added solid phase on the enhancement of thermal conductivity. Experimental data for SiC nanoparticles in water and ethylene glycol was presented. The thermal conductivity of SiC nanofluid was measured using a transient hot wire method. The effects of the morphologies (size and shape) of the added solid phase on the enhancement of the thermal conductivity of the nanoparticle suspension were studied. This study was one of the first to supply such data. Furthermore, it was one of the first to report the effects of morphology on thermal conductivity enhancement. It highlighted the deviation in the existing Hamilton Crosser model with spherical and cylindrical assumptions. The study considers just one type of nanoparticle (SiC). However, only two particle sizes were considered. In the study, it was assumed that heat transfer between the particles and fluid takes place at the particle surface interface. Heat transfer is expected to be more efficient and rapid for a system with a larger interfacial area. As the particle sizes decrease, the effective thermal conductivity of the suspension improves. Higher thermal conductivities were obtained by adding SiC nanoparticles. Furthermore, it was observed in the study that a linear relationship

existed between low volume fraction in the (1 – 5%) volume fraction range and the thermal conductivity enhancements.

Murshed et al. (2005) studied the thermal conductivity of TiO_2 water nanofluid in their paper. A more convenient measurement of the thermal conductivity of nanofluids was created – A transient hot-wire apparatus with an integrated correlation model. A relationship was established between particle volume fraction, shape, and thermal conductivity. The study focused on conveniently measuring nanofluids' thermal conductivity and comparing results with the theoretical prediction. The study was one of the first to collect and compare such data with theoretical models. However, only one type of nanofluid was used. They pointed out that traditional models fail due to a lack of accounting of the effects of (1) Particle size, (2) Particle Brownian motion, (3) Nano layering, (4) effects of nanoparticle clustering—an integrated correlation model allowed for a more precise and convenient measurement of the thermal conductivity of nanofluids. Further efforts to develop a suitable model to predict the thermal conductivity of nanofluids will consider other factors that are important in enhancing the heat transfer performance of nanofluids.

Komeilibirjandi et al. (2020) studied the thermal conductivity of nanofluids containing two nanoparticles and predicted it by using correlation and artificial neural network. The GMDH (Group method of data handling) Neural network was applied to model the thermal conductivity of CuO-nanofluids. Water and ethylene glycol were the base fluids. % volume fraction, nanoparticle size, temperature, and thermal conductivity of the base fluid were considered. Data used were extracted from experimental studies in the literature.

It is worth knowing that most researchers, as outlined above, have attempted this modelling. Furthermore, researchers that attempt the generalised model form have fixed their models to only the nanofluid types collected. Implying no other nanofluid type outside their collected data can be accounted for.

Ramezanizadeh et al. (2019) mentioned the two types of nanofluids: conventional or single-material nanofluids and hybrid nanofluids. They reviewed proposed models for predicting the thermal conductivity of various researchers. The following conclusions can be drawn from their report (Ramezanizadeh et al., 2019):

a) The reviewed models were not tested with out-of-sample data.

b) Many models were made for a specific nanofluid (meaning they only covered one nanoparticle and base fluid type). The percentage of such models was 89% (23) out of all 26 models reviewed.

c) The remaining three (3) models were designed to cover more than one nanofluid. However, they were limited in the number of nanofluids on which they could make predictions due to the numerous nanofluid types that exist in the literature plus those that can be fabricated. A further study of the modelling approach used by these researchers reveals that a shift in convention in the choice of model features might solve this problem. For example, one researcher Ahmadloo and Azizi (2016) considered numbers that would differentiate each nanoparticle type and base fluid. Although this helped add a distinct factor to the conventional inputs of particle size, volume fraction, and temperature, the resulting model was still limited to 15 nanofluid types and could not be applied beyond those nanofluids. Also, adding ordinate numbers as opposed to encoding (one-hot types) has been shown in machine learning to bias models by making those with higher numbers more critical.

d) For the final two models of the three in (c) . They could not distinguish between nanofluid types due to the features they selected, so they were only accurate in a limited range of parameters and thus not useful outside of those ranges.

e) The models' focus was curve fitting, not prediction.

The other group of models studied by Ramezanizadeh et al. (2019) are the correlation types with low accuracy and a narrow range where they hold; Hence, they are usually avoided.

In this study, the predictors used as input were chosen so that they uniquely represented the nanoparticle and base fluid data and could also apply to other nanoparticles and base fluids not available in the collected data. This ensures that it can be used to make predictions based on the numerical values of the predictors only and hence be a more general model. As compared to the work of other researchers such as Ahmadloo and Azizi (2016), as mentioned above, used predictors that were only uniquely identified with the nanoparticle and base fluid in the collected data; hence, they could not be used on a general basis for predicting the thermal conductivity of single material nanofluids not included in the collected data. Moreover, our approach in this study is to create a generalised model that accounts for all single-material nanofluids using a novel feature selection algorithm.

Experimental Measurements and Description of the Experimental Setup and Procedures

Data used in this study were obtained from experimental data reported in the following articles (Patel et al., 2010):

The report's experimental setup for measuring thermal conductivity utilised a transient hot wire apparatus. The measurement cell consisted of a 15 cm long platinum wire with a diameter of 100 μm. The platinum wire served both as a heater and a thermometer. It was placed in a glass container filled with the test liquid and formed an arm of a Wheatstone bridge. An analytical solution for the temperature distribution was employed to determine the thermal conductivity of the test liquid. This solution assumes an infinitely long line heat source continuously heating a semi-infinite medium. The platinum wire was electrically insulated to prevent interference. The validity of the measurement technique was established by comparing the obtained thermal conductivity values with literature values for various fluids such as water, ethylene glycol, transformer oil, xylene, and toluene. The results showed that the measurements obtained from the transient hot wire apparatus were within 1.2% of the literature values, indicating its reliability. However, it should be noted that this equipment is not suitable for measuring the thermal conductivity of fluids with high electrical conductivities. Nonetheless, it proved effective for measuring the thermal conductivity of oxide nanofluids, which was the focus of their study. Overall, the transient hot wire equipment employed in the study provided a robust and validated method for measuring thermal conductivity, ensuring accurate and reliable data for the analysis of nanofluids.

Machine Learning Techniques:

Machine learning (ML) techniques (Ewim et al., 2020; Ewim et al., 2021; Géron, 2022; Jiang et al., 2020; Meng et al., 2020; Sharma et al., 2022; Zhu et al., 2021) have revolutionised regression analysis by providing powerful tools for predicting continuous numerical outcomes. This section will explore several ML regression techniques commonly used in various domains. These techniques include neural networks, gradient boosting, random forest, support vector machine (SVM), linear models, decision trees, and naive Bayes regression models. Moreover, they have been investigated for nanofluid thermal conductivity predictions in this study along with the application of the novel feature selection algorithm proposed by this study.

Neural Networks

Neural networks are ML models inspired by the human brain's neural structure. They consist of interconnected layers of artificial neurons that can learn complex patterns and relationships. Neural networks have been successfully applied to regression tasks because they capture non-linear relationships in the data (Chiniforooshan Esfahani, 2023; Genzel et al., 2022; Hornik et al., 1989; Kamsuwan et al., 2023; Kannaiyan et al., 2019; Mijwil, 2018; Ekene Jude Onyiriuka, 2023; Ekene J Onyiriuka, 2023; Peng et al., 2020).

Gradient Boosting

Gradient boosting is an ensemble learning method that combines multiple weak models, typically decision trees, to create a robust predictive model. It trains new models to correct the errors made by previous models, gradually improving the overall prediction accuracy (Friedman, 2001).

Random Forest

Random forest is another ensemble learning technique that constructs a collection of decision trees and combines their predictions to make accurate predictions. It reduces overfitting by introducing randomness in tree-building (Breiman, 2001; Gholizadeh et al., 2020; Tan et al., 2022).

Support Vector Machine (SVM)

SVM is a popular ML algorithm used for regression tasks. It aims to find the best hyperplane that separates the data into different classes while minimising the error in the training instances. SVM can handle linear and non-linear regression problems (Razavi et al., 2019; Vapnik, 1999).

Linear Model

Linear regression is a simple and widely used ML technique for regression analysis. It assumes a linear relationship between the input features and the target variable. The goal is to find the best-fit line that minimises the sum of squared differences between the predicted and actual values (Géron, 2022).

Decision Trees

Decision trees are versatile ML models that make predictions by partitioning the feature space into regions based on simple decision rules. They are interpretable and can capture non-linear relationships in the data. Decision trees can be used for regression and classification tasks (Breiman et al., 1984).

Naive Bayes Regression Model:

Naive Bayes regression is based on Bayes' theorem and assumes that the input features are conditionally independent given the target variable. Despite its simplicity, naive Bayes can provide reasonable predictions, especially when the independence assumption holds (Rish, 2001).

These ML regression techniques offer various options for analysing and predicting continuous variables. The choice of technique depends on the specific problem, dataset characteristics, interpretability requirements, and computational considerations. Researchers and practitioners often compare and combine these techniques to achieve the best performance for their regression tasks (Sharma et al., 2022; Witten et al., 2016; Yashawantha & Vinod, 2021; Zhu et al., 2021).

Cross-validation

Cross-validation is a machine learning technique used to estimate the ability of a machine learning model on unknown data. In this process, a small sample is used to assess how the model will perform. This data is called "out-of-bag" data. It is a popular strategy since it is simple and produces a less biased or optimistic estimate of a model’s predictive ability than other processes, such as a simple train-test split. Cross-validation ensures a fair comparison of the models (Brownlee, 2020a).

To compare machine learning algorithms well, we ensured that each algorithm was evaluated on the same data and in the same way. Cross-validation is a resampling technique for evaluating machine learning models on a small sample of data. Although there are several cross-validation methods, we chose the k-fold cross-validation method because it was the most fitting for this study - for evaluating models without bias. However, researchers Brownlee (2020b) reported an alternative method called stratified cross-validation, which is suitable for cross-validating imbalanced datasets. However, it is only applicable to classification problems. Hence, it does not apply to our study. The process of k-fold cross-validation includes a parameter, k, which specifies the number of groups into which a given data sample should be sectioned. 5-fold cross-validation refers to cross-validation where the dataset is split into five sections. The cross-validation method used in this study was the 5-fold cross-validation method, which is applied to evaluate every algorithm to ensure the same evaluation on all models.

The figure below shows the k-fold algorithm.

Iteration 01	Test	Train	Train	Train	Train
Iteration 02	Train	Test	Train	Train	Train
Iteration 03	Train	Train	Test	Train	Train
Iteration 04	Train	Train	Train	Test	Train
Iteration 05	Train	Train	Train	Train	Test

Figure 1 The 5-fold algorithm

The general procedure is as follows as shown in Figure 1:

1. Randomized shuffling of the dataset.
2. Divide the dataset into k distinct sections.
3. For each distinct section:
    i. Use the section as a test data set.
    ii. Use the remainder of the section as a training data set.
    iii. Fit each model to the training set (ii) and evaluate it on the test set (i).
    iv. Save the evaluation score and note the model.
4. Steps (i) through (iv) should be repeated for x number of models.
5. Report the predictive ability of each model by summarising the model's average evaluation score.

Evaluation Metrics

The evaluation metrics are used to measure the performance of the predictive model. Standard metrics for regression tasks include:

Root mean squared (RMSE) Error (Hastie et al., 2009): it is a popular evaluation metric for regression tasks. It is derived from the Mean Squared Error (MSE) as seen in equation 1 by taking the square root of the average of the squared differences between the predicted values and the actual values. The rationale behind using RMSE as an evaluation metric is like that of MSE, but with some additional considerations RMSE, like MSE, provides a measure of the average prediction error. However, by taking the square root of MSE, RMSE is expressed in the same units as the target variable, making it more interpretable and easier to relate to the original scale of the problem. For example, if the target variable represents the temperature of a fluid in ^{o}C, RMSE will also be expressed in ^{o}C. Like MSE, RMSE also emphasises more significant errors by squaring them. However, by taking the square root of MSE, RMSE balances penalises significant errors and maintaining interpretability. It allows a more intuitive

understanding of the typical magnitude of errors in the model's predictions. RMSE enables direct comparison of models or different scenarios, as it provides a scale-dependent standard metric. When comparing models, lower RMSE values indicate better performance, indicating that the model's predictions are closer to average. RMSE is related to the standard deviation of the errors. It measures the typical spread or dispersion of the errors around the actual values. Smaller RMSE values suggest a more concentrated distribution of errors, indicating better accuracy and precision in the model's predictions.

$$RMSE = \sqrt{\frac{1}{n}\sum_{i=1}^{n}(h_i - {h_i}^{pred})^2} \quad (1)$$

RSQUARED (Gareth et al., 2013), is a widely used evaluation metric for regression tasks. It measures the proportion of the variance in the dependent variable that is predictable from the independent variables as seen in equations (2) – (5). RSQUARED measures how well the regression model fits the observed data. It quantifies the proportion of the total variation in the dependent variable that the independent variables can explain. Higher RSQUARED values indicate a better fit and suggest that the model accounts for a more significant proportion of the variation in the target variable. RSQUARED allows for comparison against a baseline model, often the mean of the dependent variable. An RSQUARED value of 1 indicates that the model perfectly predicts the target variable, while a value of 0 suggests that the model does not provide any improvement over the baseline model. RSQUARED has a straightforward interpretation as the proportion of variance explained. It provides a convenient measure to communicate the model's predictive power to non-technical researchers, such as decision-makers.

$$\bar{h} = \frac{1}{n}\sum_{i=1}^{n} h_i \quad (2)$$

$$SS_{reg} = \sum_i ({h_i}^{pred} - \bar{h})^2 \quad (3)$$

$$SS_{tot} = \sum_i \left(h_i - \bar{h}\right)^2 \quad (4)$$

$$R^2 = \frac{SS_{reg}}{SS_{tot}} \quad (5)$$

Mean Squared Error (MSE) (Hastie et al., 2009), is a commonly used evaluation metric for regression tasks. It measures the average squared difference between predicted and actual values as shown in equation (6). MSE measures the average prediction error by considering the squared differences between the predicted and actual values. It penalises more significant errors due to the squaring operation, providing a way to assess the accuracy of the model's predictions. MSE is mathematically convenient and has desirable properties for optimisation. It is differentiable, allowing efficient

gradient-based optimisation algorithms commonly used in machine learning. This property makes MSE practical for training regression models using gradient-based optimisation techniques. MSE can be decomposed into the sum of variance and bias terms, known as the bias-variance trade-off. This decomposition provides insights into the model's performance by assessing the balance between overfitting (low bias, high variance) and underfitting (high bias, low variance). By minimising MSE, the model aims to find the optimal balance between bias and variance for improved generalisation.

Differentiable and Mathematically Convenient:

$$MSE = \frac{1}{n}\sum_{i=1}^{n}(h_i - {h_i}^{pred})^2 \quad (6)$$

Mean Absolute Error (MAE) (Gareth et al., 2013), is a commonly used evaluation metric for regression tasks. It measures the average absolute difference between predicted and actual values as seen in equation (7).

$$MAE = \frac{1}{n}\sum_{i=1}^{n}\left|h_i - {h_i}^{pred}\right| \quad (7)$$

MAE is less sensitive to outliers compared to other error metrics like MSE. Since MAE calculates the absolute difference, it does not heavily penalise significant errors. This makes MAE more robust to outliers, minimising their influence on the overall error measurement. MAE has a straightforward interpretation as the average absolute difference between the predicted and actual values. It represents the average magnitude of the errors, providing an intuitive understanding of the model's performance. MAE is easily understandable by non-technical researchers, making it suitable for communication. MAE is mathematically simple and computationally efficient. It does not involve squaring the differences, simplifying calculations and reducing the computational complexity of evaluating the error metric.

Methods

The procedure to evaluate the predictive model involves the following: The trained model was used to make predictions on the validation dataset. Moreover, the above evaluation metrics were computed using the predicted values and the corresponding actual values from the validation dataset.

The calculated metrics are presented in Table 2. The validation RMSE is used to sort the table from best to worse.

Data Exploration and Models

The variables were collected for analysis, selecting which features might be necessary for modelling the thermal conductivity of nanofluids.

The nanofluid data set was collected from experimental studies. It consisted of 348 data points.

Conceptualisation and parameter selection

Conceptualisation in this context is formulating a novel parameter selection method for predicting the thermal conductivity of all single-material nanofluids. Parameter selection is the selection of the training data characteristics learned during the learning process. In this study, there is a shift from parameter selection based solely on statistics to selection based on physics and reduction of an initially large dimensional space. It describes a feature engineering technique where all variables possible are selected to increase the dimensional space of a dataset by increasing the number of descriptive features. The goal is to find an optimal physical dimensional set of features that make each data point distinct from the others. Even though these extra variables may not have high importance in predicting the target variables, their presence in the model helps to make the predictions unique. This is a different approach from conventional feature engineering. In conventional feature engineering, feature engineering aims to create new variables from existing ones to improve the performance of a machine learning model by providing more information to the model (Patel, 2021).

In this case, the new variables are not derived from the existing variables but are other independent variables that further define the characteristics of what is being predicted.

It is important to remember that feature engineering is an iterative process that necessitates a thorough understanding of the problem and the data at hand.

Proposed Algorithm for parameter selection

Here we discuss the procedure for selecting parameters according to the novel method discussed above to predict the thermal conductivity of all single-material nanofluids.

1) Check the problem being solved.
2) List all the possible features (Start with the largest number of features/dimensional space possible).

3) Manually drop features that have no meaning or direct implication to the thermal conductivity of a fluid. For example, using single-material nanofluids:

    a) Fluid features - Temperature
    b) Multiphase features – Volume fraction and particle size
    c) Material features
        i) Nanoparticle material: Any two intensive properties will fix the material of the nanoparticle type (Callister, 2007; Cengel et al., 2011; Moran et al., 2010).
        ii) Base fluid material: Any two intensive properties will fix the material of the base fluid type (Callister, 2007; Cengel et al., 2011; Moran et al., 2010).

    So, these three feature groupings define a nanofluid.

4) Apply statistical methods to select features according to 3) out of all other features.

5) At the end of steps 3) – 5), you should have a reasonable number of features and optimal accuracy.

Note that this parameter selection focuses on accuracy and enhanced model learning for generalisation. Accuracy is still of utmost importance.

Other feature selection algorithm

The section presents the Minimum redundancy maximum relevance (MRMR) and RReliefF.

Minimum redundancy maximum relevance (MRMR)

1. Begin by picking the most relevant feature from a set and add it to a selected set (S).
2. Check the remaining features (Sc) for those with relevant information but not redundant with the ones in S.
3. If such features exist, add the most relevant of them to S.
4. Keep doing this until there are no more non-redundant features left in Sc.
5. Find the Sc feature with the highest value considering its ability to contribute new information - Mutual Information Quotient (MIQ) while balancing relevance and redundancy.
6. Add this feature to S and repeat Step 4 as needed.
7. Include Sc features with zero relevance into S, randomly.

The algorithm chooses features that are informative and distinct, resulting in an optimized subset for analysis.

RReliefF
Initialize the weights W_{dy}, W_{dj}, $W_{dy \wedge dj}$, and W_j to 0.

The algorithm then follows these steps for a certain number of iterations, denoted by 'updates.'

For each iteration 'i' and for a randomly chosen observation x_r

Find the k-nearest observations to x_r.

m is the number of iterations specified by `'updates'`.

Update the intermediate weights as follows:

$$W_{dy}^{i} = W_{dy}^{i-1} + \Delta_y(x_r, x_q) * d_{rq}$$

$$W_{dj}^{i} = W_{dj}^{i-1} + \Delta_j(x_r, x_q) * d_{rq}$$

$$W_{dy \wedge dj}^{i} = W_{dy \wedge dj}^{i-1} + \Delta_y(x_r, x_q) * \Delta_j(x_r, x_q) * d_{rq}$$

The $\Delta_y(x_r, x_q)$ calculates the difference in continuous response y between observations x_r and x_q normalized by the range of response values:

$$\Delta_y(x_r, x_q) = \frac{|y_r - y_q|}{\max(y) - \min(y)}$$

Where:

y_r is the response value for observation x_r

y_q is the response value for observation x_q.

d_{rq} is a distance function.

After updating all intermediate weights for each iteration, RReliefF calculates the predictor weights W_j using the formula:

$$W_j = \frac{W_{dy \wedge dj}}{W_{dy}} - \frac{W_{dj} - W_{dy \wedge dj}}{m - W_{dy}}$$

Preprocessing of experimental data for training and validation

Preprocessing experimental data for training and validation involves several steps to ensure the data is in a suitable format and quality for ML regression analysis. The following are essential components of data preprocessing for training and validation: The removal of any irrelevant or redundant data that did not contribute to the regression task. This includes removing duplicates, handling missing values, and addressing outliers. Missing values can be imputed using techniques such as mean, median, or advanced imputation methods like regression imputation. However, this study did not impute missing values since the data had no missing values.

Feature Selection and Modelling

In this study, the modelling process is approached from the standpoint of feature selection.

To start the modelling procedure, we first designed it for reproducibility. This was achieved by using a default and consistent random seed generator. The data is then partitioned into two sets in an 80:20 ratio, 80% for training (252 observations) and 20% (69 observations) for later out-of-bag testing. And 10% of the 80% for testing (27 observations). The 5-fold cross-validation was carried out to select the model without bias fairly.

The response (Percentage enhancement of thermal conductivity – “ENT”) was specified. Moreover, the rest of the variable was specified as the predictors.

Results

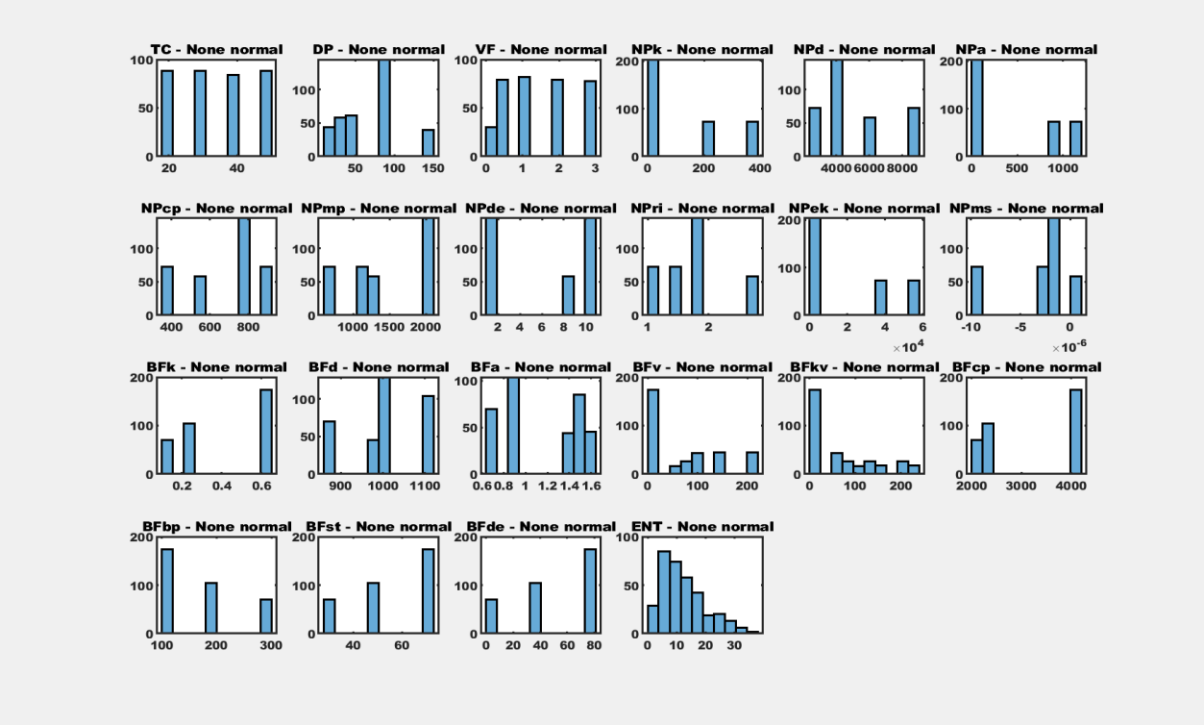

Figure 2 A Histogram plot of each variable

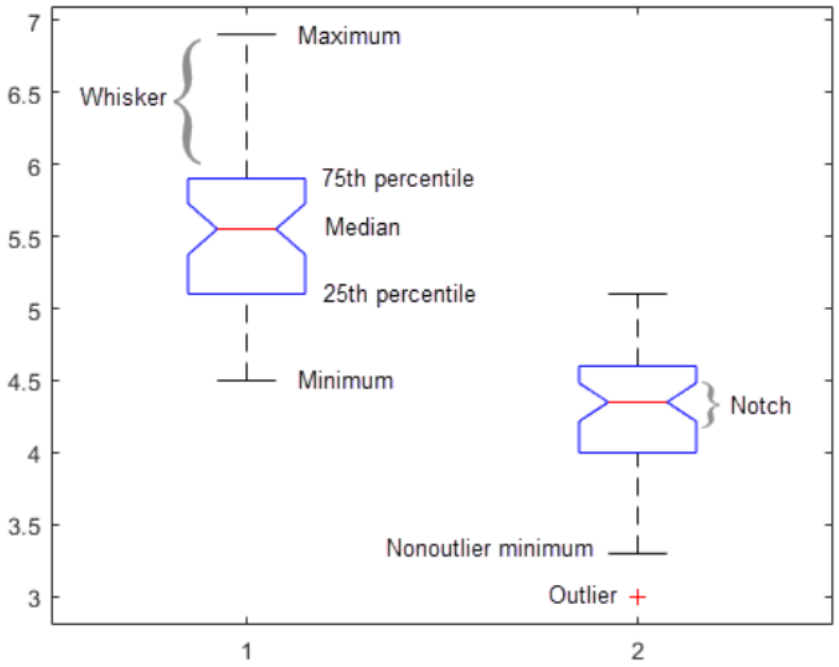

Figure 3a. Box plot anatomy (MathWorks, 2022)

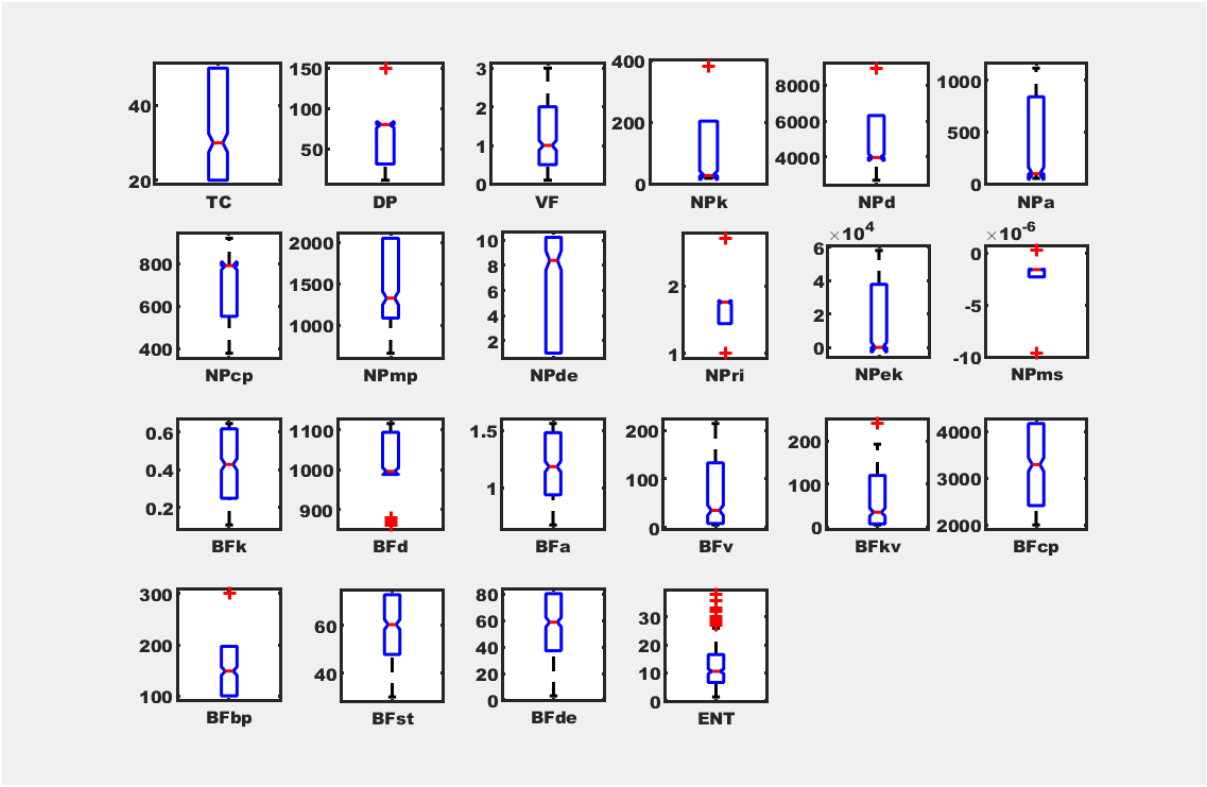

Figure 3b. Box plot of the variables

Table 1. Common feature selection algorithm

Feature selection type	Brief description of the feature selection algorithm	Selected features and their importance	Model performance	
Minimum redundancy maximum relevance (MRMR)	The MRMR (Minimum Redundancy Maximum Relevance) algorithm aims to identify an optimal feature subset highly relevant to the response variable and maximally dissimilar.	VF = 0.2279, TC = 0.2000	RMSE (Validation)	5.65
			MSE (Validation)	31.96
			RSQUARED (Validation)	0.40

			MAE (Validation)	4.57
			MAE (Test)	5.34
			MSE (Test)	39.61
			RMSE (Test)	6.29
			RSQUARED (Test)	0.25
FTest (Importance > 25)	This involves conducting separate chi-square tests for each predictor variable to determine if there is a significant association between the predictor and the response.	VF = 50.7728, DP = 31.8726, NPk = NPa = NPcp = NPmp = NPri = NPek = NPms = NPd = 26.5023	RMSE (Validation)	3.50
			MSE (Validation)	12.27
			RSQUARED (Validation)	0.78
			MAE (Validation)	2.64
			MAE (Test)	2.33
			MSE (Test)	9.72
			RMSE (Test)	3.12

			RSQUARED (Test)	0.77
RReliefF (> Abs (0.01))	The RReliefF algorithm considers the consistency of predictor values among neighbours with the same response values. It penalises predictors exhibiting inconsistent values among neighbouring instances with the same response while rewarding predictors demonstrating differing values among neighbours with different response values.	VF = 0.1515, BFv = 0.0142, BFkv = 0.0126, DP = -0.0092	RMSE (Validation)	2.66
			MSE (Validation)	7.07
			RSQUARED (Validation)	0.86
			MAE (Validation)	1.94
			MAE (Test)	1.95
			MSE (Test)	7.39
			RMSE (Test)	2.72
			RSQUARED (Test)	0.90

Table 2. Novel Feature selection algorithms (NFSA)

Feature selection type	Brief description of the feature selection algorithm	Selected features and their importance	Model performance	
Novel Feature selection algorithm is based on similar skewness and data resemblance.	This selects variables that have close to or the same statistical characteristics.	TC, DP, VF, NPk, NPd, BFkv, BFv	RMSE (Validation)	1.74
			MSE (Validation)	3.01
			RSQUARED (Validation)	0.94
			MAE (Validation)	1.14
			MAE (Test)	1.01
			MSE (Test)	2.26
			RMSE (Test)	1.50
			RSQUARED (Test)	0.95
Novel Feature selection algorithm is based on different skewness and data	This selects variables that have dissimilar. Statistical characteristics, differing values	TC, DP, VF, NPk, NPmp, BFkv, BFv	RMSE (Validation)	1.83
				3.34

resemblance. (The best)	among neighbours with different response values.		MSE (Validation)	
			RSQUARED (Validation)	0.94
			MAE (Validation)	1.23
			MAE (Test)	0.99
			MSE (Test)	2.14
			RMSE (Test)	1.46
			RSQUARED (Test)	0.97

Discussion

Data analysis

The total number of data rows collected was 348, with 22 columns including the response variable.

The variables are represented by the following nomenclature for ease of reference, as shown in Table 1:

Figure 2 showcases histograms portraying the characteristics of each variable, including the response variable "ENT" response variable. Visual scrutiny of these histograms swiftly indicates that none of the variables conforms to a normal distribution, prompting the requirement for models attuned to handling such non-normal data distributions. Therefore, a range of modelling methodologies comes into view. Notably, robust linear regression (Maronna et al., 2019) emerges as a

promising method, particularly due to its reliable coefficient estimates even in the presence of outliers. Likewise, non-parametric models, including decision trees, random forests, and support vector machines (Kurani et al., 2023), surface as possible modelling options, capable of understanding intricate relationships without making such assumptions about data distribution. Furthermore, ensemble models, represented by boosting and bagging (Mohammed & Kora, 2023), also exhibit their strength to enhance predictive accuracy. This proves invaluable when dealing with non-normal data and intricate nonlinear relationships. Additionally, the potency of neural networks (Cong & Zhou, 2023) becomes evident, owing to their remarkable capacity for detecting patterns and relationships even amidst complex data representation. It's noteworthy that, the author avoids data transformation of the response variable since that could potentially lead to data leakage because data transformation holds the risk of inadvertent data leakage as noted by Osborne (2010) where knowledge from the target variable infiltrates the transformation process, affecting the model outcomes. In conclusion, Figure 2 effectively visualizes the histogram plots of diverse variables, exposing their departure from normality. Consequently, a suite of modelling options is proposed, encompassing robust linear regression, non-parametric models (e.g., decision trees, random forests, support vector machines), ensemble models (e.g., boosting, bagging), and neural networks. These selections are apt for handling data exhibiting non-normal distributions. The selection among these modelling approaches should be guided by the specific data characteristics.

Figure 3b presents the box plot for each variable, offering a visual summary of their distribution characteristics, including skewness, symmetry, and potential outliers. The structure of the box plot is depicted in Figure 3a. Box plots allow for a concise representation of multiple variables, facilitating the identification of differences in central tendency and variability among them. The box plot provides several important features for each variable. The rectangular box represents the interquartile range (IQR), encompassing the middle 50% of the data. The line within the box represents the median, indicating the central tendency of the variable. The whiskers extend from the box, indicating the data range within 1.5 times the IQR. Values beyond the whiskers are considered potential outliers and are displayed as individual data points. By examining the box plots in Figure 3b, we can observe the distributional

characteristics of each variable. Skewness can be observed by considering the asymmetry of the box and whiskers. The whisker lengths are significantly different, suggesting unequal variability. Outliers are visually identifiable as can be observed by data points lying beyond the whiskers. The side-by-side presentation of multiple variables in Figure 3b allows for an easy comparison of their central tendencies and variabilities. Differences in box lengths, medians, and whisker lengths among the variables indicate variations in their distributions. The utilisation of box plots aids in understanding the distributional properties of each variable and enables the identification of potential outliers and variations in central tendency and variability across multiple variables. We can observe similar data characteristics between the variables regarding skewness, making it possible to create some groupings. In contrast, some variables are single and do not fall under similarity groupings. The following groups 1 to 12 show the variables that have similar relationships with themselves by visual examination as observed in the box plot in Figure 3.

Group 1: Nanofluid temperature

Group 2: Particle size diameter, Nanoparticle density, Nanoparticle thermal conductivity

Group 3: Volume fraction, Base fluid surface tension

Group 4: Nanoparticle thermal diffusivity, Base fluid dielectric constant

Group 5: Nanoparticle-specific heat capacity, Nanoparticle electrical conductivity

Group 6: Nanoparticle melting point, Base fluid specific heat capacity

Group 7: Nanoparticle dielectric constant, Base fluid density

Group 8: Nanoparticle refractive index, Base fluid boiling point

Group 9: Nanoparticle magnetic susceptibility

Group 10: Base fluid thermal conductivity, Base fluid thermal diffusivity

Group 11: Base fluid viscosity

Group 12: Base fluid kinematic viscosity, Percentage enhancement of nanofluid thermal conductivity

Groups 1, 9, and 11 are very different from the rest.

Results analysis

In the appendix, the table presents the results of the model selection process. The neural networks emerged as the best basic model based on the cross-validated set's root mean squared error (RMSE). The selected neural network consisted of three fully

connected layers with sizes of 10, 10, and 10, respectively. The Rectified Linear Unit (ReLU) was used as the activation function, and the regularisation strength was set to zero. The implementation of the neural network had a variable learning rate and a validation check stopping criteria. Additionally, the data were standardised before training the model. To further optimise the neural network, Bayesian optimisation was employed. The optimisation process was guided by the estimated improvement per second plus 30 iterations. The hyperparameter search range included the number of fully connected layers (1-3), the size of the first layer (1-300), the size of the second layer (1-300), the size of the third layer (1-300), and the choice of the activation function (ReLU, tanh, sigmoid, or none). The regularisation strength varied between 3.9683 x 10^(-08) and 396.8254. Data standardisation was considered a binary choice (yes/no). The optimised hyperparameters for the neural network were determined as follows: two fully connected layers with sizes of 64 and 10, respectively. The ReLU activation function was utilised, the regularisation strength was set to 392.6291, and the data were standardised. However, it was observed that the performance of the optimised neural network was not satisfactory. The validation RMSE for the optimised model was 14.472, which was higher than the non-optimised version. The mean squared error (MSE) was 209.443, the R-squared (RSQUARED) was -2.841, and the mean absolute error (MAE) was 12.482. For the test set consisting of 27 observations, the MAE was 9.096, the MSE was 125.532, the root mean squared error (RMSE) was 11.204, and the RSQUARED was -1.932. This observation is possibly due to overfitting the models parameters to the data hence the poor performance on the validation set and test set. In order to perform feature selection, a copy of the most accurate model was used. Table 1 presents the results of the analysis using standard feature selection algorithms. The Minimum Redundancy Maximum Relevance (MRMR) algorithm identified VF and TC as the selected features with respective importance scores of 0.2279 and 0.2000. The model's performance based on validation data included an RMSE of 5.65, an MSE of 31.96, an RSQUARED of 0.40, and an MAE of 4.57. For the test set, the MAE was 5.34, the MSE was 39.61, the RMSE was 6.29, and the RSQUARED was 0.25. Another feature selection algorithm, FTest, was employed with an importance threshold of 25. This approach involved conducting separate chi-square tests for each predictor variable to determine their significant association with the response. The resulting selected features and their importance scores were VF (50.7728), DP (31.8726), and others with importance scores of 26.5023. The model's performance improved compared to the MRMR-selected features, with an RMSE of 3.50, an MSE of 12.27, an RSQUARED of 0.78, and an MAE of 2.64 for the validation set. For the test set, the MAE was 2.33, the MSE was 9.72, the RMSE was 3.12, and the RSQUARED was 0.77. The RReliefF algorithm

was also applied with a threshold of importance greater than 0.01. This algorithm considers the consistency of predictor values among neighbours with the same response values. The selected features and their importance scores were VF (0.1515), BFv (0.0142), and BFkv (0.0126), while DP had a negative importance score of -0.0092. The model's performance improved further, with an RMSE of 2.66, an MSE of 7.07, an RSQUARED of 0.86, and an MAE of 1.94 for the validation set. For the test set, the MAE was 1.95, the MSE was 7.39, the RMSE was 2.72, and the RSQUARED was 0.90. Table 2 presents the results of novel feature selection algorithms (NFSA). One NFSA algorithm was based on selecting variables with similar statistical characteristics, selecting TC, DP, VF, NPk, NPd, BFkv, and BFv. This algorithm achieved improved performance, with an RMSE of 1.74, an MSE of 3.01, an RSQUARED of 0.94, and an MAE of 1.14 for the validation set. For the test set, the MAE was 1.01, the MSE was 2.26, the RMSE was 1.50, and the RSQUARED was 0.95. The second NFSA algorithm focused on selecting variables with different statistical characteristics, selecting TC, DP, VF, NPk, NPmp, BFkv, and BFv. This algorithm achieved the best model performance, with an RMSE of 1.83, an MSE of 3.34, an RSQUARED of 0.94, and an MAE of 1.23 for the validation set. For the test set, the MAE was 0.99, the MSE was 2.14, the RMSE was 1.46, and the RSQUARED was 0.97. Based on the results from Table 2, it is evident that the novel feature selection algorithm with different statistical characteristics provided the best model performance, achieving the lowest RMSE for the validation set. This result emphasises and encourages researchers to develop models in this manner since it leads to better models in terms of accuracy and generalisation.

It is worth noting that further investigation and experimentation are necessary to validate the findings and potentially explore alternative modelling approaches or feature selection methods. The following study's limitations should also be acknowledged, such as the sample size, potential biases, and the context of the analysis. Future research could address these limitations to provide a more comprehensive understanding of the studied phenomena and potentially improve model performance by applying the novel feature selection algorithm for other scenarios like hybrid nanofluids and similar technologies.

Practical significance of the developed predictive model

By developing this model, it is possible to study and optimise nanofluids numerically before creating them. It enhances the ability to edit conventional fluids to fit any fluid description of our desire, especially the fluid's thermal properties. Also, it is to be noted that by editing the base fluids by adding nanoparticles, we can obtain numerous fluids

(nanofluids as there are permutations of the features of the nanoparticles and base fluids) and adequately model their characteristics.

Conclusions

This research presents a novel approach for modelling single-material nanofluids, considering their constituents, the specific fluid characteristics, and the problems being addressed. The developed approach has demonstrated high accuracy in modelling nanofluids.

The significance of this study lies in its potential to advance our understanding of nanofluid behaviour by examining the individual and combined effects of variables on the thermophysical properties of nanofluids and providing researchers a road map on how to select features for nanofluid modelling so that we can have more general and accurate models. Furthermore, this methodological process for modelling as detailed in this study serves to suggest a process for researchers to apply when modelling nanofluids' thermophysical properties. By delving into these relationships, researchers can gain valuable insights into the underlying mechanisms governing nanofluid behaviour, leading to improved design and optimisation of nanofluid systems.

The ability to accurately model single material nanofluids opens up new possibilities for investigating and resolving the anomalous heat transfer enhancement observed in these fluids. Furthermore, it allows for the customisation of nanofluids to meet desired thermal properties, providing greater control over their application in various fields.

Overall, this research contributes to the growing body of knowledge on nanofluids, offering a promising avenue for further exploration and understanding of their thermophysical properties. The developed modelling approach sets the stage for future studies aimed at harnessing the full potential of nanofluids in enhancing heat transfer and achieving desired thermal characteristics. It is to be noted that the work is purely computational hence researchers can look to validate these claims experimentally. Also applying these to hybrid nanofluid serves as a significant future work.

List of Abbreviations

BFa - Base fluid thermal diffusivity (m^2/s) e+07

BFbp - Base fluid boiling point (^oC)

BFcp - Base fluid specific heat capacity (J / (kg. K))

BFd - Base fluid density (kg/m^3)

BFde - Base fluid dielectric constant (-)

BFk - Base fluid thermal conductivity (W/ (m.K))

BFkv - Base fluid kinematic viscosity (m^2/s) e+07

BFst - Base fluid surface tension (mN/m)

BFv - Base fluid viscosity (Pa.s)

DP - Particle size diameter (nm)

ENT - Percentage enhancement of nanofluid thermal conductivity (%)

GMDH – Group method of data handling

GPR – Gaussian Process Regressor

$\bar{h}$ - Mean value of observed heat transfer coefficient MAE – Mean Absolute Error

ML – Machine Learning

MRMR – Minimum Redundancy Maximum Relevance

MSE – Mean Squared Error

n - Number

NFSA - Novel feature selection algorithms

NPa - Nanoparticle thermal diffusivity (m^2/s) e+07

NPcp - Nanoparticle-specific heat capacity (J / (kg. K))

NPd - Nanoparticle density (kg/m^3)

NPde - Nanoparticle dielectric constant (-)

NPek - Nanoparticle electrical conductivity (mMS/m)

NPk - Nanoparticle thermal conductivity (W/ (m.K))

NPmp - Nanoparticle melting point (^oC)

NPms - Nanoparticle magnetic susceptibility (-)

NPri - Nanoparticle refractive index (-)

ReLU – Rectified Linear Unit

RMSE – Root Mean Squared Error

$SSreg$ - Explained sum of squares

$SStot$ - Total sum of squares

SVM – Support Vector Machine

TC - Nanofluid temperature (^{o}C)

VF - Volume fraction (%)

Superscript

$pred$ - Prediction

Subscript

i - Data point

Declarations

Ethics approval and consent to participate

Not Applicable

Consent for publication

Not Applicable

Availability of data and material

All data sources were referenced in the manuscript body.

Competing interests

The author declares that there are no competing interests.

Funding

TET Fund sponsored the studies at the University of Leeds.

Authors' contributions

EJO was the main author and only author and carried out all the work in the study.

Acknowledgements

The author wishes to thank Dr Jongrae Kim and Professor David Barton for their invaluable advice on the methods and presentation of the work. The author also

wishes to thank the Tertiary Education Trust Fund (TET Fund) for providing funding for the studies and the University of Leeds for creating the right environment.

References

Ahmadloo, E., & Azizi, S. (2016). Prediction of thermal conductivity of various nanofluids using artificial neural network. *International Communications in Heat and Mass Transfer*, *74*, 69-75. https://doi.org/10.1016/j.icheatmasstransfer.2016.03.008

Breiman, L. (2001). Random forests. *Machine learning*, *45*, 5-32.

Breiman, L., Friedman, J., Olshen, R., & Stone, C. (1984). Classification and regression trees–crc press. *Boca Raton, Florida*.

Brownlee, J. (2020a). *A Gentle Introduction to k-fold Cross-Validation*. Retrieved May 5th 2022 from https://machinelearningmastery.com/k-fold-cross-validation/

Brownlee, J. (2020b, July 2020). *How to Fix k-Fold Cross-Validation for Imbalanced Classification*. Retrieved May 27th 2022 from https://machinelearningmastery.com/cross-validation-for-imbalanced-classification/

Callister, W. D. (2007). An introduction: material science and engineering. *New York*, *106*, 139.

Cengel, Y. A., Boles, M. A., & Kanoğlu, M. (2011). *Thermodynamics: an engineering approach* (Vol. 5). McGraw-hill New York.

Chiniforooshan Esfahani, I. (2023). A data-driven physics-informed neural network for predicting the viscosity of nanofluids. *AIP Advances*, *13*(2), 025206. https://doi.org/10.1063/5.0132846

Cong, S., & Zhou, Y. (2023). A review of convolutional neural network architectures and their optimizations. *Artificial Intelligence Review*, *56*(3), 1905-1969. https://doi.org/10.1007/s10462-022-10213-5

Ewim, D. R. E., Adelaja, A., Onyiriuka, E., Meyer, J., & Huan, Z. (2020). Modelling of heat transfer coefficients during condensation inside an enhanced inclined tube. *Journal of Thermal Analysis and Calorimetry*, 1-13. https://doi.org/10.1007/s10973-020-09930-2

Ewim, D. R. E., Okwu, M. O., Onyiriuka, E. J., Abiodun, A. S., Abolarin, S. M., & Kaood, A. (2021). A quick review of the applications of artificial neural networks (ANN) in the modelling of thermal systems.

Friedman, J. H. (2001). Greedy function approximation: a gradient boosting machine. *Annals of statistics*, 1189-1232. https://doi.org/10.1214/aos/1013203451

Gareth, J., Daniela, W., Trevor, H., & Robert, T. (2013). *An introduction to statistical learning: with applications in R*. Spinger.

Genzel, M., Macdonald, J., & Marz, M. (2022). Solving inverse problems with deep neural networks-robustness included. *IEEE Transactions on Pattern Analysis and Machine Intelligence*. https://doi.org/10.1109/TPAMI.2022.3148324

Géron, A. (2022). *Hands-on machine learning with Scikit-Learn, Keras, and TensorFlow*. " O'Reilly Media, Inc.".

Gholizadeh, M., Jamei, M., Ahmadianfar, I., & Pourrajab, R. (2020). Prediction of nanofluids viscosity using random forest (RF) approach. *Chemometrics and*

Intelligent Laboratory Systems, *201*, 104010. https://doi.org/10.1016/j.chemolab.2020.104010

Hastie, T., Tibshirani, R., Friedman, J. H., & Friedman, J. H. (2009). *The elements of statistical learning: data mining, inference, and prediction* (Vol. 2). Springer.

Hornik, K., Stinchcombe, M., & White, H. (1989). Multilayer feedforward networks are universal approximators. *Neural networks*, *2*(5), 359-366. https://doi.org/10.1016/0893-6080(89)90020-8

Jiang, C., Mi, J., Laima, S., & Li, H. (2020). A novel algebraic stress model with machine-learning-assisted parameterization. *Energies*, *13*(1), 258. https://doi.org/10.3390/en13010258

Kamsuwan, C., Wang, X., Piumsomboon, P., Pratumwal, Y., Otarawanna, S., & Chalermsinsuwan, B. (2023). Artificial neural network prediction models for nanofluid properties and their applications with heat exchanger design and rating simulation. *International Journal of Thermal Sciences*, *184*, 107995. https://doi.org/10.1016/j.ijthermalsci.2022.107995

Kannaiyan, S., Boobalan, C., Nagarajan, F. C., & Sivaraman, S. (2019). Modeling of thermal conductivity and density of alumina/silica in water hybrid nanocolloid by the application of Artificial Neural Networks. *Chinese Journal of Chemical Engineering*, *27*(3), 726-736. https://doi.org/10.1016/j.cjche.2018.07.018

Komeilibirjandi, A., Raffiee, A. H., Maleki, A., Alhuyi Nazari, M., & Safdari Shadloo, M. (2020). Thermal conductivity prediction of nanofluids containing CuO nanoparticles by using correlation and artificial neural network. *Journal of Thermal Analysis and Calorimetry*, *139*, 2679-2689. https://doi.org/10.1007/s10973-019-08838-w

Kurani, A., Doshi, P., Vakharia, A., & Shah, M. (2023). A comprehensive comparative study of artificial neural network (ANN) and support vector machines (SVM) on stock forecasting. *Annals of Data Science*, *10*(1), 183-208. https://doi.org/10.1007/s40745-021-00344-x

Maronna, R. A., Martin, R. D., Yohai, V. J., & Salibián-Barrera, M. (2019). *Robust statistics: theory and methods (with R)*. John Wiley & Sons.

MathWorks. (2022). Statistics and Machine Learning Toolbox: Documentation (R2022a).

Meng, M., Zhong, R., & Wei, Z. (2020). Prediction of methane adsorption in shale: Classical models and machine learning based models. *Fuel*, *278*, 118358. https://doi.org/10.1016/j.fuel.2020.118358

Mijwil, M. M. (2018). *Artificial Neural Networks Advantages and Disadvantages*. https://www.linkedin.com/pulse/artificial-neural-networks-advantages-disadvantages-maad-m-mijwel/

Mohammed, A., & Kora, R. (2023). A comprehensive review on ensemble deep learning: Opportunities and challenges. *Journal of King Saud University-Computer and Information Sciences*. https://doi.org/10.1016/j.jksuci.2023.01.014

Moran, M. J., Shapiro, H. N., Boettner, D. D., & Bailey, M. B. (2010). *Fundamentals of engineering thermodynamics*. John Wiley & Sons.

Murshed, S., Leong, K., & Yang, C. (2005). Enhanced thermal conductivity of TiO2—water based nanofluids. *J International Journal of Thermal Sciences*, *44*(4), 367-373. https://doi.org/10.1016/j.ijthermalsci.2004.12.005

Onyiriuka, E. J. (2023). Predicting the accuracy of nanofluid heat transfer coefficient's computational fluid dynamics simulations using neural networks. *Heat Transfer*.

Onyiriuka, E. J. (2023). Single phase nanofluid thermal conductivity and viscosity prediction using neural networks and its application in a heated pipe of a circular cross section. *Heat Transfer*.

Osborne, J. (2010). Improving your data transformations: Applying the Box-Cox transformation. *Practical Assessment, Research, and Evaluation*, *15*(1), 12. https://doi.org/10.7275/qbpc-gk17

Patel, H. (2021). *What is Feature Engineering—Importance, Tools and Techniques for Machine Learning*. Medium. Retrieved 15th July from https://towardsdatascience.com/what-is-feature-engineering-importance-tools-and-techniques-for-machine-learning-2080b0269f10

Patel, H. E., Sundararajan, T., & Das, S. K. (2010). An experimental investigation into the thermal conductivity enhancement in oxide and metallic nanofluids. *Journal of Nanoparticle Research*, *12*(3), 1015-1031. https://doi.org/10.1007/s11051-009-9658-2

Peng, Y., Parsian, A., Khodadadi, H., Akbari, M., Ghani, K., Goodarzi, M., & Bach, Q.-V. (2020). Develop optimal network topology of artificial neural network (AONN) to predict the hybrid nanofluids thermal conductivity according to the empirical data of Al2O3–Cu nanoparticles dispersed in ethylene glycol. *Physica A: Statistical Mechanics and its Applications*, *549*, 124015. https://doi.org/10.1016/j.physa.2019.124015

Ramezanizadeh, M., Alhuyi Nazari, M., Ahmadi, M. H., Lorenzini, G., & Pop, I. (2019). A review on the applications of intelligence methods in predicting thermal conductivity of nanofluids. *Journal of Thermal Analysis and Calorimetry*, *138*(1), 827-843. https://doi.org/10.1007/s10973-019-08154-3

Razavi, R., Sabaghmoghadam, A., Bemani, A., Baghban, A., Chau, K.-w., & Salwana, E. (2019). Application of ANFIS and LSSVM strategies for estimating thermal conductivity enhancement of metal and metal oxide based nanofluids. *Engineering Applications of Computational Fluid Mechanics*, *13*(1), 560-578. https://doi.org/10.1080/19942060.2019.1620130

Rish, I. (2001). An empirical study of the naive Bayes classifier. IJCAI 2001 workshop on empirical methods in artificial intelligence,

Sharma, P., Ramesh, K., Parameshwaran, R., & Deshmukh, S. S. (2022). Thermal conductivity prediction of titania-water nanofluid: A case study using different machine learning algorithms. *Case Studies in Thermal Engineering*, *30*, 101658. https://doi.org/10.1016/j.csite.2021.101658

Tan, K. X., Ilyas, S. U., Pendyala, R., & Shamsuddin, M. R. (2022). Assessment of thermal conductivity and viscosity of alumina-based engine coolant nanofluids using random forest approach. AIP Conference Proceedings, https://doi.org/10.1063/5.0099553

Vapnik, V. (1999). *The nature of statistical learning theory*. Springer science & business media.

Witten, I. H., Frank, E., Hall, M. A., & Pal, C. J. (2016). *Data Mining: Practical machine learning tools and techniques*. Morgan Kaufmann.

Xie, H., Wang, J., Xi, T., Liu, Y., Ai, F., & Wu, Q. (2002). Thermal conductivity enhancement of suspensions containing nanosized alumina particles. *Journal of Applied Physics*, *91*(7), 4568-4572. https://doi.org/10.1063/1.1454184

Yashawantha, K. M., & Vinod, A. V. (2021). ANN modelling and experimental investigation on effective thermal conductivity of ethylene glycol: water nanofluids. *Journal of Thermal Analysis and Calorimetry*, *145*(2), 609-630. https://doi.org/10.1007/s10973-020-09756-y

Zhu, G., Wen, T., & Zhang, D. (2021). Machine learning based approach for the prediction of flow boiling/condensation heat transfer performance in mini channels with serrated fins. *International Journal of Heat and Mass Transfer*, *166*, 120783. https://doi.org/10.1016/j.ijheatmasstransfer.2020.120783

Appendix

Basic modelling and comparison step across various machine learning algorithms

Model Type	RMSE (Validation)	MSE (Validation)	RSQUARED (Validation)	MAE (Validation)	MAE (Test)	MSE (Test)	RMSE (Test)	RSQUARED (Test)	Preset
Neural Network	1.707	2.912	0.947	1.196	0.792	1.547	1.244	0.964	Trilayered Neural Network
Gaussian Process Regression	1.871	3.501	0.936	1.299	1.006	2.185	1.478	0.949	Exponential GPR
Gaussian Process Regression	1.929	3.720	0.932	1.390	0.923	1.447	1.203	0.966	Squared Exponential GPR
Gaussian Process Regression	1.931	3.729	0.932	1.377	0.941	1.441	1.200	0.966	Matern 5/2 GPR
SVM	1.935	3.743	0.931	1.515	0.950	1.658	1.288	0.961	Quadratic SVM
Gaussian Process Regression	2.032	4.128	0.924	1.422	0.919	1.422	1.193	0.967	Rational Quadratic GPR
SVM	2.131	4.540	0.917	1.491	0.789	1.160	1.077	0.973	Cubic SVM
Neural Network	2.185	4.776	0.912	1.542	0.619	0.561	0.749	0.987	Narrow Neural Network
Neural Network	2.222	4.937	0.909	1.502	0.743	0.947	0.973	0.978	Bilayered Neural Network
Ensemble	2.359	5.567	0.898	1.672	1.165	2.062	1.436	0.952	Boosted Trees
Neural Network	2.529	6.395	0.883	1.641	0.655	0.790	0.889	0.982	Medium Neural Network

Stepwise Linear Regression	2.573	6.620	0.879	1.988	1.546	2.977	1.725	0.930	Stepwise Linear
Neural Network	2.590	6.707	0.877	1.632	0.797	1.761	1.327	0.959	Wide Neural Network
SVM	2.679	7.176	0.868	1.940	1.159	2.492	1.579	0.942	Medium Gaussian SVM
Ensemble	2.964	8.788	0.839	2.225	1.514	3.575	1.891	0.916	Bagged Trees
Tree	3.188	10.164	0.814	2.447	1.555	3.760	1.939	0.912	Fine Tree
Linear Regression	3.387	11.470	0.790	2.319	1.828	5.000	2.236	0.883	Interactions Linear
Linear Regression	3.530	12.459	0.771	2.889	2.045	6.297	2.509	0.853	Linear
Linear Regression	3.570	12.747	0.766	2.911	2.050	6.340	2.518	0.852	Robust Linear
SVM	3.712	13.777	0.747	2.949	2.001	7.062	2.657	0.835	Linear SVM
Tree	4.004	16.028	0.706	3.091	2.235	7.242	2.691	0.831	Medium Tree
SVM	4.394	19.305	0.646	3.193	2.393	11.682	3.418	0.727	Coarse Gaussian SVM
SVM	4.468	19.962	0.634	3.009	3.002	17.704	4.208	0.586	Fine Gaussian SVM
Tree	5.164	26.672	0.511	4.082	3.579	19.630	4.431	0.541	Coarse Tree
Kernel	6.134	37.623	0.310	4.747	4.428	29.106	5.395	0.320	Least Squares Regression Kernel

Kernel	7.101	50.417	0.075	5.540	5.077	42.941	6.553	-0.003	SVM Kernel

Chapter 7 Discussion

7.1 Analysis of key findings

The research began with creating a model that accurately predicts what modelling assumptions to use for different nanofluid simulation cases. From this study it was observed that the single phase model was the worst for simulating nanofluids in terms its accuracy. Having identified that the single-phase model was not as accurate as other approaches, improving the single phase model became a motivation. This led to the creation of a neural network model, that takes as input nanoparticle specific heat, density, thermal conductivity, particle size, volume fraction, temperature of the fluid, density, specific heat capacity, and thermal conductivity of the base fluid and returns the thermal conductivity and takes a similar set of input to return the viscosity. These being very accurate are then passed to the single phase general equations solver which then solves and requests for the thermal conductivity and viscosity at every solution step. Although this is more accurate it led to the higher computational time and effort. Also since the inputs of the neural network were temperature dependent it led to a non-linear solution which reduces the stability of the solution and can sometimes lead to the solution failing at some nodes. The feature selection algorithm in Chapter 6 broke the ground in the art of feature selection for machine learning problems especially nanofluid thermal conductivity modelling by considering the physics of the problem and using that as a basis for feature selection instead of just the application of statistical tools. The approach showed very high accuracy, uniqueness and generalization of the ensuing model.

When studying nanofluids, researchers and engineers face multiple challenges to improve the accuracy and versatility of their models. These challenges stem from the knowledge that different assumptions can lead to different levels of accuracy when simulating nanofluids, which encompass a wide range of configurations and flow conditions. This research tackles the following three challenges in nanofluid modelling and prediction.

One major challenge is creating a predictive model that can accurately determine the best method for simulating a particular nanofluid. The unique configurations and flow conditions of each nanofluid require different approaches, making it crucial to develop a model that can suggest the most effective assumption for a given scenario. Such a model would prove invaluable for researchers and engineers seeking to improve the accuracy of their nanofluid simulations [12].

The second challenge involves improving the accuracy of single-phase models that are used to simulate nanofluids consisting of a single material. The goal is to incorporate a temperature-based neural network model as an additional equation in the governing equations of the single-phase model. This innovative approach aims to provide a more precise representation of thermal conductivity and viscosity in single-material nanofluids. By taking into account the temperature-dependent behaviour of thermal conductivity and viscosity and developing a neural network to replace these terms, a wider range of conditions can be studied. This will result in a more reliable model for simulating nanofluids using the single-phase model [13].

Lastly, there is a broader challenge in developing a universal method for predicting the thermophysical properties of single-material nanofluids and the need to overcome the limitations of current models that rely on simplified modelling. A more comprehensive approach to nanofluid modelling and understanding of the features of nanofluids could lead to generalised models that would be extremely valuable for researchers and engineers trying to predict these properties accurately [14].

This study aimed to present solutions to the problem of modelling nanofluids and develop an algorithm to predict the accuracy of nanofluid heat transfer coefficient computational fluid dynamics (CFD) simulations using neural networks. The results and analyses presented shed light on the performance of various models under different conditions, allowing us to draw insightful conclusions.

The data collection process involved compiling a dataset from literature sources encompassing various nanofluid configurations and flow geometries. This dataset was then used to train, validate, and test the neural network algorithm. The selected input parameters for the algorithm included particle size, particle volume fraction, wall thermal condition, thermophysical property assumption, model type, particle type, host fluid, and geometry. The output variable was the average percentage error in predicting the heat transfer coefficient.

The neural network model architecture was chosen based on experimentation and optimisation. It consisted of one hidden layer with 170 neurons, and the Rectified Linear Unit (ReLU) activation function was used for the input and hidden layers. The neural network was trained using the RMSprop optimisation algorithm and evaluated using performance metrics such as Mean Absolute Error (MAE), Root Mean Squared Error (RMSE), and R-squared (R^2) values.

The performance of the neural network model was assessed through various analyses. The algorithm demonstrated its ability to accurately predict the heat transfer coefficient's percentage error for different nanofluid simulations. The R^2 value of 0.80 indicated a strong correlation between the predicted and actual errors,

highlighting the model's predictive capabilities. The algorithm's performance was also validated through repeated training runs.

The study's results provided valuable insights into the accuracy of different models under varying conditions. It was observed that the dispersion, Buongiorno, and discrete phase models exhibited consistently high accuracy across a wide range of Reynolds numbers, particle sizes, and volume fractions. These models proved to be versatile and reliable choices for nanofluid simulations. In contrast, the single-phase model (SPM) showed inferior performance and should be employed only when other modelling options are not feasible.

Furthermore, the analysis indicated that the accuracy of the models tended to decrease with increasing Reynolds numbers, highlighting the challenges of simulating nanofluids in turbulent flow regimes. The choice of thermophysical property assumption also played a significant role in model accuracy, with constant property assumptions generally performing better [12].

In the context of nanofluid heat transfer simulations, the accurate prediction of heat transfer coefficients is of paramount importance in numerous industrial and scientific applications. The findings of this study have significant implications for optimising thermal management systems, enhancing energy efficiency, and designing advanced cooling technologies.

The study developed and applied a neural network-based approach for predicting the thermal conductivity and viscosity of single-material nanofluids. The study aimed to demonstrate the improved accuracy of simulations using these predicted properties in a heated pipe of circular cross-section. The results and discussions below summarise the findings of this study.

Several researchers have made efforts to address the challenges in nanofluid simulations through numerical methods. For instance, [134] explored heat transfer and laminar flow of nanofluids in a three-dimensional flow geometry. [124] focused on convective heat transfer in the developing region of a tube, while [136] studied turbulent flow in circular tubes. [131] emphasised accurate forced convection heat transfer prediction. Despite these efforts, discrepancies and inconsistencies among studies remain, underscoring the need for improved and efficient modelling techniques.

The neural network-based approach presented in this study offers a promising solution to these challenges. The study successfully predicted the viscosity and thermal conductivity of various single-material nanofluids by training neural network models using experimental data. These predictions were then integrated into a

single-phase simulation and solved using the finite element method. The accuracy of the predictions was validated against experimental data not included in the training dataset. The obtained results exhibited excellent agreement, with an average percentage error of 0.679%, showcasing the reliability and generalisation capabilities of the neural network models. It is noteworthy that the models were temperature-based, making them closer to the real scenarios.

The introduction highlighted the difficulties in numerical studies of nanofluids, including discrepancies arising from different formulations and the need for expensive experimental validations. The study's primary goal was to tackle these challenges by developing accurate neural network models for nanofluid properties.

The architecture of the neural network models used for predicting nanofluid viscosity and thermal conductivity was detailed. The viscosity prediction model comprised a hidden layer with 10 neurons, utilising the Log-Sigmoid transfer function. The thermal conductivity prediction model shared a similar architecture. Both models incorporated inputs such as nanoparticle properties, base fluid properties, volume fraction, particle size, and fluid temperature.

The performance of the neural network models was meticulously assessed. The mean squared error plot demonstrated the convergence of the network during training. The error histogram indicated balanced fitting among training, validation, and testing data. The change of gradient, mu, and validation fail plot highlighted consistent and optimal network training and testing, with decreasing gradients as training progressed.

Grid convergence analysis established that the simulation results accurately match with experimental data. The extra fine mesh yielded results very close to experimental data, confirming grid independence and precise resolution of thermal characteristics. Simulation results were validated against experimental data for various nanofluids, including CuO-water, TiO_2-water, and ZrO_2-water. Temperature profile plots along the pipe's length exhibited excellent agreement between simulation and experimental data. Average percentage errors fell within acceptable limits, further affirming the models' accuracy [13].

In this study also, a novel and innovative approach for the predictive modelling of thermal conductivity in single-material nanofluids was introduced. The key contribution of this research lies in the development of a comprehensive methodology that takes into account the fluid's constituents, specific characteristics, and material properties. Unlike conventional methods that rely heavily on statistical feature selection, this study proposed an approach grounded in the physical

properties of the fluid, enabling a more generalised and accurate model. A critical yet often overlooked aspect of predictive modelling.

The comparison of various machine learning algorithms allowed for a comprehensive evaluation of the model's performance. The neural network emerged as the best basic model, demonstrating its ability to capture complex relationships within the data. However, an optimised neural network did not yield improved results, suggesting the effect of overfitting.

The exploration of different feature selection algorithms sheds light on the significance of variable selection. The traditional Minimum Redundancy Maximum Relevance (MRMR) approach identified Volume Fraction (VF) and Temperature (TC) as essential features. Importantly, novel feature selection algorithms were introduced, offering a fresh perspective on the modelling process. One novel algorithm focused on selecting variables with similar statistical characteristics, while the other emphasised variables with different statistical characteristics. Notably, the latter algorithm achieved the best model performance, underlining the importance of choosing diverse features for enhanced predictive accuracy.

Histogram plots and box plots provided insights into the distribution of variables. None of the features exhibited a normal distribution, indicating the need for models that can accommodate non-normal data. This insight guided the selection of suitable modelling techniques, such as robust linear regression, non-parametric models, ensemble models, and neural networks.

The practical significance of the developed predictive model is noteworthy. The model offers the capability to numerically study and optimise nanofluids, enabling the tailoring of conventional fluids to achieve desired thermal properties. This breakthrough enhances researchers' ability to manipulate fluid properties for specific applications, revolutionising fields reliant on thermal conductivity.

The approach outlined in this study for predictive modelling of thermal conductivity in single-material nanofluids presents a significant advancement in the field of fluid dynamics, heat transfer and materials science. By delving into the intricate interactions between fluid constituents and their thermal properties, the research offers a fresh perspective on how nanofluids can be optimised for various applications. Moreover, the comparison of different machine learning algorithms adds another layer of credibility to the study's findings. The neural network's superiority in capturing intricate relationships within the data underscores its potential as a powerful tool in nanofluid research. However, the intriguing finding that an optimised neural network did not yield significant improvements over the basic model

suggests that there might be inherent limits to the complexity of the relationships that can be effectively tuned [14].

7.2 Limitations

In simulating nanofluids, researchers as observed in the literature survey, often use a hit-and-miss approach to decide which simulation method to apply. However, a new study has developed a model that uses machine learning to determine the best simulation approach for different nanofluid and flow scenarios. Additionally, researchers commonly apply the single-phase model without considering the temperature-based thermophysical properties of nanofluids as an input to the model, resulting in less accurate models. The study suggests that better accuracy can be achieved by modelling the temperature-based thermophysical properties of nanofluids and applying them as equations in the single-phase model, although doing that increases the computational cost considerably as the model is called for each new numerical solution. Finally, instead of relying solely on statistics for feature selection, this study proposes a physics-based and methodical approach to develop generalised nanofluid thermophysical property models.

These are the study's limitations:

1. The study was conducted solely through computational methods without any experimental research being carried out.
2. The amount of available data considered may be considered insufficient, and the validity of the data applied can be questioned as it was sourced from other open literature.
3. The study did not test very complex neural network architectures, with the largest network being a tri-layered neural network.
4. A temperature profile plot was used to show accurate results of 0.679%, but it may not be the best variable for drawing conclusions as temperature changes are minimal.
5. The single-phase model was based on a particular non-open source software (COMSOL), which may make its broader application difficult.
6. The results of the single-phase model were tested in a very simple geometry, and it is unclear if the results can be applied to other geometries of varying complexities.
7. The generalised modelling strategy was not tested for other scenarios apart from thermal conductivity, and although it was tested with test data, it was not validated experimentally.

Chapter 8 Conclusions and outlook

The findings have identified key insights and implications to help engineers and researchers effectively design and optimise heat exchangers, cooling systems, and thermal management solutions. Accurately predicting nanofluid thermal and flow characteristics has been proven to be possible while considering other factors like its generalisation. Nanofluids have been extensively studied, and the following findings have been established in the present study:

1. The three (3) modelling assumptions namely dispersion, Buongiorno, and discrete phase model (DPM) showed high accuracy in modelling nanofluids. They all have an accuracy within 5%, with the dispersion model being the best for both constant and temperature-dependent property assumptions. The discrete phase model (DPM) model seems to do better in turbulent flow than in laminar flow, while the Buongiorno models do better under laminar flow conditions.
2. The single phase model and mixture models were observed to be the worst and only recommended where there are no other choices.
3. The accuracy of the single phase model can be considerably improved by the substitution of the thermophysical properties of the nanofluid with an accurate machine learning model.
4. The feature selection method based on physics of the problem is a highly effective machine learning modelling strategy with the possibility of higher accuracy and generalization.
5. Neural network models are considerably effective in modelling nanofluids thermophysical properties.

Nanofluids have gained substantial attention for their potential to enhance heat transfer properties. The study's identification of accurate simulation models provides a valuable roadmap for future nanofluid research. Researchers can focus on utilising the most reliable models, leading to a deeper understanding of nanofluid behaviour and its impact on heat transfer performance.

As industries continue to explore sustainable energy technologies, nanofluid-based heat transfer systems play a crucial role. The ability to accurately predict nanofluid heat transfer coefficients allows for developing efficient and eco-friendly energy conversion and storage systems, contributing to a greener and more sustainable future.

The study's insights into the effect of particle size, particle volume fraction, and base fluid on heat transfer coefficients can guide materials scientists in designing nanoparticles optimised for heat transfer applications. This could lead to the development of novel nanomaterials with tailored properties, impacting heat transfer and various other fields.

In industries that rely on precise temperature control and heat dissipation, such as electronics manufacturing, predicting heat transfer coefficients accurately is crucial. Manufacturers can maintain consistent product quality and optimise manufacturing processes by selecting appropriate models and accounting for nanofluid behaviour.

The algorithm developed in this study could serve as a valuable educational and training tool. Engineers, students, and researchers entering the nanofluid heat transfer simulations field can use this tool to quickly assess the accuracy of different models and make informed decisions in their work.

The study underscores the importance of collaboration between researchers in fluid dynamics, nanotechnology, materials science, and engineering. Cross-disciplinary efforts can lead to developing more comprehensive and accurate models that capture the complexities of nanofluid behaviour across various scenarios.

The research findings substantially impact nanofluid applications in diverse industries and technologies. Accurate simulations of nanofluid behaviour are vital for optimising product development, enhancing heat transfer, and improving energy efficiency. The neural network-based approach efficiently captures complex nanofluid behaviour, reduces reliance on time-consuming experiments, and accelerates the implementation of nanofluid-based technologies.

The broader implications of this research are profound. As industries continue to seek more efficient and effective thermal management solutions, the ability to tailor nanofluids with desired thermal properties becomes increasingly valuable. The predictive model developed in this study serves as a practical tool for designing and optimising nanofluids and opens up possibilities for innovation in diverse fields, such as electronics cooling, renewable energy systems, and biomedical applications.

8.1 Conclusions

In summary, this research study collectively represents a significant advancement in the field of nanofluid research, with a focus on predictive modelling, simulation accuracy, and understanding nanofluid behaviour.

The study addresses the challenge of simulation accuracy by developing neural network-based models for predicting the best modelling assumptions to apply in nanofluid simulation such that the researcher has the least error possible. It presents an algorithm that leverages neural networks to predict the accuracy of nanofluid heat transfer coefficient simulations. This algorithm demonstrates its effectiveness in predicting percentage errors for diverse nanofluid configurations and flow geometries, offering valuable insights for engineering applications and enhancing the reliability of heat transfer coefficient predictions.

The study also improves the single-phase simulation assumption by using accurate and temperature-based thermophysical properties.

The study introduces an innovative approach to predict thermal conductivity in single-material nanofluids, developing a generalised feature selection algorithms approach and utilising various machine learning techniques. This model not only offers a powerful tool for optimising nanofluid compositions but also sets a new standard for future research by emphasising careful feature selection and its broader implications for the study, engineering, and exploitation of nanofluids in various industries.

Together, these studies underscore the potential of nanofluid research to drive innovation and transformation across various sectors. They offer powerful tools and methodologies that enhance our understanding of nanofluid behaviour and its applications, setting the stage for a future where nanofluids redefine the frontiers of thermal management, energy efficiency, and technological progress. As we continue to explore the intricacies of nanofluid dynamics, these pioneering efforts propel the field toward new horizons, fostering enhanced understanding and unparalleled advancements.

8.2 Future directions

The field of nanofluid research has a lot of potential for practical applications. To advance this field, many future research directions need to be explored. These include addressing the complexity of multi-material nanofluids, exploring dynamic and transient behaviour, nanoparticle distribution patterns, and the impact of nanoparticle shape.

Here are some specific investigations that are worth carrying out:

1. Conduct experimental testing and validation of nanofluid simulation results and modelling predictions.

2. Apply the generalised nanofluid thermal conductivity modelling approach to multi-material nanofluids.
3. Optimize nanofluid features to achieve desired properties and behaviour.
4. Use molecular dynamic simulation to study hybrid nanofluids.
5. Study the impact of nanofluid features on its behaviour.
6. Investigate the steady-state and transient behaviour of hybrid nanofluids.
7. Applying reinforcement learning to optimize nanofluids performance.
8. Apply machine learning to predict hybrid nanofluid thermal and flow characteristics.

References

1. Bhattad, A., J. Sarkar, and P. Ghosh, *Hydrothermal performance of different alumina hybrid nanofluid types in plate heat exchanger: experimental study.* Journal of Thermal Analysis and Calorimetry, 2020. **139**: p. 3777-3787.
2. Stalin, P.M.J., et al., *Investigations on thermal properties of CeO2/water nanofluids for heat transfer applications.* Materials Today: Proceedings, 2021. **47**: p. 6815-6820.
3. Mahian, O., et al., *Recent advances in using nanofluids in renewable energy systems and the environmental implications of their uptake.* Nano Energy, 2021. **86**: p. 106069.
4. Gray, N., *Water Science and Technology: An Introduction*. 2017: CRC Press.
5. Holden, J., *Water resources: an integrated approach*. 2019: Routledge.
6. Choi, S.U. and J.A. Eastman, *Enhancing thermal conductivity of fluids with nanoparticles*. 1995, Argonne National Lab., IL (United States).
7. Xie, H., et al., *Thermal conductivity enhancement of suspensions containing nanosized alumina particles.* Journal of applied physics, 2002. **91**(7): p. 4568-4572.
8. Das, S.K., et al., *Temperature dependence of thermal conductivity enhancement for nanofluids.* ASME Transition Jounal of Heat Transfer, 2003. **125**(567).
9. Wang, X. and A.S. Mujumdar, *Heat transfer characteristics of nanofluids: a review.* International journal of thermal sciences, 2007. **46**(1): p. 1-19.
10. Venerus, D.C., et al., *Viscosity measurements on colloidal dispersions (nanofluids) for heat transfer applications.* Applied rheology, 2010. **20**(4).
11. Buongiorno, J., et al., *A benchmark study on the thermal conductivity of nanofluids.* Journal of Applied Physics, 2009. **106**(9): p. 094312.
12. Onyiriuka, E.J., *Predicting the accuracy of nanofluid heat transfer coefficient's computational fluid dynamics simulations using neural networks.* Heat Transfer, 2023. **52**(4): p. 3389-3410.
13. Onyiriuka, E.J., *Single phase nanofluid thermal conductivity and viscosity prediction using neural networks and its application in a heated pipe of a circular cross section.* Heat Transfer, 2023. **52**(5): p. 3516-3537.
14. Onyiriuka, E., *Predictive modelling of thermal conductivity in single-material nanofluids: a novel approach.* Bulletin of the National Research Centre, 2023. **47**(1): p. 140.
15. Rohrer, H., *The nanoworld: chances and challenges.* Microelectronic Engineering, 1996. **32**(1): p. 5-14.
16. Sohn, L.L., *A quantum leap for electronics.* Nature, 1998. **394**(6689): p. 131-132.
17. Choi, S.U.S., *Nanofluids: From Vision to Reality Through Research.* Journal of Heat Transfer, 2009. **131**(3).
18. Iqbal, M., et al., *Critical analysis of thermal conductivity enhancement of alumina–water nanofluids.* Journal of Thermal Analysis and Calorimetry, 2023. **148**(18): p. 9361-9389.
19. Ramzan, M., et al., *Model-based comparison of hybrid nanofluid Darcy-Forchheimer flow subject to quadratic convection and frictional heating with multiple slip conditions.* Numerical Heat Transfer, Part A: Applications: p. 1-21.

20. Abdelaziz, A.H., et al., *Mixed convection heat transfer utilizing Nanofluids, ionic Nanofluids, and hybrid nanofluids in a horizontal tube.* Alexandria Engineering Journal, 2022. **61**(12): p. 9495-9508.
21. Wang, L. and J. Fan, *Nanofluids research: key issues.* (1556-276X (Electronic)).
22. Ali, A.R.I. and B. Salam, *A review on nanofluid: preparation, stability, thermophysical properties, heat transfer characteristics and application.* SN Applied Sciences, 2020. **2**(10): p. 1636.
23. Yasmin, H., et al., *Reproduction of nanofluid synthesis, thermal properties and experiments in engineering: A research paradigm shift.* Energies, 2023. **16**(3): p. 1145.
24. Zhu, H.T., Y.-s. Lin Ys Fau - Yin, and Y.S. Yin, *A novel one-step chemical method for preparation of copper nanofluids.* (0021-9797 (Print)).
25. Zhu, D., et al., *Dispersion behavior and thermal conductivity characteristics of Al2O3–H2O nanofluids.* Current Applied Physics, 2009. **9**(1): p. 131-139.
26. Bobbo, S., et al., *Analysis of the parameters required to properly define nanofluids for heat transfer applications.* Fluids, 2021. **6**(2): p. 65.
27. Choudhary, S., A. Sachdeva, and P. Kumar, *Time-based analysis of stability and thermal efficiency of flat plate solar collector using iron oxide nanofluid.* Applied Thermal Engineering, 2021. **183**: p. 115931.
28. Lee, J.H., D.H. Kam, and Y.H. Jeong, *The effect of nanofluid stability on critical heat flux using magnetite-water nanofluids.* Nuclear Engineering and Design, 2015. **292**: p. 187-192.
29. Bhattacharjee, S., *DLS and zeta potential – What they are and what they are not?* Journal of Controlled Release, 2016. **235**: p. 337-351.
30. Fedele, L., et al., *Experimental stability analysis of different water-based nanofluids.* Nanoscale Research Letters, 2011. **6**(1): p. 300.
31. Angayarkanni, S.A. and J. Philip, *Review on thermal properties of nanofluids: Recent developments.* Advances in Colloid and Interface Science, 2015. **225**: p. 146-176.
32. Sadeghy, R., et al., *Investigation of alumina nanofluid stability using experimental and modified population balance methods.* Advanced Powder Technology, 2016. **27**(5): p. 2186-2195.
33. Tantra, R., P. Schulze, and P. Quincey, *Effect of nanoparticle concentration on zeta-potential measurement results and reproducibility.* Particuology, 2010. **8**(3): p. 279-285.
34. Nabati Shoghl, S., J. Jamali, and M. Keshavarz Moraveji, *Electrical conductivity, viscosity, and density of different nanofluids: An experimental study.* Experimental Thermal and Fluid Science, 2016. **74**: p. 339-346.
35. Haghighi, E.B., et al., *Shelf stability of nanofluids and its effect on thermal conductivity and viscosity.* Measurement Science and Technology, 2013. **24**(10): p. 105301.
36. Chen, H., et al., *Predicting thermal conductivity of liquid suspensions of nanoparticles (nanofluids) based on rheology.* Particuology, 2009. **7**(2): p. 151-157.
37. Chiesa, M. and A. Simonsen, *The Importance of Suspension Stability for the Hot-wire Measurements of Thermal Conductivity of Colloidal Suspensions.* 2007.

38. Singh, A.K. and V.S. Raykar, *Microwave synthesis of silver nanofluids with polyvinylpyrrolidone (PVP) and their transport properties.* Colloid and Polymer Science, 2008. **286**: p. 1667-1673.
39. Mukherjee, S. and S. Paria, *Preparation and stability of nanofluids-a review.* IOSR Journal of Mechanical and civil engineering, 2013. **9**(2): p. 63-69.
40. Wei, X., et al., *Synthesis and thermal conductivity of Cu2O nanofluids.* International Journal of Heat and Mass Transfer, 2009. **52**(19-20): p. 4371-4374.
41. Martínez, V.A., D.A. Vasco, and C.M. García–Herrera, *Transient measurement of the thermal conductivity as a tool for the evaluation of the stability of nanofluids subjected to a pressure treatment.* International communications in heat and mass transfer, 2018. **91**: p. 234-238.
42. Karthikeyan, N., J. Philip, and B. Raj, *Effect of clustering on the thermal conductivity of nanofluids.* Materials Chemistry and Physics, 2008. **109**(1): p. 50-55.
43. Singh, U. and N.K. Gupta, *Stability issues and operating limitations of nanofluid filled heat pipe: A critical review.* Materials Today: Proceedings, 2023.
44. Alktranee, M., et al., *Effect of zirconium oxide nanofluid on the behaviour of photovoltaic–thermal system: An experimental study.* Energy Reports, 2023. **9**: p. 1265-1277.
45. Kazem, H.A., et al., *Effect of temperature on the electrical and thermal behaviour of a photovoltaic/thermal system cooled using SiC nanofluid: an experimental and comparison study.* Sustainability, 2022. **14**(19): p. 11897.
46. Wu, P., A.D. Nikolov, and D.T. Wasan, *Nanofluid Structural Forces Alter Solid Wetting, Enhancing Oil Recovery.* Colloids and Interfaces, 2022. **6**(2): p. 33.
47. Olabi, A., et al., *Geometrical effect coupled with nanofluid on heat transfer enhancement in heat exchangers.* International Journal of Thermofluids, 2021. **10**: p. 100072.
48. Amoo, O.M., A. Ajiboye, and M.O. Oyewola, *Analysis of thermophysical and transport properties of nanofluids using machine learning algorithms.* International Journal of Thermofluids, 2024. **21**: p. 100566.
49. Komeilibirjandi, A., et al., *Thermal conductivity prediction of nanofluids containing CuO nanoparticles by using correlation and artificial neural network.* Journal of Thermal Analysis and Calorimetry, 2020. **139**(4): p. 2679-2689.
50. Ahmed, H., H. Mohammed, and M. Yusoff, *Heat transfer enhancement of laminar nanofluids flow in a triangular duct using vortex generator.* Superlattices and Microstructures, 2012. **52**(3): p. 398-415.
51. Hamilton, R.L. and O. Crosser, *Thermal conductivity of heterogeneous two-component systems.* Industrial & Engineering chemistry fundamentals, 1962. **1**(3): p. 187-191.
52. Maxwell, J.C., *Maxwell on molecules and gases*. 1986: Mit Press.
53. Dogonchi, A. and D. Ganji, *Analytical solution and heat transfer of two-phase nanofluid flow between non-parallel walls considering Joule heating effect.* Powder technology, 2017. **318**: p. 390-400.
54. Maiga, S.E.B., et al., *Heat transfer enhancement by using nanofluids in forced convection flows.* International journal of heat and fluid flow, 2005. **26**(4): p. 530-546.

55. Khanafer, K., K. Vafai, and M. Lightstone, *Buoyancy-driven heat transfer enhancement in a two-dimensional enclosure utilizing nanofluids.* International journal of heat and mass transfer, 2003. **46**(19): p. 3639-3653.
56. Corcione, M., *Empirical correlating equations for predicting the effective thermal conductivity and dynamic viscosity of nanofluids.* Energy Conversion and Management, 2011. **52**(1): p. 789-793.
57. Rudyak, V.Y. and A.V. Minakov, *Thermophysical properties of nanofluids.* The European Physical Journal E, 2018. **41**(1): p. 15.
58. Meyer, J.P., et al., *The viscosity of nanofluids: a review of the theoretical, empirical, and numerical models.* J Heat Transfer Engineering, 2016. **37**(5): p. 387-421.
59. Sharifpur, M., S.A. Adio, and J.P. Meyer, *Experimental investigation and model development for effective viscosity of Al2O3–glycerol nanofluids by using dimensional analysis and GMDH-NN methods.* J International Communications in Heat Mass Transfer, 2015. **68**: p. 208-219.
60. Adio, S.A., et al., *Experimental investigation and model development for effective viscosity of MgO–ethylene glycol nanofluids by using dimensional analysis, FCM-ANFIS and GA-PNN techniques.* J International Communications in Heat Mass Transfer, 2016. **72**: p. 71-83.
61. Al-Rashed, A.A., et al., *Numerical investigation of non-Newtonian water-CMC/CuO nanofluid flow in an offset strip-fin microchannel heat sink: thermal performance and thermodynamic considerations.* J Applied Thermal Engineering, 2019. **155**: p. 247-258.
62. Adio, S.A., M. Sharifpur, and J.P. Meyer, *Investigation into effective viscosity, electrical conductivity, and pH of γ-Al2O3-glycerol nanofluids in Einstein concentration regime.* J Heat Transfer Engineering, 2015. **36**(14-15): p. 1241-1251.
63. Adio, S.A., M. Sharifpur, and J.P. Meyer, *Factors affecting the pH and electrical conductivity of MgO–ethylene glycol nanofluids.* J Bulletin of Materials Science, 2015. **38**(5): p. 1345-1357.
64. Adio, S.A., M. Sharifpur, and J.P. Meyer, *Influence of ultrasonication energy on the dispersion consistency of Al2O3–glycerol nanofluid based on viscosity data, and model development for the required ultrasonication energy density.* J Journal of Experimental Nanoscience, 2016. **11**(8): p. 630-649.
65. Adio, S.A., et al., *Thermohydraulic and entropy characteristics of Al2O3-water nanofluid in a ribbed interrupted microchannel heat exchanger.* Heat Transfer.
66. Liu, X., et al., *An experimental investigation on the rheological behavior of nanofluids made by suspending multi-walled carbon nanotubes in liquid paraffin.* Journal of Molecular Liquids, 2020. **300**: p. 112269.
67. Demirkır, Ç. and H. Ertürk, *Rheological and thermal characterization of graphene-water nanofluids: Hysteresis phenomenon.* International Journal of Heat and Mass Transfer, 2020. **149**: p. 119113.
68. Birkman, H., *The viscosity of concentrated suspensions and solution.* The Journal of Chemical Physics, 1952. **20**(4): p. 571.
69. Einstein, A., *Über die von der molekularkinetischen Theorie der Wärme geforderte Bewegung von in ruhenden Flüssigkeiten suspendierten Teilchen.* Annalen der physik, 1905. **322**(8): p. 549-560.
70. Krieger, I.M. and T.J. Dougherty, *A mechanism for non-Newtonian flow in suspensions of rigid spheres.* Transactions of the Society of Rheology, 1959. **3**(1): p. 137-152.

71. Singh, P.K., et al., *Entropy generation due to flow and heat transfer in nanofluids.* International Journal of Heat and Mass Transfer, 2010. **53**(21-22): p. 4757-4767.
72. Onyiriuka, E., et al., *Evaluation of single-phase, discrete, mixture and combined model of discrete and mixture phases in predicting nanofluid heat transfer characteristics for laminar and turbulent flow regimes.* Advanced Powder Technology, 2018.
73. Khanafer, K. and K. Vafai, *A critical synthesis of thermophysical characteristics of nanofluids.* International Journal of Heat and Mass Transfer, 2011. **54**(19-20): p. 4410-4428.
74. Géron, A., *Hands-On Machine Learning with Scikit-Learn, Keras, and TensorFlow: Concepts, Tools, and Techniques to Build Intelligent Systems*. 2019: O'Reilly Media.
75. Samuel, A.L., *Some Studies in Machine Learning Using the Game of Checkers.* IBM Journal of Research and Development, 1959. **3**(3): p. 210-229.
76. Zou, J., Y. Han, and S.-S. So, *Overview of Artificial Neural Networks*, in *Artificial Neural Networks: Methods and Applications*, D.J. Livingstone, Editor. 2009, Humana Press: Totowa, NJ. p. 14-22.
77. Zhang, Z., *Decision tree modeling using R.* (2305-5839 (Print)).
78. James, G., et al., *Linear Regression*, in *An Introduction to Statistical Learning: with Applications in Python*, G. James, et al., Editors. 2023, Springer International Publishing: Cham. p. 69-134.
79. Orrù, P.F., et al. *Machine Learning Approach Using MLP and SVM Algorithms for the Fault Prediction of a Centrifugal Pump in the Oil and Gas Industry*. Sustainability, 2020. **12**, DOI: 10.3390/su12114776.
80. Yoon, J., *Forecasting of Real GDP Growth Using Machine Learning Models: Gradient Boosting and Random Forest Approach.* Computational Economics, 2021. **57**(1): p. 247-265.
81. Guo, G., et al. *KNN Model-Based Approach in Classification*. in *On The Move to Meaningful Internet Systems 2003: CoopIS, DOA, and ODBASE*. 2003. Berlin, Heidelberg: Springer Berlin Heidelberg.
82. Esfahani, J.A., et al., *Comparison of experimental data, modelling and non-linear regression on transport properties of mineral oil based nanofluids.* Powder Technology, 2017. **317**: p. 458-470.
83. Ahmadi, M.H., et al., *Thermal conductivity ratio prediction of Al2O3/water nanofluid by applying connectionist methods.* Colloids and Surfaces A: Physicochemical and Engineering Aspects, 2018. **541**: p. 154-164.
84. Akilu, S., et al., *Machine learning analysis of thermophysical and thermohydraulic properties in ethylene glycol- and glycerol-based SiO2 nanofluids.* Scientific Reports, 2024. **14**(1): p. 14829.
85. Ajila, F., et al., *Prediction of nanofluid thermal conductivity and viscosity with machine learning and molecular dynamics.* Thermal Science, 2024(00): p. 5-5.
86. Topal, H.İ., et al., *Dynamic viscosity prediction of nanofluids using artificial neural network (ANN) and genetic algorithm (GA).* Journal of the Brazilian Society of Mechanical Sciences and Engineering, 2024. **46**(7): p. 429.
87. Nik Salimi, N.E.B., et al., *Rheological behavior predictions of non-Newtonian nanofluids via correlations and artificial neural network for thermal applications.* Digital Chemical Engineering, 2024. **12**: p. 100170.

88. Bahiuddin, I., et al., *Review of modeling schemes and machine learning algorithms for fluid rheological behavior analysis.* 2024. **33**(1).
89. Hemmat Esfe, M., et al., *Presenting the best correlation relationship for predicting the dynamic viscosity of CuO nanoparticles in ethylene glycol - water base fluid using response surface methodology.* Arabian Journal of Chemistry, 2024. **17**(1): p. 105467.
90. Qu, M., et al., *A new model for viscosity prediction for silica-alumina-MWCNT/Water hybrid nanofluid using nonlinear curve fitting.* Engineering Science and Technology, an International Journal, 2024. **50**: p. 101604.
91. Davoudi, A., et al., *Numerical simulation on heat transfer of nanofluid in conical spiral heat exchanger.* Progress in Computational Fluid Dynamics, an International Journal, 2021. **21**(1): p. 52-63.
92. Chen, Y., et al., *Numerical simulation and analysis of natural convective flow and heat transfer of nanofluid under electric field.* International Communications in Heat and Mass Transfer, 2021. **120**: p. 105053.
93. Chen, W.-C. and W.-T. Cheng, *Numerical simulation on forced convective heat transfer of titanium dioxide/water nanofluid in the cooling stave of blast furnace.* International Communications in Heat and Mass Transfer, 2016. **71**: p. 208-215.
94. Sekrani, G. and S. Poncet *Further Investigation on Laminar Forced Convection of Nanofluid Flows in a Uniformly Heated Pipe Using Direct Numerical Simulations*. Applied Sciences, 2016. **6**, DOI: 10.3390/app6110332.
95. Jang, S.P. and S.U.S. Choi, *Role of Brownian motion in the enhanced thermal conductivity of nanofluids.* Applied Physics Letters, 2004. **84**(21): p. 4316-4318.
96. Alimoradi, H., et al., *A parametric study of subcooled flow boiling of Al2O3/water nanofluid using numerical simulation and artificial neural networks.* Nanoscale and Microscale Thermophysical Engineering, 2022. **26**(2-3): p. 129-159.
97. Fardi, M. and Y. Khan, *Numerical simulation of squeezing Cu–Water nanofluid flow by a kernel-based method.* International Journal of Modeling, Simulation, and Scientific Computing, 2022. **13**(01): p. 2250005.
98. Bahiraei, M., S. Mostafa Hosseinalipour, and M. Hangi, *Prediction of convective heat transfer of AlO-water nanofluid considering particle migration using neural network.* Engineering Computations, 2014. **31**(5): p. 843-863.
99. Anoop, K., T. Sundararajan, and S.K. Das, *Effect of particle size on the convective heat transfer in nanofluid in the developing region.* International journal of heat and mass transfer, 2009. **52**(9-10): p. 2189-2195.
100. Mahfouz, A.B., *Viscosity prediction and optimization of ZnO-coconut oil nanofluids using numerical simulation.* Materials Today: Proceedings, 2021. **42**: p. 1437-1441.
101. Ueki, Y., et al., *Thermophysical properties of carbon-based material nanofluid.* International Journal of Heat and Mass Transfer, 2017. **113**: p. 1130-1134.
102. Mohamed, R., *Application of artificial neural network model for prediction of thermo–physical properties of carbon nanotubes (CNTs) containing nanofluid.* Journal of Nanofluids, 2019. **8**(1): p. 199-204.
103. Asadi, A., A.N. Bakhtiyari, and I.M. Alarifi, *Predictability evaluation of support vector regression methods for thermophysical properties, heat transfer*

performance, and pumping power estimation of MWCNT/ZnO–engine oil hybrid nanofluid. Engineering with Computers, 2021. **37**(4): p. 3813-3823.
104. Hemmat Esfe, M., et al., *Experimental determination of thermal conductivity and dynamic viscosity of Ag–MgO/water hybrid nanofluid.* International Communications in Heat and Mass Transfer, 2015. **66**: p. 189-195.
105. Hemmat Esfe, M., S. Wongwises, and M. Rejvani, *Prediction of thermal conductivity of carbon nanotube-EG nanofluid using experimental data by ANN.* Current Nanoscience, 2017. **13**(3): p. 324-329.
106. Mukesh Kumar, P.C. and R. Kavitha, *Prediction of nanofluid viscosity using multilayer perceptron and Gaussian process regression.* Journal of Thermal Analysis and Calorimetry, 2021. **144**(4): p. 1151-1160.
107. Rashidi, S., et al., *Volume of fluid model to simulate the nanofluid flow and entropy generation in a single slope solar still.* Renewable Energy, 2018. **115**: p. 400-410.
108. Mahdavi, M., M. Sharifpur, and J.P. Meyer, *A novel combined model of discrete and mixture phases for nanoparticles in convective turbulent flow.* Physics of Fluids, 2017. **29**(8): p. 082005.
109. Akbari, M., A. Behzadmehr, and F. Shahraki, *Fully developed mixed convection in horizontal and inclined tubes with uniform heat flux using nanofluid.* International Journal of Heat and Fluid Flow, 2008. **29**(2): p. 545-556.
110. Akbari, M., N. Galanis, and A. Behzadmehr, *Comparative assessment of single and two-phase models for numerical studies of nanofluid turbulent forced convection.* International Journal of Heat and Fluid Flow, 2012. **37**: p. 136-146.
111. Albojamal, A. and K. Vafai, *Analysis of single phase, discrete and mixture models, in predicting nanofluid transport.* International Journal of Heat and Mass Transfer, 2017. **114**: p. 225-237.
112. Akbarinia, A. and A. Behzadmehr, *Numerical study of laminar mixed convection of a nanofluid in horizontal curved tubes.* Applied Thermal Engineering, 2007. **27**(8-9): p. 1327-1337.
113. Bahiraei, M., *A comprehensive review on different numerical approaches for simulation in nanofluids: traditional and novel techniques.* J Journal of dispersion science technology, 2014. **35**(7): p. 984-996.
114. Behroyan, I., et al., *Turbulent forced convection of Cu–water nanofluid: CFD model comparison.* J International Communications in Heat, 2015. **67**: p. 163-172.
115. Bianco, V., et al., *Numerical investigation of nanofluids forced convection in circular tubes.* Applied Thermal Engineering, 2009. **29**(17-18): p. 3632-3642.
116. Bianco, V., O. Manca, and S. Nardini, *Numerical investigation on nanofluids turbulent convection heat transfer inside a circular tube.* International Journal of Thermal Sciences, 2011. **50**(3): p. 341-349.
117. Chen, Y., Y. Li, and Z. Liu, *Numerical simulations of forced convection heat transfer and flow characteristics of nanofluids in small tubes using two-phase models.* J International Journal of Heat Mass Transfer, 2014. **78**: p. 993-1003.
118. Ghanbarpour, M., R. Khodabandeh, and K. Vafai, *An investigation of thermal performance improvement of a cylindrical heat pipe using Al 2 O 3 nanofluid.* Heat and Mass Transfer, 2017. **53**(3): p. 973-983.

119. Godson, L., et al., *Enhancement of heat transfer using nanofluids—an overview.* Renewable and sustainable energy reviews, 2010. **14**(2): p. 629-641.
120. He, Y., et al., *Numerical investigation into the convective heat transfer of TiO2 nanofluids flowing through a straight tube under the laminar flow conditions.* Applied Thermal Engineering, 2009. **29**(10): p. 1965-1972.
121. Hejazian, M., M.K. Moraveji, and A. Beheshti, *Comparative study of Euler and mixture models for turbulent flow of Al2O3 nanofluid inside a horizontal tube.* International Communications in Heat and Mass Transfer, 2014. **52**: p. 152-158.
122. Heris, S.Z., M.N. Esfahany, and G. Etemad, *Numerical investigation of nanofluid laminar convective heat transfer through a circular tube.* Numerical Heat Transfer, Part A: Applications, 2007. **52**(11): p. 1043-1058.
123. Heris, S.Z., M.N. Esfahany, and G. Etemad, *Investigation of CuO/water nanofluid laminar convective heat transfer through a circular tube.* Journal of Enhanced Heat Transfer, 2006. **13**(4).
124. Moraveji, M.K., et al., *Modeling of convective heat transfer of a nanofluid in the developing region of tube flow with computational fluid dynamics.* International communications in heat and mass transfer, 2011. **38**(9): p. 1291-1295.
125. Rostamani, M., et al., *Numerical study of turbulent forced convection flow of nanofluids in a long horizontal duct considering variable properties.* J International Journal of Heat Mass Transfer, 2010. **37**(10): p. 1426-1431.
126. Lotfi, R., Y. Saboohi, and A. Rashidi, *Numerical study of forced convective heat transfer of nanofluids: comparison of different approaches.* International Communications in Heat and Mass Transfer, 2010. **37**(1): p. 74-78.
127. Vanaki, S.M., et al., *Numerical study of convective heat transfer of nanofluids: a review.* 2016. **54**: p. 1212-1239.
128. Utomo, A.T., et al., *The effect of nanoparticles on laminar heat transfer in a horizontal tube.* International Journal of Heat and Mass Transfer, 2014. **69**: p. 77-91.
129. Saberi, M., M. Kalbasi, and A. Alipourzade, *Numerical study of forced convective heat transfer of nanofluids inside a vertical tube.* International Journal of Thermal Technologies, 2013. **3**(1): p. 10-15.
130. Saha, G., *Heat transfer performance investigation of nanofluids flow in pipe*. 2016, University of Glasgow.
131. Özerinç, S., A. Yazıcıoğlu, and S. Kakaç, *Numerical analysis of laminar forced convection with temperature-dependent thermal conductivity of nanofluids and thermal dispersion.* International Journal of Thermal Sciences, 2012. **62**: p. 138-148.
132. D'Orazio, A., Z. Nikkhah, and A. Karimipour. *Simulation of copper–water nanofluid in a microchannel in slip flow regime using the lattice Boltzmann method with heat flux boundary condition*. in *Journal of Physics: Conference Series*. 2015. IOP Publishing.
133. Brownlee, J. *How to Choose an Activation Function for Deep Learning*. 2021; Available from: https://machinelearningmastery.com/choose-an-activation-function-for-deep-learning/.
134. Vajjha, R.S., D.K. Das, and P.K. Namburu, *Numerical study of fluid dynamic and heat transfer performance of Al2O3 and CuO nanofluids in the flat tubes*

of a radiator. International Journal of Heat and Fluid Flow, 2010. **31**(4): p. 613-621.
135. Wollblad, C. *Your Guide to Meshing Techniques for Efficient CFD Modeling*. 2018 11/07/2024]; Available from: https://www.comsol.com/blogs/your-guide-to-meshing-techniques-for-efficient-cfd-modeling.
136. Namburu, P.K., et al., *Numerical study of turbulent flow and heat transfer characteristics of nanofluids considering variable properties.* International Journal of Thermal Sciences, 2009. **48**(2): p. 290-302.